March 2022

Alaska Department of Transporation & Public Facilities

R&M Consultants, Inc.

Updated Findings Report

Beach Road Landslide, Haines, Alaska

Professional Services Agreement No. 25213018
IRIS Program No. SDRER00317

LANDSLIDE TECHNOLOGY
A DIVISION OF CORNFORTH CONSULTANTS

LANDSLIDE TECHNOLOGY
A DIVISION OF CORNFORTH CONSULTANTS

GEOTECHNICAL INVESTIGATION, UPDATED FINDINGS REPORT
BEACH ROAD LANDSLIDE, HAINES, ALASKA

Professional Services Agreement No. 25213018
IRIS Program No. SDRER00317

March 18, 2022

Report To:
Alaska Department of Transportation & Public Facilities
6860 Glacier Highway
Juneau, Alaska 99811-2506

Submitted To:
R&M Consultants, Inc.
9101 Vanguard Drive
Anchorage, Alaska 99507

Prepared By:
Landslide Technology, a Division of Cornforth Consultants, Inc.

George Machan, P.E.
Senior Associate Engineer

Charlie Hammond, R.G., C.E.G.
Senior Associate Geologist

Benjamin George, P.E., C.E.G.
Senior Associate Engineer

Table of Contents

List of Tables

List of Figures

List of Appendices

EXECUTIVE SUMMARY

The Beach Road Landslide in Haines, Alaska occurred on December 2, 2020 when regional weather produced an 'atmospheric river' that delivered historic precipitation and caused significant snowmelt. Landslide Technology (LT) along with prime consultant R&M Consultants, Inc. (R&M) were contracted by the State of Alaska Department of Transportation and Public Facilities (DOT&PF) to conduct a geotechnical investigation and analysis of slopes within the Beach Road Area of Concern (AOC). Three phases of investigation were performed, and several preliminary reports were prepared. This Findings Report details geologic evaluations, summarizes interpretations and analyses, describes conclusions and opinions regarding geologic hazards, and provides recommendations for monitoring, management and possible mitigation of the geologic hazards.

Section 1 describes the investigation scope of work, chronology of the December 2020 atmospheric event and resulting landslides, and lists the various interim technical documents prepared during the investigation.

Section 2 describes the regional geology. There has been accretion of terranes onto the western margin of the ancient North American tectonic plate, igneous intrusion, faulting and significant uplift, and most recently the advancement and retreat of continental glaciation. These processes have combined to form complex geologic assemblages and structural elements.

Section 3 describes our evaluations of site geology and geomorphology, and presents interpretations of stratigraphy and subsurface material units comprising the landslide and adjacent hillsides. Geologic processes have deformed the materials within the hillside that now contribute to marginal stability. Groundwater conditions were also evaluated, including current levels and potential storm surge levels. Groundwater and surficial runoff played a major role in landslide triggering. The weather event produced historic precipitation and significant snowmelt that caused elevated groundwater pressures resulting in artesian flows.

Section 4 describes the geotechnical analysis of slope stability. The analyses evaluated the stability preceding and during the December 2020 storm event, including parametric modeling of groundwater levels that contributed to landslide instability. Analyses were also performed for current, post-landslide conditions to characterize stability going forward, particularly during groundwater surges associated with high-precipitation events combined with snowmelt. The stability of the adjacent hillside slopes to the east and west of the landslide was evaluated, confirming higher levels of stability than the landslide area. Seismic stability analyses were performed to model the possible reduction in slope stability due to earthquakes.

Section 5 describes modeling of potential fluid runouts of debris flows. Liquefiable conditions exist at the Mt. Riley mid-slope benches where deposits of fine-grained colluvium can be impacted by artesian groundwater pressures. Modeling was used to simulate potential flow paths and extents, based on several assumed potential liquefaction source areas. The analyses indicate a wide range of possible flow paths and extents to consider.

Section 6 presents qualitative assessments of various types of geologic hazards, including the estimated likelihood of occurrence, relative level of potential consequences, and relative risk based on the studies performed. The results of the qualitative analysis are presented on a Risk Informed Decision Matrix.

Section 7 presents conclusions, describes concepts for mitigation options, and provides recommendations.

In our opinion, the catastrophic 2020 landslide occurred due to a combination of factors in this localized section of the Mt. Riley hillside, including: upper zone of displaced fractured weathered bedrock (tilted, deformed, crushed, inflated), concentrated surface water, 'thick' accumulation of liquefiable fine-grained colluvium, strong groundwater recharge, and artesian groundwater. The small debris flow slide located west of the landslide area did not result in a catastrophic slide since the bedrock appears more competent (i.e., less weathered/fractured/deformed) than the rock mass in the landslide area. Elsewhere within the AOC, the slopes may have experienced erosion, particularly in swales and drainages, but did not experience landslides or liquefied flows. The bedrock appears more competent (i.e., less weathered/fractured/deformed) than in the landslide area, the mid-slope colluvium was of insufficient thickness, and/or the groundwater did not rise to liquefiable artesian levels.

In our opinion, the remnant slide mass of the catastrophic landslide is marginally-stable during normal groundwater conditions, but may experience movement during increased groundwater levels during moderate to large storms. If large slump blocks are displaced from the headscarp area, which could be caused by large storms or earthquakes, the materials would collapse into the headscarp and onto the landslide mass below. The likely result would be a decrease in landslide stability, with potential mobilization of remnant slide mass.

Rockfall from the headscarp and upper lateral scarps is likely, but would generally be localized and result in very small loading onto the landslide mass, which would have negligible effects on landslide stability and not cause remnant slide mass movement. Boulders that are displaced will likely not travel far downslope due to the roughness and softness of the slide debris surface, and will likely not reach Beach Road due to the gentle ground slopes in the lower landslide debris flow area.

Elsewhere within the AOC, it is anticipated that the slopes on both sides of the landslide will continue to experience erosion and to weather/deform in-place, producing more rockfall and colluvium. Localized debris flows, slumps, and creep of colluvium slopes may occur. In our opinion, large deep-seated landslides in the bedrock slope would be unlikely. Slides may occur in colluvial deposits on the hillside slopes, particularly during significant storms that cause high increases in groundwater levels and artesian pressures.

Earthquakes can reduce stability and possibly trigger movement of the landslide and adjacent hillside slopes, depending on the size and location of the seismic events.

In our opinion, fluid runout flows and debris flows may occur in deposits of fine-grained colluvium due to artesian groundwater pressures as a result of significant rainfall events that cause colluvial soils to liquefy. A range of debris flow runout extents may be possible. The analyses and interpretations presented in this report are rough approximations due to the uncertainty in the modeled larger debris flow extents based the limited available data.

There are several approaches to deal with landslides and marginally-stable slopes, including: 1) stabilization, 2) avoidance, 3) management, 4) maintenance, and 5) partial mitigation.

Monitoring geotechnical and weather instruments should be continued to establish baseline conditions and to further improve the understanding of the effects weather and groundwater have on the site. A long-term goal would be to develop correlations between weather events, groundwater pressures, and ground movements. Threshold values to warn residents of potentially hazardous conditions may be determined once baselines are established and the effects of weather and groundwater have on slope stability.

Changes across the AOC and areas surrounding the AOC could be understood if periodic lidar data is collected. Monitoring could be conducted periodically, initially on an annual basis and decreased to a five-year period or longer should baseline comparisons show stable conditions.

We recommend preparing a plan for maintenance of infrastructure (i.e., roadway and utilities). Items to consider when preparing a plan could include environmental factors, storm water runoff, debris flows, and slide movement/creep.

Consider the construction of partial mitigation drainage measures to reduce the risk of liquefaction and slope instability by limiting potential increases in groundwater pressure surges (particularly artesian pressures) during large storms and snowmelt. Horizontal drains and/or trench drains constructed in colluvial materials at the Mt. Riley mid-slope benches may achieve partial mitigation.

Due to the high likelihood of hazard associated with the landslide area, we recommend avoiding construction of buildings within the active landslide limits, possibly including a buffer zone along the boundaries of the landslide or a hazard overlay where there is uncertainty whether the landslide may widen and whether debris flow paths/extent may run beyond the existing landslide impact area. Limiting activities within the landslide area during periods of significant precipitation is also recommended. Caution signs could be maintained to warn visitors of geologic hazard risks along the north-facing hillside of the AOC. Consideration of options would also likely include increased public awareness.

A subsequent work phase could develop recommendations and details for the mitigation and/or management approaches the Borough wants to pursue.

1 INTRODUCTION

This Updated Findings Report for the Beach Road Landslide has been prepared to document the geotechnical studies authorized by the State of Alaska Department of Transportation and Public Facilities (DOT&PF) as described in Agreement No. 25213018 (IRIS Program No. SDRER00317). Three phases of work were conducted. Phase 1 included conducting a desktop study of available information, performing a winter reconnaissance, and preparing a preliminary findings report. Phase 2 was conducted to provide additional assessment of site conditions and geologic hazards, investigation of subsurface conditions via test pits, and installation of surface monitoring instrumentation. Phase 3 work included investigation of subsurface conditions via exploratory borings and installation of subsurface instrumentation. Details of the scope of work for Phase 1 were provided in the *Winter Reconnaissance – Preliminary Findings Report* submitted on April 8, 2021. This report includes information provided therein; however, is focused on the Phase 2 and 3 efforts. A detailed scope of work for Phase 2 and 3 follows.

1.1 Scope of Work

The geotechnical scope for Phase 2 and 3 included the following.

1. Geotechnical consultation assistance for the Haines Borough. This included on-call geotechnical support during development of the Borough's approach to managing the Beach Road Landslide Area of Concern (AOC).
2. Geotechnical on-site support for access and recovery. LT provided geotechnical support during Borough on-site access and recovery efforts including review of on-going landslide conditions, training on-site spotters, and observing debris removal efforts.
3. Spring field reconnaissance of the slide area and adjacent hillside slopes within the AOC.
4. Surface instrumentation across the tension cracks east of the slide area.
5. Subsurface investigations including test pits, exploratory borings, and installation of subsurface instrumentation.
6. Coordination of geophysical subsurface investigations conducted by Siemens & Associates.
7. Preparation of this updated findings report, which included interpretation and development of geologic models, performing stability modeling, and conducting runout analyses.

1.2 Slide Event and Response Background

On December 2, 2020, damaging storms impacted several Southeast Alaska communities. The greater Haines Borough was impacted by flooding, landslides, and debris flows, causing widespread and severe infrastructure damage, mandatory and voluntary evacuations, and loss of life. Several local, state and federal agencies responded along with local contractors to assist the Haines Borough with the initial response. On behalf of the Haines Borough and Emergency Operations Centers, the State of Alaska Department of Natural Resources (DNR)-Division of Geological and Geophysical Surveys (DGGS) and DOT&PF deployed a team of geoscientists with different specialties to assist by collecting data to support decision making by the Local and State Emergency Operations Center (EOC) teams. The teams arrived in Haines between the December 4 and 6, 2020. The most severe

impact was a large landslide event along Beach Road, which completely destroyed two homes, significantly damaged another home, blocked road access and disrupted utilities to approximately 20 homes (refer to Figure 1 and Figure 2). Two residents of these homes are unaccounted for and are presumed to have perished during the event. After ten days of on-site analysis, Search and Rescue (SAR) operations and re-occupancy of several homes; these operations were halted pending further evaluations of landslide stability and hazards.

The weather event was considered a very strong atmospheric river followed by a series of additional strong and moist weather fronts from December 1 through 8, 2020. This weather event produced historic extreme precipitation along with significant snowmelt, as described by Jacobs (2021a & 2021b). The temperature in Haines at the time of the storm was above freezing and rose into the mid-40s °F. The downtown Haines COOP weather station reported 6.62 inches of precipitation by 8:00 am December 2, 2020, which exceeded the previous historic daily record set in 2005. The heavy rain continued and the snow level rose above 2,500 feet elevation. The 48-hour precipitation recorded at the downtown Haines COOP weather station was 8.54 inches, and the weather station at the Haines airport recorded 10.26 inches in 48 hours. Jacobs performed an evaluation and estimated the storm return interval to be on the order of 200 to 500 years.

1.2.1 Description of the Landslide Event and Related Factors

The resulting rainfall and snowmelt produced a significant amount of runoff. Area residents were surprised by the unusually high amounts of stormwater and runoff water in their yards and along/across the Beach Road. Water discharge from a couple springs near the residences and road appeared to flow at rates far greater than previously observed. A water-supply well, located on the Anderson residence at the east end of Beach Road, was overflowing from the top of the casing extending above the ground surface, indicating a rise in artesian groundwater pressures (Anderson, 2020). Domestic wells for several properties along Beach Road had previously been installed through shallow overburden and into deep bedrock over 200 feet deep to reach suitable groundwater, with prior flows typically of only a few gallons per minute. Residents observed excessive runoff, including unusual discharge of water appearing to flow from the roots of trees. Surface runoff water caused erosion of ditches and parts of the roadway, and residents attempted to regrade some ditches to divert flows from sheeting across the road.

In the early afternoon on December 2, 2020, shortly before 2 pm, residents in the Slate residence (located near the shore, immediately east of the landslide) heard a loud noise like a large slab of ice sliding off a roof. They stepped outside and saw the debris flow landslide moving with trees tilting in all directions, along with sounds of popping, breaking and snapping of trees, sounding like a train or big jet. They hurried inside their home for protection, then looked out the window to the west and saw the debris flow landslide extending downslope into the inlet water and realized homes had been washed away (Slate, 2020). This was followed within a few minutes by another phase of flow sliding. The sliding material was more fluid this time and the tree trunks were generally laying on the landslide debris as it flowed to the shoreline and further into the inlet water. This lasted possibly a minute or less. The Slates recorded a video of this second flow landslide (Slate, 2020). Electric power to the house was lost immediately concurrent with the first debris flow.

In the early afternoon on December 2, 2020, the occupants of the Messano house (located on the upslope side of Beach Road, immediately west of the landslide) had just driven back to the house from downtown, and had to find a location to park to avoid standing water and eroded areas. They were still in their car when they heard a loud rumbling noise, which caused them to look up. They then saw trees and boulders rapidly moving/flowing very close to their east, and saw the flowing debris push a parked car that impacted the Messano house. The landslide event lasted approximately a half minute, and then a few minutes later they heard a second debris flow event, but could not see it from their location due to the westerly pileup of debris from the first flow landslide.

The debris from the landslide covered a 650-foot portion of Beach Road, cutting off access to the residents to the east of the landslide on this dead-end road. After the landslide event, it was necessary to evacuate residents by boat, as Beach Road had been rendered impassable.

1.2.2 Emergency Evaluations

Emergency evaluations of the debris landslide and hillside were subsequently performed by the DGGS, along with support from DOT&PF, Haines Borough and EOC, Haines Avalanche Center, National Weather Service (NWS, NOAA), and local geologists. Reconnaissance was performed of the landslide and adjacent terrain in early December, and a helicopter and drone were utilized to perform aerial evaluations and imaging. DNR staff accessed the headscarp area on December 11 and 12 and evaluated exposed rock conditions. Aerial photographs, lidar imaging and videos were obtained of the post-failure conditions. The reconnaissance documented the various materials and conditions comprising the slide debris, the relative geometry and topography of the ground surface of the landslide scarp and debris, surface water flows and springs, and identified a tension crack extending from the headscarp towards the east a reported distance of approximately 160 feet. This tension crack prompted further assessment of the hillside to the east of the landslide.

The reconnaissance verified that the slide debris consists of a heterogeneous mix of cobble and boulder-sized rocks, detached rock blocks, soil, vegetation and trees. Surface water flowed into the headscarp from upslope, apparently from a localized depression (hollow basin or pond-like feature) that concentrated water from melting snow, creating a waterfall down the face of the headscarp. Springs were evident in the middle portion of the slide debris, which resulted in several streams coursing downslope. By December 9, 2020, the runoff from upslope of the headscarp had reduced significantly, and only a trickle was flowing by December 12, 2020 and no water or seepage was observed in the rock slopes comprising the headscarp. The headscarp was observed to consist of fractured and jointed bedrock.

An ortho-aerial photo was developed from the December 2020 post-slide photography to assess the landslide and adjacent hillside slopes. Figure 2 shows the aerial photo, which includes the approximate locations of private properties and roads. The extent of sliding and impacts to the terrain were visible. The length of the landslide was determined to be approximately 2,300 feet from the headscarp to the shoreline. The width of the upper landslide area was approximately 300 to 400 feet, and the width along the road and shoreline was approximately 650 feet. Locations of large rock blocks and clusters of boulders on the surface of the slide debris were evident in the aerial photo. Drainage channels on the slide debris were also identified on the aerial photo.

Lidar data was available at the site with a data set collected by DGGS in May 2014 and subsequent to the event in December 2020. The 2014 and 2020 lidar data were evaluated to identify apparent changes in the ground surface and to interpret geomorphology of the hillside. The images showed the irregular topography and areas incised by springs and streams. It became apparent that the 2014 lidar image did not extend all the way up to the headscarp, which limited the evaluations. Hillshade models were developed from the lidar terrain data, and 3D images were created by DGGS to discern geomorphic conditions.

Preliminary evaluations as part of the emergency response were performed to evaluate the hillside terrain east of the landslide for possible landslide features to identify geologic hazards. Of concern were drainage channels, scarps, linear and arcuate changes in ground surface, differential erosion and jointing of bedrock, and mounds of bedrock separated by gently sloped areas.

Haines Borough adopted a DGGS map delineating the AOC, which showed the properties included in the evacuated zone (December 18, 2020). The AOC was defined as an area that "could be impacted by a potential landslide originating at the fracture site" and that this area "remains an area of elevated concern with unknown stability." The approximate boundary of the AOC is shown on Figure 2.

1.2.3 Initial Landslide Monitoring

Survey monitoring was performed by local surveyor Dave Smith with Southeast Roadbuilders. Survey points were established above the landslide headscarp and close to the Messano house, including a boulder located in the slide debris east of the Messano house. Data through February 12, 2021 did not detect any movement of the survey points.

A series of "time lapse" photos of the upper landslide debris made by the Haines Avalanche Center from December 22, 2020 to February 5, 2021 did not discern any major movement of the slide debris. This matched observations by local residents that the slide debris began to get firmer, and that most of the slide debris did not appear to be noticeably moving.

1.2.4 Interim Temporary Access Road

After almost two months of apparently relative minor to negligible ground movement, a local contractor constructed a temporary corduroy road across the landslide in late January 2021. The temporary road was authorized by Haines Borough to allow residents to retrieve belongings and to mitigate concerns at their properties. The surface of the slide debris appeared to be less saturated and was somewhat firmer to walk on. This construction effort took two and a half days to accomplish. Portions of the debris exhibited wet conditions, and the hydraulic Cat 335 excavator experienced localized buoyant conditions (like being on a waterbed). The western portion of the debris (the first 100 feet of the temporary road) was extremely soft and saturated. A "rocky" ridge was encountered between 100 and 150 feet from the western flank of the landslide. The middle and eastern area of slide debris contained more boulders and was relatively firmer. Many tree trunks were in the slide debris. The roadbed was developed by reinforcing the subgrade with logs and pushing boulders into muddy zones. One culvert was installed in a drainage area approximately 200 feet west of the eastern end of the temporary access road. Reportedly a 30-inch diameter steel pipe.

1.3 Geotechnical Studies

R&M Consultants, Inc. (R&M) and Landslide Technology (LT) were contracted by the DOT&PF in January 2021 to conduct a geotechnical study of the landslide and areas adjacent to the slide within the Haines Borough AOC. A series of studies were performed that are discussed herein and submitted reports are listed in Section 1.4. Phase 1 of the work included reviewing available information related to the landslide event, performing a desktop study of geomorphic features within the AOC, conducting a winter surface reconnaissance, and preparing a preliminary findings report.

A winter reconnaissance was performed at the project site following a review of available information related to the landslide event (and the days preceding) and developing geomorphic interpretations of pre- and post-slide lidar images. The goal of the reconnaissance was to: i) check observations obtained from the desktop review and geomorphic interpretations, ii) observe and document landslide features, iii) observe and document surficial and outcrop geology, iv) assess surficial hydraulic conditions, and v) estimate groundwater conditions.

Two geotechnical engineers and one engineering geologist from LT performed the winter reconnaissance between February 22 and March 1, 2021. The reconnaissance was performed via: i) helicopter over-flights, ii) traversing the landslide area and the slopes adjacent to and above the landslide within the AOC, iii) walking the limits of Beach Road and observing surficial conditions adjacent and behind local residences, iv) conversations with local residents, and v) excavating test pits along the interim road.

During the reconnaissance, surficial observations were hampered by relatively heavy snow cover. Up to three feet of snow was encountered in and adjacent to the landslide area and drifts thicker than six feet were encountered at higher elevations near and south of the headscarp of the landslide. Phase 1 work was documented in a *Winter Reconnaissance – Preliminary Findings Report* submitted on April 8, 2021.

Phase 2 and 3 of the geotechnical study included the scope of work detailed above. Upon authorization by the DOT&PF, several efforts were implemented. Initial work included conducting additional test pits upslope of Beach Road along alignment and at higher elevations on the slide mass. A geotechnical engineer was onsite from June 23 to 29, 2021 to observe and direct test pit excavations, log exposed materials, and collect representative samples for laboratory testing. Upon completion of the test pit explorations and associated laboratory testing, an interim memo *Phase 2 Test Pit and Laboratory Testing Results* was prepared and submitted on September 1, 2021 (revised February 3, 2022).

The test pit work was then followed by a Spring Reconnaissance conducted from July 5 through 12, 2021 by two geotechnical engineers and one engineering geologist from LT. The reconnaissance was conducted to collect additional surficial observations to supplement the Phase 1 findings. The landslide and surrounding slopes west and east of the upper slopes were traversed to observe and map: site geology, prominent landslide features, landslide debris, and surface water within the landslide. A *Spring Surface Reconnaissance Memo* was prepared as an interim submittal provided on September 8, 2021.

While LT conducted the spring reconnaissance, several other activities were also occurring. Siemens & Associates (Siemens) conducted geophysical surveys of the slide body and areas adjacent to the slide. Siemens crews were onsite from July 5 to 15, 2021. They performed seismic refraction (p-wave)

and linear microtremor (s-wave) surveys along six alignments and electrical resistivity surveying techniques along two alignments. Siemens submitted a *Results of Geophysical Exploration, Data Report* on January 21, 2022.

LT had an engineer on site during debris removal operations between July 12 and 21, 2021. LT assisted with slide monitoring during removal activities, observed conditions of materials being excavated, evaluated potential scour areas within the original road grade, assessed groundwater/runoff conditions, and documented results of the removal activities. The thickness of the debris steadily increased from the margins of the slide towards the center. Surface water runoff was observed in two primary drainages in the slide mass: major runoff on the western side, and more minor runoff on the eastern side. Culverts (24-inch corrugated HDPE pipe) were installed for each of those two drainages, and the drainage path upslope of each culvert was armored with rock. The upslope side of the roadway was laid back to a 2H:1V slope above the ditch. Two local areas of the roadway were observed to have been locally scoured by the slide debris runout. Observations are summarized in the July 27, 2021 memo *Interim Road Debris Removal.*

Phase 2 included installation of surface monitoring equipment. Installation locations were identified during the spring reconnaissance and installed by LT personnel from July 12 to 20, 2021. Instrumentation included installing six extensometers and placing 21 geodetic prisms on the slide body and scarp features. Details of the extensometers are provided in the interim memo *Surface Extensometer Instrumentation Installation* submitted on August 26, 2021.

In November 2021, R&M Consultants, Inc. installed additional prisms for control points outside of the slide and a robotic total station south of Beach Road. A secure shelter was constructed to house the total station to minimize tampering and provide protection during inclement weather. The robotic total station is periodically surveying the installed prisms to monitor for surficial movement on the landslide. Details of the total station installation and the initial measurements of the prisms were offered by R&M in their December 30, 2021 report titled *Haines Beach Road Landslide, Total Station Monitoring Site Installation Report*.

Phase 3 work included completing 12 exploratory borings, installing 24 vibrating wire piezometers and 12 ShapeArray® in-place slope inclinometers, performing downhole acoustic and optical televiewing, and conducting laboratory testing of representative samples. The subsurface exploration work was conducted by several LT personnel from August 28 to October 31, 2021. Preliminary results of the exploratory work, associated laboratory testing, and monitoring was provided in the *Investigation Report, Borings and Subsurface Instrumentation, Beach Road Landslide* submitted on March 18, 2022.

The 2014 lidar data has evolved during the completion of the three phases of work. During Phase 1 and a portion of Phase 2, the 2014 lidar data had a gap at the top of the slide area that was critical for interpretation. In late summer 2021, the data gap was filled with additional processing of over-flight data, and a complete 2014 surface of the area before the 2020 slide was created for the reviews detailed in this report.

Likewise, the *Investigation Report, Borings and Subsurface Instrumentation* report did not include a complete set of laboratory testing results. Uniaxial compression strength, x-ray diffraction (XRD), and petrographic testing were outsourced to a specialty laboratory and had not been completed prior to December 30, 2021.

1.4 Previously Submitted Reports

The interim reports and memos detailed above have been summarized below. Key reference items contained within these documents are indicated.

- Winter Reconnaissance – Preliminary Findings Report, Beach Road Landslide, Haines, Alaska, April 8, 2021.
    - Photographs of December, 2020 landslide impacts
    - Photographs of winter reconnaissance
    - Rock outcrop structural analyses
    - Draft test pit logs
    - Initial laboratory tests
    - Initial geologic interpretations, maps and cross sections
    - Preliminary assessments
- Haines Beach Road Landslide, Winter Survey Reconnaissance, Survey Report (R&M Consultants, Inc.), April 8, 2021.
- Surface Extensometer Instrumentation Installation, Beach Road Landslide, Haines, Alaska, August 26, 2021.
- Spring Surface Reconnaissance Memo, Haines Beach Road Landslide – NTP2 Task 5.1, September 8, 2021.
    - Rock structure data summary stereonets
    - Photographs of spring reconnaissance
    - Surface observations of landslide features
    - Updated geologic interpretations and map
- Investigation Report, Borings and Subsurface Instrumentation, Beach Road Landslide, Haines, Alaska, March 18, 2022.
    - Drilling and sampling details
    - Boring logs, core sample photos, downhole imagery,
    - Laboratory testing
    - Instrument installation details and initial data plots
- Haines Beach Road Landslide, Total Station Monitoring Site Installation Report, Haines, Alaska (R&M Consultants, Inc.) December 30, 2021.
    - Survey prism locations
    - Surveying method and installation

- Results of Geophysical Exploration, Data Report, Beach Road Landslide, Haines, Alaska, (Siemens & Associates) January 21, 2022.
- Phase 2 Test Pit and Laboratory Testing Results, Haines Beach Road Landslide – NTP2 Task 5.3, September 1, 2021 (revised February 3, 2022).
    - Test pit location map
    - Test pit logs
    - Test pit photographs

2 REGIONAL GEOLOGY

The Beach Road Landslide site is located on the east side of Haines, Alaska, approximately 75 miles northwest of Juneau, Alaska as shown on Figure 1. Haines lies at the northern end of the Alexander Archipelago on the Chilkat Peninsula. The Chilkat Peninsula is bounded on the northeast by the Chilkoot Inlet and on the southwest by the Chilkat Inlet. These two waterways form the northern extension of the Lynn Canal as shown on Figure 1.

The Chilkat Peninsula and the southeast region of Alaska has undergone considerable changes over geologic time. There has been accretion of terranes onto the western margin of the ancient North American tectonic plate, metamorphism, igneous intrusion, faulting and significant uplift. Most recently the area has been subjected to advancement and retreat of continental glaciation. These processes have combined to form the complex geologic assemblages and structural elements through the region. A regional geologic map is provided on Figure 3.

The Chilkat Peninsula is comprised of rock materials that are part of the lithotectonic Wrangellia Terrane (Brew and Ford, 1994). The basal part of the Wrangellia terrane consists of Paleozoic volcanic flows and breccias that are locally intruded by Late-Paleozoic granitic rocks of the Skolai arc and Cretaceous ultramafic rock bodies.

The regional area and the Chilkat Peninsula have undergone significant tectonic deformation, which resulted in the geologic structure currently present. Tectonism accreted the terrane and rock assemblages to the North American Continent and in the process, they were structurally deformed and faulted. The Chilkat River fault, which trends northwest to southeast, is the eastern local segment of the Denali fault system. The Denali fault system is a right-lateral feature with a number of splays. A major unnamed fault splay cuts across the Chilkat Peninsula south of Haines and connects with the Lutak Inlet-Chilkoot Inlet fault, which is north-northwest to south-southeast trending. This splay cuts through the Triassic basalts that make up the Chilkat Peninsula.

At the site of the Beach Road Landslide, the in-place bedrock has been previously mapped consisting of layered ultramafic intrusive rocks. These intrusive rocks are predominantly clinopyroxenite, typically containing hornblende and biotite (Gehrels and Berg, 1992). According to local geological experts who reside in Haines, visible plagioclase is rare to non-existent. In addition, exposed contacts between the ultramafics and the nearby mapped metabasalt are rare or non-existent. Felsic intrusions of diorite, granodiorite, and tonalite are locally observed intruding the ultramafics.

Petrographic and X-Ray Diffraction (XRD) analysis conducted as part of this most recent phase of the project has indicated the rock sampled from the landslide area consists of ultramafic and mafic rock types. The ultramafics appear to be predominant and consist primarily of clinopyroxenite. The mafic rock includes primarily gabbro, but also includes lamprophyre and dolerite. Chemical analysis results from the XRD testing differ slightly from the petrography in that the results include chemical differences, likely due to weathering, alteration, and secondary minerals. Figure 4 provides a typical ophiolite sequence of oceanic lithosphere, which illustrates the types of rocks that could be expected as the original source of the rock.

In addition to faulting and intruded rock, the landscape and topography at the site have been heavily influenced by glaciation. The area has been covered by glaciers likely several times during the

Pleistocene Epoch (Lemke and Yehle, 1972). Marine deposits located several hundred feet above sea level indicate the land has been uplifted relative to sea level (i.e., glacial rebound) since the last major deglaciation of the region approximately 12,000 to 10,000 years ago. The rate of relative uplift due to deglaciation rebound in the Haines area has been estimated to be nearly an inch per year (Larson, et al., 2005). This would correlate with the entire Beach Road Landslide being previously below sea level.

3 SITE GEOLOGY

The following geology discussion includes a general description of the setting, followed by a review of geologic and engineering geologic testing and the geomorphic material units that make up the hillside. These descriptions support the development of geotechnical engineering characteristics.

3.1 General Description

The landslide occurred on slopes that generally face north-northeast on the northern peak of Mt. Riley. This peak is a prominent component of the Chilkat Peninsula to the south and east of Haines. The landslide is approximately 2,300 feet long horizontally from the headscarp to the shoreline. The width of the upper landslide area is approximately 300 to 400 feet, and the width along the road and shoreline is approximately 650 feet. Figure 2 shows the extents of the landslide.

Figure 5 and Figure 6 are topography and slope shade maps based on the 2014 lidar data set, respectively. An oblique view of the 2014 and 2020 slope shade is provided on Figure 7, side by side with a 2020 slope shade for demonstration of slope conditions before and shortly after the landslide.

The landslide extends from sea level up to elevation 865 feet at the headscarp. Overall the north-facing slope is approximately 22° (40%). However, in the AOC below elevation approximately 320 feet, its lower slopes average approximately 11° (19%), while its upper slopes average approximately 37° (75%). Local sections of the upper slopes in the AOC are as steep as 65 to 80°. To the south and above the landslide's headscarp, the mountainous slopes are variable, but less steep in general.

Vegetation in the AOC appears to be a mixed lowland forest of shrubs and evergreen and deciduous trees. The Haines Borough and the Chilkat Peninsula are in the Maritime Zone per the Western Regional Climate Center. Typical daily temperature ranges from 0° to 80°, ±10°. Typical rainfall ranges from 1.5 inches per month during the summer to over 8 inches per month in the winter, and snowfall can range from 10 to 40 inches per month November through March (https://wrcc.dri.edu/summary/ Climsmak.html, accessed Feb 2022).

3.2 Change Detection

Elevation change detection was completed in ESRI ArcMap by comparing raster datasets created from the 2014 and 2020 lidar data sets. The results of the change detection are provided on Figure 8. The following is a description of observed changes on the landslide and throughout the AOC.

Within the landslide area, a maximum elevation decrease of 54.7 feet is within the steeper slopes of the upper landslide area. The maximum elevation increase of 18.4 feet corresponds to material deposited on and upslope of the Mt. Riley mid-slope benches.

Elevation changes within the lower landslide are variable and represent areas of scour and deposition. These elevation changes range from an approximate 8-foot decrease to an approximately 7-foot increase. Elevation increases within the lower slide area are especially prominent along both the east and west margins of the landslide. Elevation decreases also occur in a scour area along the western edge of the landslide. Elevation change at the toe of the landslide are representative of deposition, with a maximum elevation increase of approximately 13 feet.

Changes in elevation outside of the landslide area were shown to be minimal to no change. One area to the west of the landslide did show a small debris flow event occurred, as observed during the winter

and spring reconnaissance. This smaller debris flow landslide was deposited onto the Mt. Riley mid-slope bench.

3.3 Geomorphologic Review of Geotechnical Materials

The *Spring Surface Reconnaissance Memo* included a geomorphic interpretation of the 2020 ground features. Interpretation of the 2014 ground features was not completed at that time due to the gap that was present in the data. Assessing the geomorphology included review of the ground reconnaissance observations and interpretation of topography/slope shade maps produced from 2014 and 2020 lidar data sets. Figure 9 is a geomorphic interpretation map of the 2014 ground surface showing rock and colluvium areas along with deposits of slumped colluvium, debris flow fans, and lobate-shaped colluvium. The 2020 geomorphic interpretation map (Figure 10) illustrates features mapped within the landslide area along with rock and colluvium areas within the AOC. Mass wasting landforms are also interpreted within the AOC, including deposits of slumped colluvium, debris flow fans, and lobate-shaped colluvium. Below is a discussion of the observed and mapped features.

Relatively thin "overburden" deposits of marine sediment and topsoil are not mapped. The marine sediments occur on the lower slopes near Beach Road, and topsoil occurs over the entire area. Other than their geologic occurrence, the marine sediment and topsoil are not significant factors in the stability modeling of the Beach Road Landslide.

Bedrock and colluvium are interpreted and mapped based on reconnaissance observations, subsurface exploration results, and the geomorphology in the AOC. Weathered and degraded rock occurs over the entire AOC. Based on the reconnaissance and explorations, it is apparent that variations in subsurface conditions result in different weathered materials.

Rock materials vary from visually fresh and in-place, to weathered and displaced. Photographs of typical rock outcrops are provided in Appendix A. The visually fresh and in-place rock occasionally forms steep cliffs on the slopes of Mt. Riley. The vast majority of the rock exposed at the ground surface is weathered. Exploratory borings encountered weathered rock and underlying in-place visually fresh rock. A transition between weathered and in-place rock was encountered in the subsurface exploratory borings.

Weathered rock materials have joints and fractures that are mechanically opened, which in general creates an inflated condition. Mechanical inflation and slope creep of the rock mass is caused by water pressure, ice pressure (freeze-thaw), and gravity. Together these result in fracturing, toppling, buckling, sliding, and general degradation of the rock. This process is illustrated on Figure 11. Chemical weathering may also be occurring, for instance, oxidation of minerals from fluctuating pressure and water chemistry. However, chemical weathering is considered a relatively minor occurrence. The amount of inflation due to creep movement appears to be variable in the AOC. For instance, rock cliffs tend to be comprised of thickly layered rock that is less inflated.

Fault gouge including sheared and crushed material, caused by pressure and friction, is also present in the rock materials. Minor occurrences of fault gouge were observed; however, these materials can be critical in specific, local stability conditions.

As the rock weathers and inflates, it degrades into colluvium through buckling, toppling, fracturing and sliding. The process appears to occur both gradually and quickly. Individual pieces of rock may

fracture slowly, or masses of colluvium and rock creep very slowly, while mass wasting events can be both slow and rapid. Types of mass wasting that are in the AOC include shallow sloughing of topsoil and colluvium, debris flows, and rockfall.

Other geomorphic slope features that are pertinent to the stability modeling include:

- Irregular and inclined benches termed the Mt. Riley mid-slope benches;
- Local slumps, lobate slope features, and debris flow fans that source (head) on the slopes above, and terminate (toe), on the Mt. Riley mid-slope benches; and
- Two prominent drainages that source high on Mt. Riley and flow into Chilkoot Inlet.

Mid-way up the slope on Mt. Riley is a series of gently inclined and discontinuous benches, generally between approximate elevations 250 to 450 feet. Slumping and creeping, generated from the slopes above the benches, soil and debris flow fans toe onto the mid-slope benches. The mid-slope benches are also areas of high groundwater, based on observed groundwater springs and groundwater pressure monitoring. To the east of the 2020 landslide, the benches are gently sloped to the north, but within 1,000 feet of the landslide, they are sloped to the west (toward the landslide). West of the 2020 landslide, the bench is gently sloped to the north.

The two prominent drainages that source high on Mt. Riley contain debris flow fans that flow across the Mt. Riley mid-slope benches, and down and across the relatively gentle slopes to Beach Road before dropping to the shore and Chilkoot Inlet. One of the prominent drainages is within the west side of the 2020 landslide. The other is approximately 2,000 feet east of the landslide.

The drainage at the 2020 landslide starts above elevation 1,000 feet, where a depression collects surface water from adjacent slopes and forms a ponded area. The pond seeps into groundwater. When the pond is full it feeds a surface drainage where a creek flows into the 2020 landslide area. The surface water seeps into the upper rock slump debris and appears to re-emerge as two spring areas flowing out of slumped slide debris near elevation 630 to 640 feet. One spring area emerges and then disappears into the boulder field in the middle of the slide. The other spring flows down a steep swale that forms a separate or side-drainage channel within the west side of the landslide. The flowing water converges at another spring area near elevation 330 to 340 feet at the toe of the mapped boulder-field. From here, the drainage flows across the Mt. Riley mid-slope benches before it continues flowing on the surface and down the west side of the lower deposits of the landslide.

The drainage approximately 2,000 feet east of the landslide starts at a spring area observed near elevation 860 feet. This drainage flows downslope, across steep rock slopes and colluvium slopes, and then across an eastern extension of the Mt. Riley mid-slope benches. Downslope of the benches it flows through a channel incised apparently in colluvium between approximate elevation 350 and 200 feet. From there it flows onto a broad and relatively gentle slope that extends down to Beach Road (i.e., historic debris flow fan).

Several geotechnical engineering material units were identified during geomorphic analyses. These units were used to prepare interpreted geologic cross sections and are based on the site geology and weathering processes. There are seven geotechnical engineering material units: three rock units and four colluvium units. These are based on geomorphic interpretation and geotechnical behavior.

Photographs of typical rock and colluvium materials are provided in Appendix A. A description of the geotechnical materials units is offered below and in more detail in Section 3.6.

- Rock slopes
  - Rock 1: in-place, relatively low degree of stress-relief and weathering, uninflated.
  - Rock 2: inflated, moderate to high stress-relief.
  - Rock 3: similar to Rock 2, but with surface morphology that indicates it has been displaced (irregular hummocky landforms combined with a headscarp/down-dropped block feature).
- Colluvium slopes
  - Colluvium 1: weathered in-place, remnants of Rock 2 and Rock 3.
  - Colluvium 2: talus, rockfall.
  - Colluvium 3: slump and flow debris, upper slopes of a debris flow fan.
  - Colluvium 4: debris flows, flood deposits, lower gentler slopes of a debris flow fan.

3.4 Analysis of Geologic Structure and Stratigraphy

The structure and mechanics of the rock and its stratigraphic geotechnical engineering condition is reviewed below.

3.4.1 Structure

Rock structural discontinuities were analyzed using the RocScience software DIPS v8.018. The analysis uses a stereonet, which is a 2D representation of planar features measured in the rock as dip and dip direction. Planar rock features at the Beach Road Landslide include fractures, joints, faults, and partings between different rock layers. Planar features were measured by hand in the field using rock structure compasses, and by an analyst using the computer program WellCAD to pick features observed in the borehole televiewer images from exploratory borings. Rock structure data is presented in the *Investigation Report, Borings, and Subsurface Instrumentation*.

Hand measurements from the Winter and Spring Reconnaissance phases were merged with subsurface data for this phase of study. Figure 12 presents stereonets of the surficial data collected by hand during the Winter and Spring reconnaissance phases. Figure 12A illustrates all of the surface rock structure data. Figures 12B, 12C, and 12D divide the dataset into clusters to illustrate data from: (B) the west of the landslide, (C) central within the landslide area, and (D) east of the landslide.

Figure 13 and Figure 14 provide stereonets of the downhole imagery data. Figure 13 is of the upper or shallow rock materials that exhibit mechanical weathering. Figure 14 is of the lower or deep rock materials that exhibit in-place, non-weathered conditions. These figures are clustered similar to Figure 12, with (A) showing all of the rock structure data, (B) showing the west side of the landslide, (C) showing the central landslide area, and (D) showing the east side of the landslide.

Several sets of discontinuities were identified. These sets combine to promote a toppling and buckling failure mechanisms. Toppling is promoted by Set 1, which tends to be steeper in surface and shallow rock data as compared to deeper rock data. It generally has a northeasterly dip direction with dip ranges from 60 to 75° in the surface and shallow measurements, and 45 to 50° in the deeper measurements. This difference in dip is interpreted to be caused by mechanical wedging and rotation of the rock layers as they topple and buckle. In addition, Set 1 appears to include two other types of

discontinuities: partings between rock layers of different texture and mineral assemblage, and exfoliation joints associated with glacial load and rebound.

Buckling tends to occur along second set of discontinuities (Set 2). This set of discontinuities dips into the slope on the order of 20 to 35°. Discontinuities from Set 3 do not appear to be critical to the stability; however, they appear to be the sides of layers and blocks that are toppling.

Hand measurements of faulted rock materials were collected during the spring reconnaissance at five locations in the rock scarps around the upper slumped block. Three of the fault measurements were oriented similar to Set 1, one was within Set 2, and one was within Set 3. One measurement within Set 1 was of sheared and decomposed rock in the headscarp below the highest elevation of the landslide. The headscarp was measured with dip/dip directions of 52/015 and 47/018.

3.4.2 Stratigraphy

Geologic and geotechnical data related to the stratigraphy of the rock materials was evaluated from surface reconnaissance and borehole data as presented. Surface reconnaissance information can be found in the *Winter Reconnaissance – Preliminary Findings Report* and *Spring Surface Reconnaissance Memo*. Borehole information can be found in the *Investigation Report, Borings and Subsurface Instrumentation* report.

The geologic stratigraphy appears to be predominantly layered pyroxenite and gabbro, which is commonly associated with oceanic lithosphere and an ophiolite sequence of rock materials. The layering is comprised of mineral assemblages, different grain size/rock texture, and intrusive dikes and veins. These all have parallel and cross cutting relationships. The layers have varying thickness, persistence, and hardness. Thickness of the layers observed during the reconnaissance ranged from a couple inches to 15 feet, with the average thickness in the 1- to 3-foot range. The layers appear to extend over distances of 10s to 100s of feet based on the length of cliff exposures. The largest outcrops observed were cliffs in the eastern AOC that had an approximate 50-foot height and 100-foot length of exposure. This would be a minimum persistence assuming that the layers also extend deep into the subsurface. However, due to the fracturing and faulting, all of the layers are likely broken/separated into smaller blocks (i.e., mechanical weathering – toppling and buckling mechanisms).

Hardness was determined by hand and in a laboratory. Hand techniques (scratching and hammer impact) were performed during the reconnaissance and borehole sampling. Laboratory technique was unconfined compressive strength (UCS) testing. The hand techniques determined the rock hardness ranges from Hard to Very Hard (R4 to R5 in rock hardness designation), which is generally 8,000 to >16,000 psi. And with weathered and crushed rock zones of Extremely Soft to Soft (R0 to R2), which is generally <100 to 4,000 psi. Laboratory testing measured compressive strength that ranges from 2,700 to 14,300 psi. Rock samples that were soft rock were not testable due to the often "soil-like" characteristics of extremely soft to soft rock. Approximately 25% of the samples that were shipped for testing did not hold up to the trimming and grinding necessary for the testing apparatus. Based on the samples provided, the failed testing appears to be associated with discontinuities that were healed or closed through geologic processes.

Zones of extremely soft (R0) to very soft (R1) rock, are typically described as "micaceous sand" when sampled in the boreholes. This rock in the subsurface appears to be fault gouge or crushed rock.

Surface exposures of faulted rock material includes fractured rock with gouge seams of clayey sand, and occasional macro and micro strain fabrics and slickensided fracture surfaces.

A geotechnical engineering classification for the rock stratigraphy is the degree of fracturing, which is expressed as RQD (Rock Quality Designation). While all the rock is fractured, rock materials that are closer to the ground surface tend to have higher variability and lower average RQD than rock that is deeper. This change is interpreted to be a transition from weathered and mechanically inflated rock to in-place, unweathered rock.

The transition from weathered to unweathered, and generally low to high RQD, was evaluated for its structural significance. The evaluation included interpretation of an apparent 3D surface that represents the location of the transition from inflated rock to in-place unweathered rock for all the borings on the upper slopes of the AOC (boreholes LT-1 through LT-10).

Based on our investigation, this rock structure transition is interpreted to represent a dislocation zone that could develop into a potential slip surface. Over geologic time, environmental processes have resulted in this transition between weathered, more highly fractured rock and un-weathered, less fractured rock. Imagery of core samples and downhole optical televiewer data was compiled in Appendix B to illustrate the conditions of the transition zone materials. Table 1 provides a summary of the materials that were sampled at the transitional zone immediately above in-place rock. The surface that was developed based on elevations of the transition zone in borings LT-1 through LT-10 is provided as Figure 15.

Table 1: Description of Weathered/Mechanically-inflated Rock Materials Immediately above Unweathered Rock 1

Boring No.	Base of Weathered Rock Elev. (Depth) (ft)	Description (from Summary Boring Logs)	Geotechnical Unit
LT-1	730.7 (50.8)	...EXTREMELY SOFT (R0) micaceous sand zone at 46.0 to 47.0 feet ...Basalt dike at 50.0 to 50.8 feet with clay film	Rock 2'
LT-2	734.8 (32.8)	...sheared and crushed zones 28.8 to 29.2, and 30.9 to 31.3, and 32.2 to 32.8 feet; slickensides on 60° fracture (90° rake) at 31.3 feet, and 30° fracture (20° rake) at 32.2 feet	Rock 2'
LT-3	685.8 (52.9)	... EXTREMELY SOFT (R0), sheared and crushed zone with micaceous sand 42.5 to 52.9 feet	Rock 3'
LT-4	350.5 (66.1)	… very highly fractured and sheared, EXTREMELY SOFT (R0) micaceous zone from 63.5 to 66.1	Rock 2'
LT-5	454.1 (26.7)	... sand- to gravel-sized rock fragments 26.3 to 26.8 feet	Colluvium 3
LT-6	870 (7.5)	DENSE to VERY DENSE, dark gray, silty, sand to gravel-sized ROCK FRAGMENTS; micaceous, moist	Colluvium 1
LT-7	824.6 (33.5)	... EXTREMLY SOFT (R0), highly weathered, micaceous zone from 30.1 to 30.9 feet ...very highly fractured zone from 33.1 to 33.5 feet	Rock 3'
LT-8	906.6 (35.2)	… EXTREMELY SOFT (R0), very highly fractured and sheared zone with up to 1/2-inch sandy clay infilling from 33.5 to 35.2 feet	Rock 2'
LT-9	638.5 (74.0)	EXTREMELY SOFT to VERY SOFT (R0-R1), gray, pervasively sheared and diced with zones reduced to sandy clay, ULTRAMAFIC ROCK	Rock 2'
LT-10	218.2 (71.8)	VERY SOFT to SOFT (R1-R2), green-gray, highly to moderately weathered, ULTRAMAFIC ROCK; very highly to highly fractured, pervasively sheared (EXTREMELY SOFT (R0)), numerous slickensides	Rock 2'
LT-11	80.0 (25.8)	DENSE, gray, gravel- to cobble-sized ROCK FRAGMENTS; silty sand infilling, subrounded rock fragments (DELTA DEPOSITS/TILL?)	Colluvium 4
LT-12	100.6 (12.5)	MEDIUM DENSE, gray to brown, slightly silty, sand- to gravel-sized ROCK FRAGMENTS; micaceous (LANDSLIDE DEBRIS) ... becomes VERY DENSE below 10.0 feet	Colluvium 4

3.5 Geologic Cross Sections

Representative cross sections were developed to characterize the landslide, two areas east of the landslide and one area west of the landslide. Interpretation of the geologic materials in the subsurface of the AOC is provided in the following series of cross sections:

- Figure 16: Interpreted 2014 Section 1 (landslide area)
- Figure 17: Interpreted 2020 Section 1 (landslide area)
- Figure 18: Interpreted 2014 Section 1A (landslide area)
- Figure 19: Interpreted 2020 Section 1A (landslide area)
- Figure 20: Interpreted 2014 & 2020 Section 2 (east of the landslide)
- Figure 21: Interpreted 2014 & 2020 Section 3 (east of the landslide)
- Figure 22: Interpreted 2014 & 2020 Section 4 (west of the landslide)

Interpretations are of the materials that comprise the slope and landslide conditions suitable for modeling and stability analysis. The subsurface geology interpretation is based on findings from the reconnaissance and exploratory borings along with geomorphic interpretation of the surface features. All of which are reviewed in the proceeding paragraphs.

3.6 Geotechnical Material Units

Geologic materials within the AOC include overburden, colluvium, and rock. While colluvium may be considered overburden, its review and discussion below is separate from overburden due to its contribution of differing geotechnical engineering conditions. Geotechnical material units of colluvium and rock are shown on the interpretive cross sections provided on Figure 16 through Figure 22.

3.6.1 Overburden

The overburden at the site has several distinct units from topsoil to marine/glacial materials. Throughout the project area, these units are relatively thin and other than their geologic occurrence, are not significant factors in the stability modeling. Material descriptions are described below.

3.6.1.1 Topsoil

A layer of topsoil is present at most locations across the site. Generally, the topsoil is on the order of 3 to 5 feet thick. These materials were observed to be very loose to loose, soft, organic, gravely, silty sand to sandy silt with trace clay. There are numerous organics with varying degree of decay and the materials are seasonally moist to wet.

3.6.1.2 Marine Sediment Characteristics

Marine sediments were observed below the topsoil and at locations below colluvial materials. This is especially true at elevations near the Beach Road alignment and grade. Marine sediments were observed to be stiff to very stiff, gray, slightly sandy, slightly clayey to clayey silt. Thickness of these materials varies with observations generally in the range of 5 to 10 feet.

3.6.1.3 Glacial Sediments/Glacial Till

Glacial sediments and till were observed at multiple elevations throughout the project area with some deposits present at higher elevations, such as adjacent to the eastern tension crack. The glacial

sediments and till are generally less than 5 feet thick and consist of medium dense to dense, gray, silty sandy gravel to gravelly, silty sand, trace clay, both with gravel- to boulder-sized rock clasts. Clasts vary in color (dark gray, light gray, brown, red-brown), weathering (fresh to decomposed), angularity (subangular to rounded), and composition (mafics/ultramafics, diorite/felsic).

3.6.2 Colluvium Material Units

Colluvium at the site has been divided into four sub-units depending on depositional environment/mode. The four sub-units are categorized as follows:

- Colluvium 1 – Weathered In-Place Inflated Rock Materials
- Colluvium 2 – Talus Deposits
- Colluvium 3 – Slumped and Flow Deposits
- Colluvium 4 – Debris Flow and Flood Deposits

3.6.2.1 Colluvium 1 (Weathered In-Place Inflated Rock Materials)

Colluvium 1 includes those inflated rock materials that are weathered in-place, which are mechanically fractured rock with characteristics of a soil matrix with rock fragments. The material has remnant rock layering/structure that is visible in exposures or as patterned and stepped ridges on the colluvial ground surface. These materials include the lobate-shaped, deep-seated creep deposits. In general, these materials are medium dense to dense, brown, gray, dark gray and black, mixed micaceous sand, and gravel-, cobble-, and boulder-sized rock clasts. Generally, they are highly weathered to visually fresh rock clasts. The clasts are derived from inflated rock, with cobbles, boulders and blocks in zones that are remnant rock layers. There are scattered zones of micaceous sand/crushed mica-rich rock, which in some instances appear to have experienced plastic rock deformation. There are occasional lens/zones of decomposed and sheared rock of fragments that vary from medium hard to very hard (R3 to R5). These materials are generally moist. Slopes of this material are up to 42°, except slopes may also be gentler where this colluvium occurs as a relatively thin layer overlying rock material.

3.6.2.2 Colluvium 2 & 3 (Talus, Slumped and Flowed Deposits)

These colluvial materials are a result of breakdown of outcropping rock and slumping of accumulations of built-up debris. Colluvium 3 is generally a mobilized lower elevation derivation of Colluvium 2. Characteristic differences between these two materials include: material density, location on the slope (i.e., higher elevation for Colluvium 2 and lower elevation for Colluvium 3), and slope angles (i.e., Colluvium 2 deposited at angle of repose 30-37°, whereas Colluvium 3 accumulates at flatter slope angles 13-20°). Descriptions of these materials are offered below.

- Materials identified as Colluvium 2 were observed to be medium dense to dense, brown to dark gray, gravely, silty sand; numerous organics, micaceous; occasional to numerous cobble-, boulder- and block-sized, subangular to angular rock clasts; moist. Slopes of this material appear to be at an angle of repose, generally 32°.
- Materials identified as Colluvium 3 were observed to be loose to medium dense, brown to gray, silty, gravelly sand to rock fragments in matrix of silty sand. Clasts are gravel-, cobble-, and boulder-sized, subrounded to subangular. There is occasional organics and the materials are seasonally moist to wet. Slopes of this material are formed by debris flow fans and

slumps. They are at an angle of repose commonly at gentler angles measured from 25° and down to 15° and 13° degrees (14° is 4H:1V).

3.6.2.3 Colluvium 4 (Debris Flow and Flood Deposits)

Colluvium 4 includes those deposits that resulted from debris flow (liquefied) materials and from flooding events associated with local drainages. These materials were observed to be loose to medium dense, gravelly sand, with gravel- to cobble-sized, rounded to subangular rock clasts with occasional organics. They are seasonally moist to wet. Slopes of this material, generally near Beach Road, measure at an overall 11° (5H:1V).

3.6.3 Rock Material Units

The rock at the site has been divided into three units: Rock 1, Rock 2, and Rock 3 with transition materials between Rock 1 and Rock 2, and between Rock 1 and Rock 3. Rock 1 consists of the 'lower' rock materials below potential slip surfaces at depths on the order of 40 to 50 feet below ground surface. Rock 1 was observed in the subsurface explorations to be less fractured and less weathered. The Rock 2 and Rock 3 materials are generally in the 'upper' 5 to 50 feet of the subsurface. Rock 2 and Rock 3 materials were observed in the subsurface explorations to be more highly fractured and have a higher degree of weathering. Transition materials at the interfaces of Rock 1 & Rock 2, and Rock 1 & Rock 3, are identified as Rock 2' and Rock 3', respectively. Detailed descriptions of the geotechnical rock units and associated strength parameters are offered below.

3.6.3.1 Rock 1 (Low Stress-Relief, In-Place, Un-Inflated)

Rock 1 is the 'lower' stratigraphic rock unit that is generally competent, in-place rock. It was observed to be hard to very hard (R4 to R5), dark gray to black, slightly weathered to visually fresh rock. It is highly to moderately fractured and occasional very highly fractured and micaceous faulted/sheared rock zones.

3.6.3.2 Rock 2 (Moderate to High Stress-Relief, Inflated)

Rock 2 was observed to be hard to very hard (R4 to R5), dark gray to black, moderately to slightly weathered with local visually fresh rock. Rock 2 is very highly to highly fractured with rock fragments from gravel- to block-sized. It contains macro voids/porosity due to mechanical weathering, occasional lens/zones of micaceous sand, and decomposed sheared rock. Slopes underlain by Rock 2 are generally 45° and steeper with local slopes up to 65°.

3.6.3.3 Transition Material Rock 2'

This unit was observed in several subsurface explorations where Rock 2 overlies Rock 1. It was generally extremely soft to soft (R0 to R2), dark gray to black, moderately to slightly weathered rock that is highly to very highly fractured, sheared and crushed. This transition material is a discontinuous crushed zone that often contains voids and macro porosity between gravel-to cobble-sized rock fragments.

3.6.3.4 Rock 3 (Moderate to High Stress-Relief, Inflated and Displaced)

Rock 3 is generally the same as Rock 2; however, geomorphic interpretations indicate this material has experienced displacement due to colluvial processes dilating and shifting the rock downslope. Slopes of this material are generally between the angle of repose and in-place rock, generally up to 42°, but locally up to 65°.

3.6.3.5 Transition Material Rock 3'

This material is similar to the transition between Rock 2 and Rock 1, and was encountered where Rock 3 overlies Rock 1. The main difference from Rock 2' is the Rock 3' is generally extremely soft to very soft rock (R0 to R1), and with lesser gravel- to block-sized rock fragments. It is interpreted as a potential shear surface for movement that occurred in December 2020 in the landslide area.

3.7 Hydrogeology Assessment

Hydrogeology of the landslide and AOC includes assessment of surface water and groundwater pressure data from the piezometer monitoring.

3.7.1 Surface Water

Surface water includes groundwater springs, seasonally intermittent creeks, and a ponded water area. Short reaches of the intermittent creeks may be perennial. Approximately 600 feet south and 70 feet higher in elevation than the landslide headscarp is a pond and wetland area that likely originated as a glacial scour. Currently it is largely infilled in with organic materials and likely sediment, but it still retains surface water during seasonal periods.

Surface water in the immediate area of the landslide headscarp is the creek that flows from the pond. The creek follows a rectangular path over the 600-foot distance, and it makes at least six right angle turns as it zigzags toward and then flows over the headscarp. In addition, the overall path of the creek flows toward azimuth 345°, oblique to the overall slope direction of 020° azimuth. Based on rock exposures along the creek, the rectangular path is controlled by the rock structure.

Two other locations of surface water were observed generally near the elevation of the landslide's headscarp during the spring reconnaissance. One groundwater spring was observed at approximate elevation 865 feet over 700 feet east of the landslide area. The other groundwater spring was at elevation 620 feet approximately 300 feet west of the landslide area. Both these springs feed creeks that flow downslope but do not enter the 2020 landslide area.

Groundwater springs mapped within the slide area are shown on Figure 10. The mapped springs include: two on the west side of the boulder field at elevations 465 and 625 feet, two near the toe of the boulder field at elevations 345 and 425 feet, one in a drainage west of the slide at elevation 475 feet, one to the east of the boulder field at elevation 405 feet, and two in the east side of the lower debris flow where it crosses the Mt. Riley mid-slope benches near elevation 270 feet. Springs within the slide area flowed downslope and remained within the slide area.

Other springs were observed on the Mt. Riley mid-slope bench, both east and west of the landslide. Springs on the bench flowed across the bench and downslope, and did not flow into the landslide area.

3.7.2 Groundwater

Groundwater pressure monitoring is performed at each boring with two piezometer installations per boring. Each borehole was installed with an upper, shallow piezometer, and a lower, deep piezometer. The piezometer sensors were installed in fractured rock. The shallow piezometers were installed at the transition zone between Rock 1 and the upper Rock 2 and Rock 3 units, or shortly below those depths. The deep piezometer tips were installed generally 20 to 40 feet deeper than the shallow tips. The

vibrating wire piezometer tips monitor groundwater pressure if they are installed within saturated groundwater conditions. Some of the piezometers are installed in dry conditions outside of a saturated zone, and appear to be monitoring atmospheric pressure.

Three general types of groundwater pressure response to precipitation are being measured with the piezometers: relatively fast, relatively slow, and no response or dry. Fast responders start to rise generally within 1 day of precipitation onset or snowmelt, depending on local conditions. Slow responders tend to start to rise within 2 to 3 days or longer.

- Eight (8) piezometers in four (4) of the borings have relatively fast groundwater pressure responses (LT-2, LT-3, LT-8 and LT-9).
- Six (6) piezometers appear to be dry or record very small pressures that appear coincident with barometric pressure. These include both piezometers in borings LT-1 and LT-5, and the shallow piezometers in borings LT-6 and LT-7. These instruments have potential to record pressures if groundwater levels rise is above the sensor tips.
- Ten (10) piezometers have relatively slow responses to precipitation. These include eight (8) sensors in borings LT-4, LT-10, LT-11 and LT-12, and the deep piezometers in borings LT-6 and LT-7.

Shallow piezometers tend to respond shortly before the response in the deep piezometers. Two of the deep piezometers, while responding after the shallow piezometers, experienced groundwater pressure increases that were faster (i.e., a higher rate) than their companion shallow piezometers. This appears to indicate that at least two of the deeper aquifers have higher conductivity than the shallower depths.

Data indicates that groundwater aquifers are influenced by fracture flow with varying conductivity. Overall, shallow fractures generally appear to be highly conductive. Deep fracture aquifers within in-place rock (Rock 1) have variable conductivity as compared to the shallow aquifers. Higher conductivity is indicated by the high rate of response in the piezometers, whereas lower conductivity is indicated by the dry/atmospheric piezometer measurements.

In addition, artesian groundwater pressure conditions are likely in Colluvium 3 and 4 due to the higher content of fine-grained soils (i.e., silts and clays) resulting in lower hydraulic conductivity. Artesian groundwater was encountered low on the slope at LT-12. Other areas of upward artesian groundwater flow are also likely, again in the Colluvium 3 and 4 materials. It is estimated the Rock 1, 2, and 3 materials along with Colluvium 1 and 2 are sufficiently free-draining to prevent artesian pressure buildup.

3.7.3 Discussion

Precipitation and snowmelt infiltrate the ground surface, which seeps vertically down through the vadose zone in colluvium, inflated rock, and fractured rock. When it encounters a static/transient water level/saturated zone, it would then flows down a hydraulic gradient seepage path.

Aquifers are anticipated to be locally perched, such as in the colluvium overlying weathered rock, and perched or confined within fractures that are open to the colluvium and within the deeper rock materials. Based on the rectangular drainage path upslope of the landslide, it is assumed that groundwater has a similar flow pattern through fractured rock aquifers.

Colluvium is interpreted to have lower conductance than the fractured rock aquifers due to development of fine-grained soils. Based on groundwater monitoring, some of the deeper aquifers have higher conductance in fractures than overlying colluvium aquifers.

Based on the locations of springs and surface waters, the groundwater within and underlying the 2020 landslide materials appears highly influenced by the drainage upslope, including the pond area, and fractured rock aquifers in both Rock 1 and Rock 2.

Groundwater pressures that occur within the Rock 2' and Rock 3' transition zones, and the overlying Rock 2 and Rock 3 material units are influencing the landslide and the stability of the north-facing hillside slopes. Therefore, groundwater pressures within these units are considered in stability models.

3.8 Precipitation and Groundwater

Precipitation data and changes in groundwater pressure have been evaluated to assess hydrogeologic response to storm-induced groundwater surges. Seasonal groundwater levels are also a condition that affects slope stability; however, the monitoring period to date is insufficient to evaluate this as a factor.

Groundwater pressures due to storm surge are controlled by the duration, intensity, and frequency of rainfall storms, and well as the hydrologic characteristics of the subsurface materials.

The average storm-related groundwater level across the landslide and the AOC is likely to be dependent on the variable nature of the subsurface materials. Storm event spikes represent a maximum groundwater level at a specific instrument.

Groundwater pressure response to precipitation events was evaluated to estimate the potential response in the event of a 100-year 24-hour rainfall of approximately 10 inches as estimated by Miller (1963). More current methods of estimating rainfall may include new information about climate; however, the Miller (1963) study is recognized and sufficient for our simplified evaluation.

Six 24-hour storms measured at the DGGS Mt. Riley weather station that were evaluated include:

- 1.4 inches 2-Oct-2021
- 1.56 inches 12-Oct-2021
- 0.99 inches 17-Nov-2021
- 2.25 inches 22-Jan-2022
- 0.81 inches 28-Jan-2022
- 1.17 inches 4-Feb-2022

The above listed storms resulted in raised groundwater levels within the landslide materials. Estimates of 100-year storm-induced groundwater surges were performed by measuring the height of individual storm surges and plotting against the amount of rainfall for each individual storm (Figure 23). Trendlines for each instrument are included to estimate potential storm-induced groundwater levels. The overall average trendline for the instruments indicates an approximate 10-foot groundwater pressure surge in the event of a 24-hour 10-inch rainfall. The range for individual instruments is from zero to 44 feet. This extrapolation is a simplification of a complex relationship between rain and groundwater; however, based on our experience, these storm surges are reasonable given the fractured rock and overlying colluvium aquifers.

4 STABILITY ANALYSES

4.1 Stability Analysis Methodology

Stability models used limit equilibrium methods as implemented in the Slope/W computer program, a module of GeoStudio 2021. Slope stability analyses were performed using the Morgenstern-Price method. The slope stability analyses were performed on five geologic cross-sections located along the landslide and the adjacent hillside, designated Sections 1A and 1 through 4 (Figure 16 through Figure 22). The locations of the sections are shown in plan view on Figure 2, Figure 9, and Figure 10. These cross-sections were developed based on borehole/groundwater data from the geotechnical investigation and utilizing lidar-developed site topography (May 2014 and December 2020).

Geologic stratigraphic controls and geomorphology of the site were critical in determining the specified slip surface. Slip surfaces were modeled using specified points though the cross section. Fully-specified surfaces were used since large portions of slip surface positions were interpreted from field investigations and instrumentation readings.

4.2 Material Properties

Based on the data collected from the field investigations, laboratory testing program, and LT's experience with similar soils and rocks, generalized soil and rock properties were developed for the materials encountered by the borings. Colluvial strengths are based on engineering judgment and past experience. Material properties were prescribed Mohr-Coulomb effective stress shear strength relationships using cohesion and angle of internal friction values.

Rock material shear strengths were estimated using Hoek-Brown analysis based on unconfined compressive shear strength test results and observed material conditions along fractures and deformed zones. The rock Mohr-Coulomb relationship was based on the Hoek-Brown failure criterion, which initially estimates strength parameters for the entire rock mass based on properties of the intact rock. Based on the discontinuity characteristics of the rock mass, reduction factors are used to modify the strength estimate of the rock mass (Hoek, 2007; Hoek et al., 2002; Hoek and Brown, 2019). The Hoek-Brown system uses a parameter called the Geologic Strength Index (GSI) to characterize quality of the rock mass. Failure of the idealized rock mass is the result of sliding along random discontinuities or rotation of blocks, with relatively little failure of the intact rock (Hoek and Brown, 2019).

The RocScience software, RSData, was used to determine a normal-shear stress relationship based upon Hoek-Brown classification parameters. Hoek-Brown classification takes the following four parameters into account:

1) Unconfined compressive strength of intact rock, σ_{ci}
2) Geological Strength Index, GSI
3) Intact Rock Parameter, m_i
4) Disturbance Factor, D

Parameters 1 and 3 were determined based on laboratory test results from unconfined compressive strength testing, and X-ray Diffraction testing (and petrographic analyses when available). Parameters 2 and 4 were determined from observations made during field reconnaissance and subsurface explorations. Table 2 contains the material parameter inputs for RSData. A failure-envelope

overburden pressure of 6,000 psf was defined in RSData to take into account the stresses anticipated for estimated shear surfaces.

Table 2: Hoek-Brown Classification of Material Parameters for Rock

Rock Unit	Intact Uniaxial Compressive Strength, σ_{ci} (psi)	Geological Strength Index, GSI	Intact Rock Parameter, m_i	Disturbance Factor, D
Rock 1	8,000	77	25	0
Rock 2	8,000	48	25	0.3
Rock 3	8,000	37	25	0.7
Rock 2'	200	45	25	0
Rock 3'	100	12	25	0

Table 3 provides a summary of the material properties used in the slope models.

Table 3: Summary of Material Properties used in Slope Stability Analysis

Material Units	Description	ϕ (degrees friction)	Cohesion (psf)	Unit Wt (pcf)
Colluvium 4	Debris Flow and Flood Deposits	30	0	130
Colluvium 3	Slumped & Flowed Deposits	32	0	130
Colluvium 2	Talus Deposits	42	0	130
Colluvium 1	Weathered In-Place Rock Materials	42	0	130
Rock 3	Mod-High Stress Relief, Inflated and Displaced Rock	55	3,400	200
Rock 3' & R3 joints	Transition Zone (translational rock block) and joints & scarps in Rock 3	30	500	180
Rock 2	Mod-High Stress Relief, Inflated Rock without displacement	64	6,200	200
Rock 2' & R2 joints	Transition Zone, discontinuous crushed materials (rotated blocks, joints in Rock 2)	42	2,000	180
Rock 1	Un-inflated In-Place Rock	68	32,200	200

The use of undrained strengths was considered in limited applications where sudden loading would cause an immediate offsetting water pressure in low-permeability surface soils, preventing the mobilization of higher effective stress and shear strengths. Colluvium 3 and 4 are materials that have relatively low permeability in comparison to other material units onsite and could develop undrained shear strength during sudden load applications. The equivalent undrained shear strength was estimated

by calculating the cohesive shear strength based on the effective overburden pressure (including the effect of groundwater buoyancy) and tan(ϕ), for ϕ of 30° and 32°, for Colluvium 4 and 3, respectively.

4.3 Groundwater Models

The stability analysis models are affected by groundwater, which causes buoyant pressures and reduces shear resistance. Groundwater levels fluctuate seasonally and in response to storms and snowmelt. Current groundwater levels are interpreted based on piezometers installed last fall after the landslide occurred. Measured groundwater levels vary across the hillside, and the responses to storm events vary among the piezometers, ranging from no response to discernable spikes.

The higher groundwater profile at the time of landslide failure during the December 2, 2020 storm is not known since no piezometers existed onsite at that time. Analyses were performed to estimate the potential increases in groundwater due to storms. Initial groundwater measurements made this winter 2021/22 were evaluated to correlate the effects of several recent storms on groundwater levels and ground movement. Storms that have occurred during the period of instrumentation monitoring were relatively small that included 0.01- to 2.25-inch precipitation events (24-hour), whereas the large storm that occurred in December 2020 was reportedly about 6 to 7 inches (24-hour portion). The 48-hour total precipitation during the December 2020 event may have been close to 10 inches based on reports from nearby weather stations. Snowmelt at that time also contributed to the spike in groundwater level. The recurrence return interval of the December 2020 storm was estimated about 200- to 500-year.

Preliminary projections of potential groundwater spikes to represent larger storms were made based on trends in the initial piezometer data. The initial piezometer data indicate an increase in groundwater of 1 to 3 feet for a 1-inch storm, and an increase in water level of 1 to 9 feet for a 2.25-inch storm, based on 24-hour precipitation records.

Extrapolating piezometer trends, groundwater spikes associated with large storms (such as 100-, 200- and 500-year recurrence intervals), could be made if there were many recorded large storms. Based on the limited data available, it is estimated that the groundwater level could possibly rise 10 feet or more during large storms.

Parametric analyses were performed to model a potential range of groundwater levels that could have contributed to triggering the landslide. The baseline groundwater profile at each cross section was based on piezometers and evidence of seepage close to those sections. Increases in the groundwater level for the parametric analyses were modeled in 5-foot increments up to an increase of 20 feet. In some cases, the modeled increases in groundwater levels plots higher than the ground surface, which would imply artesian conditions. These conditions would be reasonable where surficial soils have low permeability. However, artesian conditions would not likely occur in free-draining materials. The parametric groundwater models were adjusted where the surficial materials are highly permeable to limit the rise to the ground surface.

4.4 Slope Stability Models

The stratigraphy in the interpreted geologic cross sections was used to develop analytical models for the slope stability analyses using the computer program Slope/W. Each of the stratigraphic units were assigned shear strengths based on the estimated material properties (see Table 3). A series of

groundwater profiles were prepared for each cross section to represent potential increases in groundwater during storms. The analysis sections are illustrated on Figure 24 through Figure 32. The interpreted landslide slump extent is designated on Section 1 with the headscarp at elevation 870 feet and the slide toe at elevation 240 feet (on the north side of the Mt. Riley mid-slope benches). The slide flow runout-area downslope of the landslide toe was not included in the stability analyses since it represents discharge of slide debris and does not provide resistance to the translational landslide slump. The interpreted transition zone and potential slip zones were inserted into the stratigraphic model using thin layers. Interpreted headscarps and slide exit toes were also modeled with thin layers. Interpreted and potential headscarps were positioned on an inclination of 65° based on measurements of fractures and joints. Analysis slip surfaces were modeled using specified points positioned within the narrow potential slip zones.

Slope stability analyses calculate relative "driving" and "resisting" forces/moments within the modeled extent of the slope and assumed depths of trial slip surfaces. The stability analyses calculate a Factor of Safety (FS) that essentially is the product of "resisting" forces/moments divided by the "driving" forces/moments. If the "driving" and "resisting" forces/moments are the same (just barely balanced), the resulting FS would be calculated 1.0. If the "driving" forces/moments are smaller than the "resisting" forces/moments, the resulting FS would be calculated greater than 1.0. If the "driving" forces/moments are larger than the "resisting" forces/moments, the resulting FS would be calculated less than 1.0, which represents an unstable creeping/moving slope condition. Technical explanations of the slope stability analysis procedures and FS formulas are presented in Slope/W and various geotechnical manuals and textbooks, including Cornforth (2005).

4.4.1 Back-Analysis (Slump Block Section 1A)

The analyses started with a back-calculation of the existing remnant slump block represented on Cross Section 1A, which utilized 2020 topography. The purpose of the analysis was to calibrate the shear strength along the Rock 3' transition zone and headscarp (east tension crack) where marginal stability exists and the instrumentation measured slight displacements along the transition zone when groundwater spikes occurred due to significant rainfall events. The results of the analysis are presented on Figure 24 and Graph 1. The analyses confirmed that the estimated Rock 3' shear strength derived using the Hoek-Brown method is reasonable, and that the FS temporarily drops below 1.0 when groundwater pressures surge, based on the interpreted model and estimated properties. This drop in FS represents the creep movement that has been observed in the ShapeArray data for the slump block.

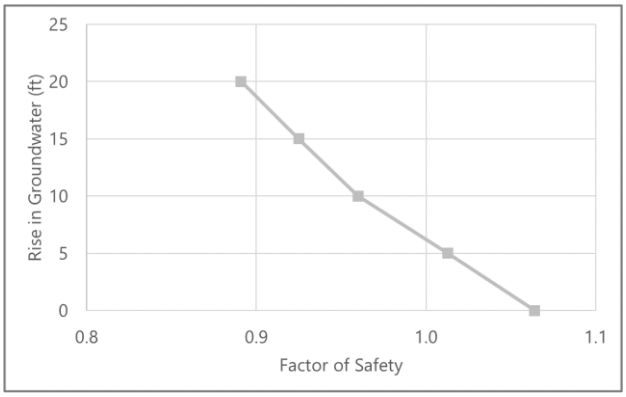

Graph 1: Section 1A – Back Analysis Results

4.4.2 Landslide Analysis (Section 1)

The landslide that occurred December 2, 2020, was modeled in two ways. One approach was to consider the entire translational landslide in a global case. The second approach modeled a lower slide

(Section 1 – Slide 1) followed by an upper slide (Section 1 – Slide 2) representing the documented two slide events that occurred. In the second approach, the lower slide (Section 1 – Slide 1) assumed that groundwater levels increased in the colluvium in the Mt. Riley mid-slope bench and caused liquefaction and/or instability of the slope, which triggered the landslide. As the initial slide occurred, the colluvium slumped and flowed, and its headscarp resulted in a loss of support to the upper rock block (Rock 3), decreasing the FS below 1.0 and causing the upper block to fail and collapse into the colluvium downslope (Section 1 –Slide 2). The global and local landslide analyses are illustrated on Figure 25 through Figure 27 and Graph 2 through Graph 4. The analysis results are plotted graphically, showing the effect of rising groundwater on the Factor of Safety, ultimately leading to failure when the FS dips below 1.0.

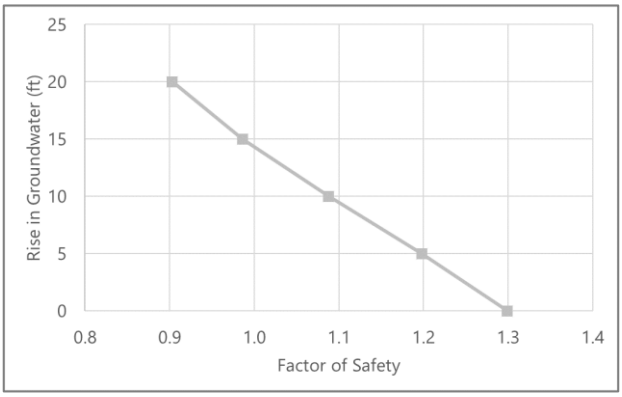

Graph 2: Section 1 – Slide 1 (Pre-Failure) Analysis Results

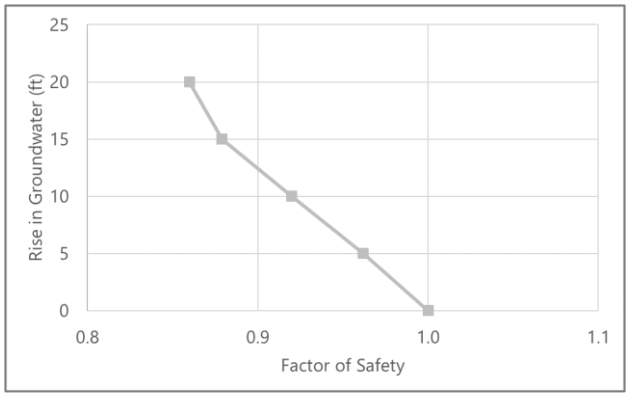

Graph 3: Section 1 – Slide 2 (Pre-Failure) Analysis Results

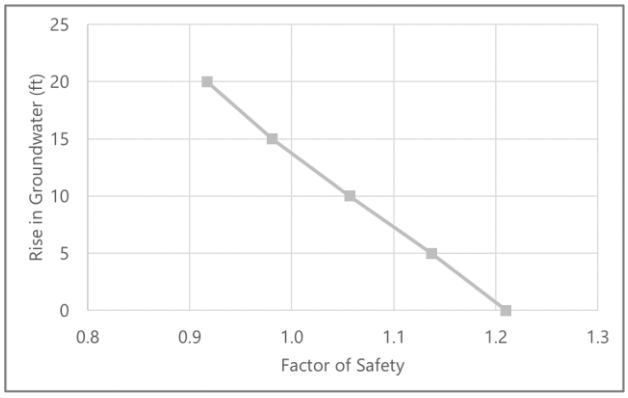

Graph 4: Section 1 – Global Slide (Pre-Failure) Analysis Results

Another series of analyses were performed to model current conditions following the landslide event, and to estimate the stability as seasonal groundwater level or storm-induced spikes occur. Two landslide slip surfaces were modeled. The first slip surface assumes the landslide head is located high on the slope, and the second slip surface assumes the head located just upslope of the Mt. Riley mid-slope bench, as illustrated on Figure 28 and Figure 29. The toe of the slide for both cases was assumed at the same location as the toe of the original landslide case. The stability analyses indicate that the FS is above 1.0 for normal conditions where there is no significant precipitation, and there would be a potential for renewed slide movement when groundwater levels increase due to significant rainfall events. The results of the analyses are presented on Figure 28 and Figure 29, and Graphs 5 and 6 (zero surcharge results).

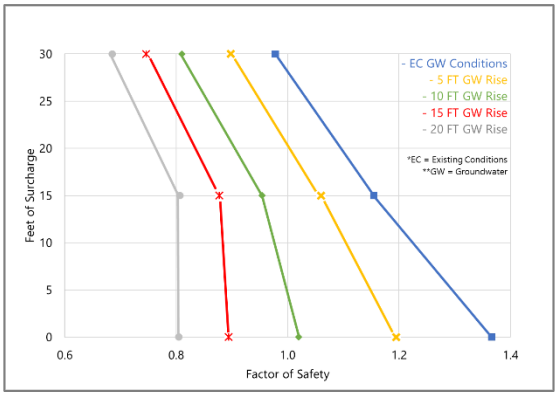

Graph 5: Section 1 – Global Slide Analysis (Post-Failure) Results

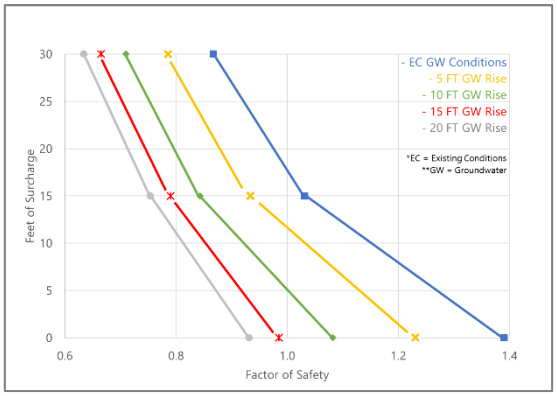

Graph 6: Section 1 – Local Slide Analysis (Post Failure) Results

In addition, analyses were performed to represent the impact and load of materials detaching from the headscarp and collapsing onto the landslide. This includes the possible failure of the eastern slump block in Section 1A and assuming the entire mass fails into and surcharges the colluvium slide debris below. Movement observed in LT-3 and LT-7 along with reconnaissance observations indicate the eastern slump block is creeping towards the slide body (i.e., in a northwest direction).

Two cases of surcharge loading were analyzed. One case assumes the surcharge loading develops high up on the landslide slope. The second case assumes the surcharge loading develops lower on the landslide, near the Mt. Riley mid-slope bench. These two surcharge cases are illustrated on Figure 28 and Figure 29, and results shown on Graphs 5 and 6. Undrained shear strength was modeled for Colluvium 3 due to the sudden surcharge loading, preventing the mobilization of higher effective stress and shear strengths. The stability analyses indicate that the first surcharge case high on the landslide would likely cause the FS to drop below 1.0 causing instability and displacement of the slide debris further downslope. The stability analyses for the second surcharge case lower on the landslide indicates that the FS would be above 1.0 for small amounts of debris collapse during normal conditions where there is no significant precipitation. With large amounts of debris, there is a potential for renewed slide movement during periods when groundwater levels are elevated due to storms.

4.4.3 Hillside Stability Analysis (Sections 2, 3 and 4)

In addition to Section 1 for the landslide area, three cross sections are used to represent hillside slopes within the AOC, designated Sections 2, 3 and 4. The stratigraphy is based on the interpreted geologic cross sections. Groundwater levels vary significantly across the hillside, influenced by localized water sources, material permeabilities, and various fractures, joints and faults. The groundwater profile at each cross section was interpreted based on nearby borings, piezometers, and evidence of surface seepage/springs.

The hillsides adjacent to the landslide exhibit in-place deformation, breakdown, erosion, rockfall, colluvial mass wasting and localized debris flows as described in the Site Geology section of this report. They do not exhibit evidence of prior translational landsliding or deep-seated slumping.

Material properties used in the stability analyses are listed in Table 3. The reasonableness of material properties was evaluated when performing analyses on Sections 1 and 1A. Since the adjacent hillsides do not have discernable landslide shear zones, the use of back-analysis was not possible. Fully-

specified trial slip surfaces were plotted along the transition from Rock 2 to Rock 1, with the interface plotted as a narrow strip designated Rock 2'. The upper and lower ends of trial slip surfaces were optimized by performing parametric analyses to identify locations that produced lower values of FS. Due to the approximations used in the modeling geometry and parameters, the resulting FS values are considered approximate. The trends of decreasing FS with increased groundwater levels are considered reasonable.

Section 2 represents the hillside immediately to the east of the landslide and east slump block (east tension crack), where boring LT-2 was drilled. The analyses show why this area of the hillside did not fail during the December 2020 storm. With groundwater at current baseline levels, the FS would be approximately 1.3. Even if the groundwater level rises 20 feet, the resulting FS would be greater than 1.0, approximately 1.1. The results of the stability analyses are presented on Figure 30 and Graph 7.

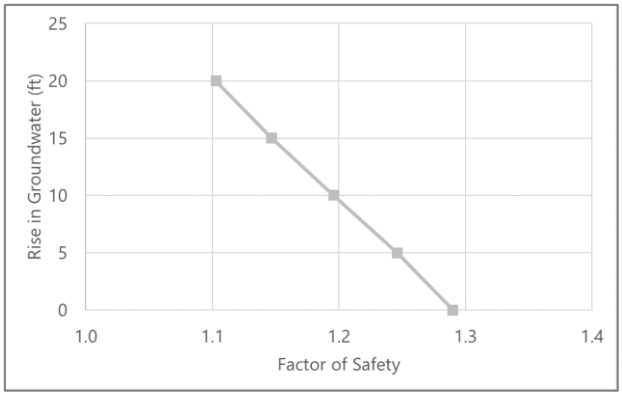

Graph 7: Section 2 Analysis Results

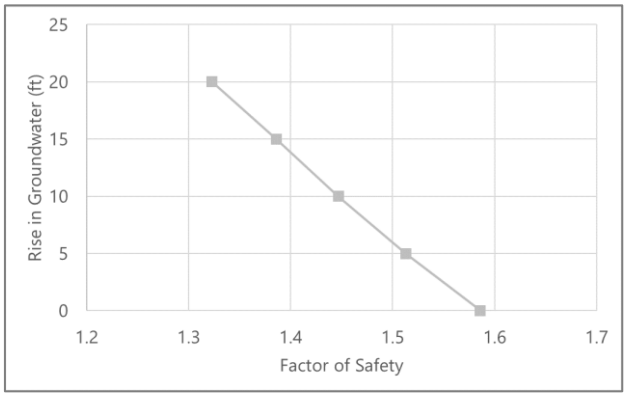

Graph 8: Section 3 Analysis Results

Section 3 represents the hillside in the east portion of the AOC, where boring LT-1 was drilled. The analyses show why this area of the hillside did not fail during the December 2020 storm. With groundwater at current baseline levels, the FS would be approximately 1.5. Even if the groundwater level rises 20 feet, the resulting FS would be greater than 1.0, approximately 1.3. The results of the stability analyses are presented on Figure 31 and Graph 8.

Section 4 represents the hillside in the west portion of the AOC, where borings LT-8, LT-9, and LT-10 were drilled. The analyses show why this area of the hillside did not fail during the December 2020 storm. With groundwater at current baseline levels, the FS would be approximately 1.3. Even if the groundwater level rises 20 feet, the resulting FS would be greater than 1.0, approximately 1.1. The results of the stability analyses are presented on Figure 32 and Graph 9.

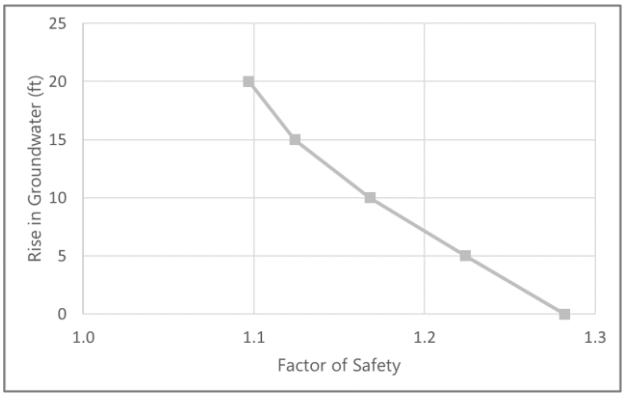

Graph 9: Section 4 Analysis Results

4.5 Seismic Stability Analysis

Seismic stability analyses were performed to evaluate possible reduction in FS due to earthquake shaking. Landslides and steep slopes subjected to earthquake ground motions can destabilize and move as accelerations within the ground cause material to deform. As part of the seismic stability evaluation, a limited review of seismic hazards was performed to understand the contributors to the seismic hazard in the vicinity of the project.

The Haines Borough is located within an active tectonic region of the Pacific Rim. The USGS seismic hazard for Alaska and the quaternary fault and fold database were reviewed to provide information on fault source parameters. The two most prominent fault systems in South Eastern Alaska are the Denali fault system (Chilkat River and Chatham Strait section) and the Fairweather fault system. The Chilkat River Section of the Denali fault is a right-lateral strike-slip fault trending southeast. The closest trace of the fault is located approximately 5 kilometers from the Beach Road Landslide site. The seismic hazard review considered probabilistic seismic hazards developed by USGS as accessed through the USGS Unified Hazard Tool. USGS Deaggregation of the probabilistic seismic hazard indicates the primary contributors to the hazard at the site are the Denali Fault and gridded seismicity, which accounts for earthquakes occurring on unknown faults and background seismicity of the region.

Pseudo-static stability analyses were performed to estimate the FS when the hillside and landslide are subject to seismic events. The USGS probabilistic seismic hazard analysis for a 1,000-year and 500-year uniform hazard peak ground acceleration (PGA) were used for seismic analyses. The 1,000-year seismic design level is similar to the seismic hazard level used to evaluate no-collapse criteria for highway bridges. The 500-year seismic event is intended to represent a more frequently occurring event.

The 1,000-year return PGA is 0.28g and the 500-year is 0.18g for the project site, assuming site class B/C (poor rock/colluvium), based on the USGS seismic hazard mapping. These PGA levels correspond to approximate magnitudes of 6.0 and 5.3 for earthquakes on the Denali Fault at a distance of about 5 kilometers from the site.

Pseudo-static stability analyses utilize a seismic coefficient to estimate earthquake forces impacting the stability of the landslide. Typically, the seismic coefficient is a proportion of the PGA, accounting for the transitory nature of the ground motions and the variability of the motions within different parts of the landslide. Analyses utilized a seismic coefficient, k_h, of 0.5*PGA = 0.14g for the 1,000-year return and 0.09g for the 500-year return. The groundwater pressure profiles used in the seismic analyses assume current conditions without estimated increased due to rainfall events. The results of the pseudo-static stability analyses are shown on Graph 10.

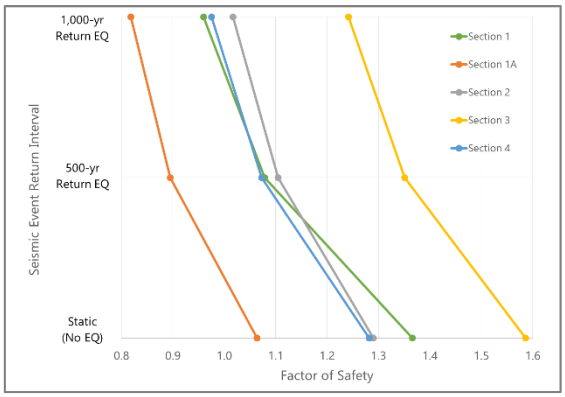

Graph 10: Pseudo-Static Seismic Stability Results

4.6 Stability Analysis Summary

The stability analyses evaluated the level of stability, expressed as Factor of Safety, for several areas on the hillside and the recent catastrophic landslide. Models were developed based on lidar-developed topography that existed prior to the December 2020 storm event and the topography following that event. The stability analysis results (FS values) are approximate due to variations that occur with material properties and groundwater levels, and are reasonable for assessing the relative stability of this area.

In our opinion, the analyses demonstrate the marginally stable and unstable conditions at the landslide, at the time of the December 2020 storm event and for the changed conditions following that storm event. The FS of the landslide would be expected to drop below 1.0 during high groundwater spikes associated with large storms, which would cause ground movement. The east slump block is expected to occasionally experience movements when FS drops below 1.0 during high groundwater spikes associated with large storms. A major storm event may cause portions of the slump block to ravel or cascade into the body of the existing landslide area, causing further displacement of the main landslide mass.

In our opinion, the relative slope stability of the hillsides within the AOC to the west and east of the landslide and slump block indicates sufficient stability even during large storms. This is evidenced by the lack of failure during the major December 2020 rain on snowstorm event, and supported by the stability analysis results.

Earthquakes can also cause geologic hazards, including reduce hillside stability. A large magnitude earthquake could cause stability of the landslide and east slump block to decrease below 1.0, based on the analysis results for a 1000-year return interval seismic event. Landslide displacements and rockfall could occur during such large earthquakes. The adjacent hillside slopes would also experience reductions in stability. Rockfall could occur in the hillsides during such large earthquakes, with a possibility of slope displacements. The seismic stability analyses assumed baseline groundwater levels. If a large earthquake occurs when groundwater levels are spiked due to significant rainfall, the FS could decrease further, with the possibility of increased ground displacements.

5 FLOW SLIDE RUNOUT MODELING

Debris flow modeling and simulations were performed to approximate and evaluate potential flow paths and extents when liquefiable soils become fluid on sloping ground. The modeling was based on the debris flows in the AOC that occurred during the December 2020 storm event and on geologic interpretations. Several computer programs exist for modeling debris flow runout; however, debris flow modeling is relatively new and evolving. Examples of available programs include Terranum Flow-R, United States Army Corps of Engineers HEC-RAS, and Stantec DebrisFlow Predictor. Terranum Flow-R was selected to perform modeling at the Mt. Riley hillside due to its simplicity and, given the results of the investigation, the additional assumptions that would be necessary for the advanced modeling methods. A summary of the Flow-R methodology is provided as background for explaining model behavior, benefits, and limitations. Use of the modeling results is cautioned due to uncertainties involved in the simulation analyses. Flow-R modeling results may be helpful for approximating flow hazards and potential consequences.

5.1 Flow-R Runout Methodology

Terranum Flow-R 2.0.6 (Flow-R) software (https://www.terranum.ch/en/products/flow-r/) was used to model potential extents and flow paths where groundwater and debris might flow following possible future rainfall events where colluvium may become liquefied and unstable (designated as 'source areas' in the modeling method). The source areas are estimated based on evidence of past flow initiation and/or geologic interpretation. The methodology is described in the following subsections.

The benefit of this debris flow modeling approach is its relative simplicity and its ability to approximately simulate possible debris flow extents and flow paths. These analyses may be performed to simulate individual events such as the debris flows associated with the 2020 Beach Road Landslide, or smaller areas like the localized debris flow that occurred west of the landslide upslope of Mt. Riley Road. A known event is needed in similar terrain to calibrate the modeling method. The 2020 Beach Road Landslide and a debris flow that occurred near the Mt. Riley Road cul-de-sac provide two different known events for calibration. The modeling can also be used to simulate potential debris flows based on assumed source areas that are interpreted to contain liquefiable materials and high groundwater pressures (with critical hydraulic gradients).

Limitations of the Flow-R approach include the following:

- Volume of debris flow material is not accounted for, which means that this model does not predict depth of debris, material accumulations, and potential for flowing over blockages.
- Mass is not accounted for, which means that the forces imparted by the debris flow are not analyzed.
- Definition of the travel angle as being from the source location to the termination location is practical for debris flows that propagate from steep terrain to shallow terrain, but may not produce realistic termination in locations where topography varies along the flow path.
- Conditions required to initiate a debris flow are assumed present; however, stability analyses and groundwater monitoring data are critical to understanding if initiation conditions are possible (i.e., presence of liquefiable soils, high groundwater pressures, significant volume of material, etc.).

5.2 Flow-R Parameters

Flow-R modeling produces a spatial distribution of possible flow paths by propagating flow elements downslope from the assumed source locations. Possible extents of a debris flow can be modeled using the exceedance of a threshold value assumed by the software. The spatial distribution of flows is controlled using model parameters. Model parameters are empirical and are dependent on movement type and calibrated to observed data. Two input files are required to perform runout modeling in Flow-R: (1) a Digital Elevation Model (DEM) of the topography for the area of concern; and (2) a raster file containing the source regions. Flow-R modeling uses lateral spreading algorithms and friction laws to model the potential propagation extent and susceptibility.

5.2.1 Lateral Spreading Algorithms

Lateral spreading algorithms control the path (direction of flow) and spreading of the modeled debris flow. Spreading is controlled by flow direction algorithms and a persistence function. Direction algorithms control the propagation of mass movements in the downslope direction based on the slope of adjacent cells. The persistence function aims at reproducing behavior of inertia, and weights the flow direction based on changes in direction with respect to the previous direction. The Holmgren (1994) direction algorithm modified by Horton et al. (2013) was used for runout model calibration and application within the AOC because it has the most extensive flow direction algorithms. The algorithm requires input of model parameters *dh* and *x*, and is influenced by DEM resolution.

The modeling parameter *dh* is an extra height added to the central cell to locally change the slope to adjacent cells. This parameter acts to smooth DEM roughness and to simulate the average height of the propagating debris flow mass. The value of parameter *dh* is estimated from field observations of debris thickness.

Modeling parameter x is a spreading exponent that controls divergence of the flow. Low values of x promote diverging flow ($x = 1$), while high values of x lead to a single flow direction ($x = \infty$). Claessens et al. (2005) suggested assuming a value for parameter x of four (4) for debris flows.

DEM resolution is selected with the objective of balancing detail and computation time. Horton et al. (2013) recommend the use of a 10-meter resolution, but the resolution oversimplified the numerous gullies and ridges within the AOC. A resolution of 16.4 feet (5 meters) was used, as it did not significantly increase computation times and maintained some of the detail of the high-resolution lidar datasets.

5.2.2 Friction Laws

Friction laws determine the runout distance of the modeled debris flow. Friction laws operate on a cell-by-cell level and control which other cells the flow would be able to reach depending on its energy. A Simplified-Friction-Limited Model was used for runout modeling of previous and potential debris flows within the AOC. This model is characterized by a minimum travel angle, represented by the gradient of a line connecting the source area to the most distant point reached by the mass movement. The travel angle is determined by calibration to a previous debris flow event.

5.3 Flow Runout Analyses

Debris flow modeling was performed to evaluate potential flow paths and extents assuming interpreted locations where soils could become fluid on sloping ground. The 2014 pre-slide topography was used for back-analysis of the two debris flows that occurred within the AOC during the December 2020 storms. The December 2020 topography was used for analysis of potential future debris flows, as it is the closest representation of the current topography. Seven interpreted source areas were identified across the hillside where susceptible colluvium and high groundwater conditions are interpreted to simulate debris flow initiation (Figure 33).

5.3.1 Model Parameter Calibration

Flow-R was initially applied to the study area by modeling the December 2020 debris flows to calibrate the values of the spreading parameter, *x*, and the travel angle. Two separate sets of calibrated parameters were obtained by using two debris flows that occurred within the AOC during the December 2020 storms. The calibration debris flows are the runout from the Beach Road Landslide and a small, localized debris flow located upslope of the Mt. Riley Road cul-de-sac, west of the landslide. The localized debris flow upslope of Mt. Riley Road contrasts with the significant runout flow associated with the Beach Road Landslide in size and runout geometry. Calibration was performed using a DEM produced from spring 2014 lidar as a proxy for pre-landslide conditions. A source area for the runout flow associated with the Beach Road Landslide was selected in the colluvium near the landslide toe. A source area for the small, localized debris flow upslope of Mt. Riley Road was selected to correspond with the narrow chute formed at the initiation location.

The calibration process involved performing Flow-R model simulations for both calibration debris flows using various combinations of *x* and travel angle until the resulting susceptibility map appeared to be similar to the actual debris flow extents. Values of *dh* were set to 13.1 feet (4 meters) and 3.3 feet (1 meter) for the Beach Road Landslide runout flows (Model A) and the localized narrow debris flow upslope of Mt. Riley Road (Model B), respectively. These are based on measured heights of debris determined by comparing the DEM ground surface topography in the 2014 and December 2020 lidar terrain models. Calibrated values of the Flow-R parameters are provided in Table 4. Calibration Flow-R maps are provided for the Beach Road Landslide runout flow in Figure 34 and for the localized debris flow upslope of Mt. Riley Road in Figure 35.

Table 4: Summary of Calibrated Flow-R Model Parameters

Model Parameter	Beach Road Landslide runout flow (Model A)	Debris flow near Mt. Riley Road (Model B)
X	12	32
Dh	13.1 feet (4 meters)	3.3 feet (1 meter)
Travel Angle	13°	27°
DEM Resolution	16.4 feet (5 meters)	16.4 feet (5 meters)

5.3.2 Modeling Potential Future Debris Flow Extents

Calibrated Flow-R parameters for Model A and Model B were used to evaluate potential flow paths from assumed flow source areas within the AOC. Recall that Model A parameters were calibrated from the significant landslide flow runout that reached the shoreline, whereas Model B parameters were calibrated from a small localized debris flow that did not reach Mt. Riley Road. Therefore, flow runout simulations using Model A calibrated parameters will appear more extensive than those estimated using Model B calibrated parameters and flow simulations.

Results for each of the flow simulations for the individual assumed source areas, applying both Model A and Model B calibrated parameters, are provided in Appendix C. Flow simulations using Model A calibrated parameters tended to estimate runout paths that would spread and flow towards the shoreline, while flow simulations using Model B calibrated parameters tended to estimate narrow paths that generally would stop on or near the Mt. Riley mid-slope bench.

Flow simulations were also performed to evaluate the combined effect of assumed Source Areas 1 to 3 located west of the landslide. Flow simulations using Model A calibrated parameters produce estimated runout paths that may flow down to the Mt. Riley mid-slope bench before converging and flowing down toward Beach Road (Figure 36). At Beach Road, the paths may spread out before flowing to the shoreline. The topography of Beach Road appears to influence possible flow spreading to the west. In comparison, flow simulations using Model B calibrated parameters produce estimated runout paths that could flow to the Mt. Riley mid-slope bench and stop (Figure 37). This is similar to the extent of the small localized debris flow that occurred during December 2020 west of the landslide.

Flow simulations for potential flow Source Area 4 (landslide toe), using Model A calibrated parameters, shows similar flow paths and extents (Figure 38) as occurred in December 2020. Simulated flows using Model B calibrated parameters for potential flow Source Area 4 do not appear realistic, and are not included.

Flow simulations were performed to evaluate the combined effect of assumed Source Areas 5 to 7 located east of the landslide within the AOC. Flow simulations using Model A calibrated parameters produce estimated runout paths that may flow down to the Mt. Riley mid-slope bench, where they may spread out and move downslope through several channels, mostly in bedrock (Figure 39). A less likely path may flow west from assumed flow source 5 into the scoured area of the Beach Road Landslide, which appears to be due to the effect of combining flows from assumed Source Areas 6 and 7. All other modeled paths could flow downslope across the existing debris fan deposits in the east area of the AOC before flowing to the shoreline. In comparison, flow simulations using Model B calibrated parameters produce estimated runout paths that generally could flow to the Mt. Riley mid-slope bench and stop (Figure 40). One possible modeled path appears it could descend 200 feet further along the prominent channel below assumed Source Area 7 before stopping on the upper reaches of the fan deposits.

5.4 Flow Runout Summary

Debris flows have occurred on the Mt. Riley hillside, and future debris flows would be reasonable to expect as an ongoing geologic hazard. The modeled potential flow extents and paths, where debris

may mobilize from assumed areas of liquefiable/marginally stable colluvium, are based on evidence of past flow initiation and/or geologic interpretation.

The modeled debris flows (using two unique model parameter calibrations in the Flow-R analyses) indicates there is a broad range of possible flow paths and extents. This conclusion is consistent with features on the hillside terrain that are indicative of prior debris flows ranging from small to large. The occurrence, location, and extent of future debris flows is difficult to forecast, and these model simulations illustrate a range of possible flows that may occur in the future.

6 GEOTECHNICAL INTERPRETATIONS AND OPINIONS

Evaluations of potential scenarios as presented in the *Winter Reconnaissance – Preliminary Findings Report*, and *Spring Surface Reconnaissance Memo* have been revisited below along with inclusion of additional scenarios that were not previously discussed. This updated assessment is qualitative and based on the culmination of geotechnical work and analyses that have been completed at the site and summarized in the preceding report sections. The work and analyses include geotechnical investigations, geologic interpretations, stability analyses, debris flow runout analyses, and qualitative risk assessments. The assessments describe the estimated likelihood of occurrence, relative level of potential consequences, and relative risk based on engineering judgment. These assessments were then plotted on a risk informed decision matrix, as described below.

6.1 Risk Informed Decision Matrix

There are many geologic hazards present in the AOC as discussed in some detail in this section. Each of the hazards has a likelihood of occurrence and a consequence if it does occur. Methodology for geotechnical probabilistic evaluations is based on publications by Silva, Lambe & Marr (2008), Genevois & Romeo (2003), and Duncan & Wright (2014). The methodology applies quantification of expert judgment as a practical alternative for determining probability of geologic hazard conditions to arrive at rational management and engineering decisions. The likelihood and consequence comprise the risk associated with the hazard. They can be plotted in a matrix format to provide a visual understanding of higher risk and lower risk hazards and to compare hazards in a relative sense. This can be done qualitatively or quantitatively. For the work here a qualitative approach was taken. The likelihood of occurrence is based on the assessment of the potential for failure scenarios (i.e., landslides, debris flows, rockfalls, etc.) to reach the lower slope areas where public activities may occur, developed property is present, or infrastructure exists. The likelihood was informed by the quantitative analyses presented in prior sections and other considerations, as described. The consequence is assessed in two separate ways – public safety and infrastructure damage that might be costly and disruptive, but not specifically tie to public safety.

A chart was developed that compares "Likelihood of Occurrence" with "Consequence or Impact" for the identified scenarios. The likelihood of occurrence is described as either: very low, low, moderate, or high. The consequence or impact is a qualitative estimate of the resulting public safety/injury and/or cost/impact to infrastructure, and is described as either: very low, low, moderate, or high.

The estimation of "Likelihood of Occurrence" and "Consequence or Impact" for the identified scenarios presented below was based on evaluations addressing many aspects of the slope/landslide and contributing factors, including the following:

- Landslide movement amount and rate
- Results of quantitative analyses reported herein, and the assumptions embodied in them
- Seasonal movement trends
- Potential for rapid movement impacting the Beach Road area (impact to infrastructure, potential for injury)
- Hazard type

- Subsurface conditions and geometry
- Groundwater influence
- Geologic uncertainties

The various aspects were qualitatively evaluated to interpret relative levels of "Likelihood of Occurrence" and "Consequence or Impact". The results were then plotted onto the risk informed decision matrix chart as provided on Figure 41.

6.2 Updated Evaluation of Geologic Hazards

6.2.1 Catastrophic Reactivation of 2020 Landslide Debris (extreme weather)

This scenario assumes a sudden release of fluid slide debris from the headscarp area, similar to the historic December 2, 2020 event. The released materials would flow all the way downslope to the road and into the ocean. This catastrophic scenario is thought to need a trigger mechanism similar to the precipitation/weather event (200+ year recurrence interval) that occurred leading up to the December 2, 2020 event. The size of this failure scenario would most likely be less than half of original mass of the recent landslide due to the fact that less mass, or volume of material to fail, is available due to the previous failure event. There appears to have been three major contributors to triggering movement in the landslide area: i) large accumulation of colluvial materials, ii) larger hydrologic basin (i.e., surface water drainage area), and iii) high groundwater pressures assumed to have occurred at the toe of the large colluvial deposit. Other factors that could influence this failure scenario include:

- Size and geometry of remnant slide mass.
- Strength and moisture content of remnant slide debris.
- Effect of groundwater and surface water infiltration on remnant slide mass.
- Slope of ground surface along potential travel path includes a midslope bedrock area with gentle grades.
- Weather (extreme/sustained precipitation, snowpack/melt).
- Large, angular blocks add strength and roughness to the slide debris in drained condition. Numerous trees and woody debris also add short-term strength.

The landslide body has significantly less volume of unconsolidated materials, slope angles are flatter than those adjacent to the slide and that were present pre-slide, and it appears the materials have a higher propensity to be free draining (i.e., buildup of pore pressures may be less prevalent). However, stability analyses indicate that under high groundwater pressure conditions the remaining colluvial mass and recently accumulated landslide debris can become unstable (see modeling of current conditions subjected to increased groundwater pressures in Section 4.4.2, including Graphs 5 and 6). The question then is what is the runout potential of mobilized material. Flow runout analyses show that the likelihood of mobilized material flowing along a similar path to what occurred in December 2020 is high (see Section 5.4 and Figure 38). However, the actual runout would be contingent on the volume of material mobilized, which is a significantly smaller volume due to the December 2020 failure.

In general, the likelihood of occurrence for this catastrophic scenario would be very low. Catastrophic reactivation would require a similar extreme weather event that would cause groundwater pressures

to trigger mobilization of remnant slide debris. As stated above, the slide has less unconsolidated material available, slopes are generally flatter, and materials appear to be more free draining.

Consequences of this catastrophic scenario are variable. There would be low to high consequence should the public be traveling on the road at the time of a reactivation. This could correlate to a low to moderate risk to public safety. Residents in homes bordering the landslide would have a moderate to high risk to public safety. There would be high consequence of damaging utilities and other infrastructure along Beach Road. Since these are permanent structures this would correlate to a moderate risk to infrastructure.

6.2.2 Localized Reactivation of 2020 Landslide Debris (normal weather)

This scenario assumes the areas of remnant/deposited slide debris become saturated causing movement. Some debris would slough and lobes would flow downslope. This scenario assumes normal precipitation weather events. It is anticipated that the slide mass in this scenario would not travel as far down the slope due to the lack of water and saturated conditions that are necessary to cause a severe liquefying event. Other factors that could influence this failure scenario include:

- Size and geometry of remnant slide mass is less than half of the original mass.
- Strength and moisture content of remnant slide debris.
- Effect of groundwater and surface water infiltration on remnant slide mass.
- Slope of ground surface along potential travel path includes the Mt. Riley mid-slope bench area with relatively gentle grades.
- Weather (sustained precipitation, snowpack/melt).
- Ground motions and forces associated with significant seismic events.
- Large, angular blocks add strength and roughness to the slide debris in drained condition. Numerous trees and woody debris add short-term strength until they rot.

The likely trigger for the December 2, 2020 event was the high groundwater pressures and surficial water runoff produced as a result of the storm event. This scenario considers normal weather patterns. As shown in our stability modeling based on recent groundwater measurements, normal weather patterns do not destabilize the remnant colluvium and accumulated slide debris (see Section 4.4.2, including Graphs 5 and 6). If remnant slide materials were to mobilize under normal weather/precipitation, the mobilized material likely would not travel as far downslope due to the lack of water and saturated conditions that would be needed to liquefy materials.

The likelihood of this landslide scenario reaching properties and infrastructure under normal weather would be low. The consequences of this scenario would be very low relating to public safety and infrastructure, since the mobilized debris would most likely be contained on the slide body. This scenario would be considered a low risk to public safety and infrastructure.

6.2.3 Boulders within 2020 Landslide Mass Rolling Downslope

This scenario assumes boulders detach from zones of slide debris (due to freeze/thaw, wetting/drying cycles, rainfall, ice-jacking, erosion, tree and woody debris rot, and other environmental factors) and roll or bounce downslope until coming to rest on a flatter slope or against an obstacle. The higher

elevation on the landslide this occurs increases the likelihood one of these boulders can reach the roadway or beyond. Other factors that could influence this failure scenario include:

- Slope of ground surface along potential travel path includes the Mt. Riley mid-slope bench area with relatively gentle grades downslope of the steep upper slope.
- Periods of sustained precipitation, resulting in increased hydrostatic pressures within slide debris.
- Wetting/drying and freezing/thawing cycles.
- Ground motions and forces associated with significant seismic events.
- Large, angular blocks add strength and roughness to the slide debris. Numerous trees and woody debris add short-term strength. Rotting of trees reduces strength and causes subsidence.
- Relatively loose, soft condition of the landslide debris and its long-term consolidation/subsidence.

As stated above, there is a gradation of the remnant slide materials with large dilated rock blocks in the higher elevations, a boulder field in the midslope areas of the landslide, and matrix-supported boulders and cobbles in the lower portions of the slide. Mobilization of the large dilated rock blocks and boulders from the midslope elevations could occur if there is loss of support, due to freeze/thaw processes, wetting/drying cycles, rainfall, ice-jacking, tree and woody debris rot, an increase in groundwater pressures, or several other factors. However, it is our interpretation that these materials would not travel significant distances due to the loose nature of the slide debris slowing down mobilized material (i.e., attenuating mobilized material) and relative shallow slopes that are present upslope of Beach Road. The small surcharge effect of boulders landing onto the remnant landslide mass would result in negligible changes in stability.

The likelihood of this boulder displacement scenario to occur and reach properties and infrastructure would be low. The consequences of this event are interpreted to be very low due to the estimated attenuation of mobilized material resulting in debris remaining on the slide body. This scenario would be considered a low risk.

6.2.4 Retrogression of 2020 Landslide Over-Steepened Scarps

This scenario assumes portions of the landslide headscarp detach, topple or slump, due to a variety of environmental factors, causing a mass of material to slide into the upper rock slump and middle boulder field areas. This process is quite common on over-steepened headscarps following a large failure event. In addition, this scenario assumes that groundwater pressures in and under the slide debris could be elevated. Other factors that could influence this scenario include:

- Retrogression would likely be limited to local areas, reaching equilibrium when the scarp slope angle is reduced to 1:1 or angle of repose. Therefore, volume of material detached during retrogression would be very small compared to volume of December 2 landslide mass.
- Structural and weathering condition of rock at headscarp (lower likelihood if scarp slopes are massive, fresh, competent rock).
- Weather (wetting/drying cycles, sustained precipitation, snowpack/melt, freeze/thaw).

- Ground motions and forces associated with significant seismic events could cause rockfall and displacement of over-steepened slopes such as the headscarp area.
- Erosion.
- Strength and moisture content of remnant slide debris.
- Effect of groundwater on headscarp and remnant slide mass.

Observations of tension cracking on both the east and west sides of the landslide indicate slumping of material from the lateral scarps is occurring. This process will continue to occur until the lateral scarps have reached an equilibrium with the new terrain formed by the landslide. It appears likely that slumped material will generally be localized with minimal effect on the remnant slide materials in the upper rock slump area and lower portions of the slide body. This scenario is a common process of over-steepened headscarps. There are several blocks on the headscarp that are inflated and will likely fall into the headscarp bowl. These appear to be localized and will likely have minimal effect on the remnant slide materials in the headscarp bowl and lower portions of the landslide body.

Materials that may mobilize from the headscarp area would be deposited on the scarp and into the landslide body. Blocks of rock that detach from the headscarp and collapse onto the landslide mass below would add relatively small surcharge loadings onto the slide, resulting in relatively small to imperceptible decreases in slope stability, which would likely not result in significant displacement of the landslide mass. In our opinion, the average deposit of collapsed materials would be less than 5 feet thick. The effect of small deposits of displaced block materials onto the landslide mass on FS can be interpolated from Graphs 5 and 6 in Section 4.4.2. Stability analyses show that additional loading (i.e., surcharging from mobilized material) does not create an unstable (i.e., FS < 1) condition.

This landslide retrogression scenario would have a low likelihood of reaching properties and infrastructure, and with very low consequences. Therefore, this scenario would be considered a low risk.

6.2.5 Slump Bounded by Tension Crack to East and West of 2020 Headscarp

This scenario assumes that the ground between the east tension crack and the headscarp of the landslide develops into a slump and that it slides toward and into the bowl of the headscarp, adding load onto the existing remnant slide debris, possibly causing reactivation of the upper landslide. The direction of sliding is interpreted towards the lateral scarp of the landslide rather than directly downslope based on inclinometer measurements of apparent deep slide block movement. Other factors that could influence this failure scenario include:

- Weather (sustained precipitation, snowpack/melt, and increases in groundwater pressures).
- Springs indicative of high hydraulic gradient of groundwater. Or whether the area is more drained due to tension crack and relief of main landslide sidescarp.
- Size, geometry and volume of slump mass.
- Constraint provided by bedrock downslope.
- Strength of materials.
- Moisture content of slump material.
- Strength and moisture content of remnant slide debris.

- Groundwater conditions within slump and within remnant slide debris.
- Ground motions and forces associated with significant seismic events could cause displacement of the slump and over-steepened slopes such as the headscarp area.

The slumping material to the east and west of the landslide could fail as large volume events. The stability analyses indicate this would require moderate groundwater pressure surges to be present that could cause large portions of the slump blocks to collapse onto the head of the landslide mass below (see Section 4.4.1 and Graph 1 for analysis of the eastern slump block).

Failure of the slump block could result in materials sliding onto the landslide mass below, resulting in a surcharge loading that would increase driving forces and reduce the stability of the landslide. The amount of displaced material is uncertain; however, for modeling purposes, the average thickness of materials potentially deposited onto the landslide mass was conservatively assumed 15 to 30 feet thick. As shown in our stability analyses, large amounts of collapsed slump blocks could cause landslide stability to decrease below FS of 1, particularly during groundwater surges (see Section 4.4.2, Graphs 5 and 6). This decrease in stability would cause displacement of the landslide mass. Flow runouts from the landslide area may be significant if high artesian groundwater conditions exist at the time of the slump collapse and surcharge loading.

This slump block scenario would have a low likelihood of reaching developed properties and infrastructure, with moderate consequences to developed properties and infrastructure, and low consequences to public safety due to limited use of the road in the immediate area of the landslide. This scenario would be considered a moderate risk.

6.2.6 Global Failure of Bedrock Slopes East and West of 2020 Landslide

This scenario evaluates the potential for a large rockslide event occurring within the slopes to the east and west of the 2020 landslide area. Potential trial slip surfaces were interpreted to be at locations where inflated rock materials (i.e., Rock 2) were identified during site reconnaissance and/or in the subsurface explorations. A trial slip surface (i.e., the 'transition' zone) was estimated based on subsurface explorations. Analyses were performed to evaluate the effect of elevated groundwater conditions. Stability analysis results relating to this scenario are provided in Section 4.4.3 and Graphs 7, 8 and 9. Factors that could influence this stability scenario include:

- Steepness/inclination of slopes.
- Weather (precipitation, snowpack/melt, runoff).
- Subsurface conditions (presence of altered/weakened bedrock, bedrock structure/faulting, discontinuity conditions, groundwater).
- Shear strength of bedrock and discontinuities.
- Ground motions and forces associated with significant seismic events could cause rockfall and displacement of over-steepened slopes.

The modes of slope degradation interpreted at the hillsides on the east and west sides of the landslide include a combination of mechanical weathering (creep movements), toppling, buckling, and basal planar mechanisms. Based on available data, the rock materials on the east and west side of the landslide do not show evidence of translational slide movement. There is evidence of relaxation of bedrock blocks due to deglaciation and colluvial development processes that could be interpreted as

mechanical degradation, toppling, buckling, etc. Subsurface explorations indicate there is a 'transition' zone between more highly fractured/moderately to highly weathered materials (i.e., upper rock unit Rock 2) and less fractured/slightly to moderately weathered materials (i.e., lower rock unit Rock 1).

The stability analyses described in Section 4.4.3 indicate stable conditions (FS > 1.0) for current groundwater levels and for storm-related water pressure surges. The analyses assumed the slopes east and west of the slide experienced the same high groundwater pressures as were imparted on the landslide area. However, the eastern and western slopes did not have a catastrophic failure. There also appears to have been three major contributors to triggering movement in the landslide area: i) large accumulation of colluvial materials, ii) larger hydrologic basin (i.e., surface water drainage area), and iii) groundwater pressures assumed to have occurred at the toe of the large colluvial deposit. The slopes east and west of the landslide may have one or two of these contributing factors, but do not appear to have the combination effect of all three.

The likelihood of this bedrock stability scenario to cause slides that reach develop properties and infrastructure would be very low. If failure of this bedrock stability scenario were to occur, there would be moderate to high consequences to public safety and infrastructure. Based on the very low likelihood of occurrence of bedrock slides in these areas and the degree of development near Beach Road, it would be considered a moderate risk. Instrumentation installed east and west of the landslide body could be monitored to further understand slope stability and potential changes. Should movement be detected, these risks could be re-evaluated.

6.2.7 Global Failure of Colluvial Slopes East and West of 2020 Landslide

This scenario assumes a large landslide occurs within overburden materials on relatively steeper slopes (i.e., the colluvial slopes). In this scenario the overburden mantle experiences instability, creep and/or more deep-seated movement. Factors that could influence this failure scenario include:

- Weather (precipitation, snowpack/melt, runoff).
- Subsurface conditions (colluvium mantle thickness/conditions, groundwater).
- Shear strength of colluvium.
- Ground motions and forces associated with significant seismic events could cause rockfall and displacement of colluvial slopes.

The accumulation of colluvial materials east and west of the landslide appears to be less significant (i.e., not as thick) than the lobe deposit that was present in the landslide area pre-slide. Mobilization of the relatively thinner deposits of colluvium could occur, but it is likely any movement would not be on the order of what was experienced in December 2020 without the mass available. Again, the colluvial slopes to the east and west of the landslide were subjected to the same weather event as the 2020 failure area; however, movement did not occur. This includes an area of lobate-shaped colluvium mapped within a drainage on the east side of the AOC, which appears to be an accumulation upslope of the Mt. Riley mid-slope benches.

Colluvial material slopes are typically deposited close to their angle of repose. This implies that the FS of colluvial slopes could be marginally stable (FS of 1.0 to 1.2). Surface water and groundwater can decrease slope stability, typically resulting in raveling, shallow slumps, and debris flows. The impact of debris flows is addressed in the scenario presented in Section 6.2.11.

The likelihood of this colluvium stability scenario to reach developed properties and infrastructure would be low to moderate, based on the degree of artesian pressure increases associated with significant rainfall events. Consequences would be low when artesian groundwater pressures are minimal; however, the consequences could increase to high during significant rainfall events and associated surges in artesian groundwater pressures causing greater slope failures. This scenario is considered a moderate to high risk event (especially in the east area of the AOC). As stated above, the installed instrumentation could inform changes to slope conditions and re-evaluation of risk associated with this scenario.

6.2.8 Weathering/Erosion of Bedrock/Colluvial Slopes East and West of 2020 Landslide

This scenario considers environmental processes that are common to the area, resulting in erosion, sloughing, creep, rockfall, and accumulation of colluvium. This scenario currently exists throughout much of the Haines area where moderate to steep slopes are present. Factors that influence this hazard scenario include:

- Weather (wetting/drying, freeze/thaw, snowpack/melt, wind, runoff).
- Subsurface conditions (bedrock, colluvium mantle, groundwater).
- Steepness of slopes.
- Ground motions and forces associated with significant seismic events.
- Shear strength of colluvium (angle of repose).

Development of colluvium due to weathering and erosional processes will continue at the site until the slopes are flattened and at equilibrium. This is common through southeast Alaska and could be considered the baseline hazard for mountainous terrain.

This slope weathering scenario would have a low likelihood of reaching developed properties and infrastructure. Colluvial creep and movement is likely to be contained on the Mt. Riley mid-slope benches. As a result, the consequences of this type of slope movement would be low. The associated risk would be considered low.

6.2.9 Seismically Triggered Slope Movements

This scenario considers earthquake related events and their effects on slope stability. Southeast Alaska is an active seismic zone that has produced high (i.e., magnitude 6 and higher) earthquakes. Periodic earthquakes will likely occur in the region. Triggering of landslides has occurred and can occur at this site. Factors that affect the potential for geologic hazard conditions when subjected to seismic motions include:

- Ground motions, forces and directions associated with significant seismic events (earthquake magnitude, proximity, and ground motion attenuation and/or amplifications).
- Subsurface conditions (bedrock, colluvium mantle, groundwater).
- Weathered and fractured condition of rock materials.
- Steepness of soil and rock slopes.
- Shear strengths of materials.

Based on pseudo-static stability analyses a 1,000-year and a 500-year return period earthquake could decrease the stability of slopes within the AOC (see Section 4.5 and Graph 10). This could trigger slope displacements, raveling materials, rockfall, slides, and debris runouts.

Large earthquakes (i.e., magnitude 6 and higher) in southeast Alaska would have a low to moderate likelihood of occurrence, with an estimated moderate to high consequence. More common earthquakes (i.e., approximate magnitude 5 and lower) would have a moderate to high likelihood of occurrence, with a low to moderate consequence.

Consequences of earthquake-induced slope failures and runout could include: impact to traveling public, impact to residential structures, and impacts to utilities. These are all high consequence incidences. This seismic hazard scenario would generally be considered a high risk.

6.2.10 Rockfall from Lateral Scarps

This scenario assumes that rockfall occurs in the over-steepened lateral scarp of the landslide. Rock would detach, topple or slump due to a variety of environmental factors, causing material to fall or slide into the bowl of the headscarp and load the existing slide remnant. Other factors that could influence this scenario include:

- Rockfall would likely be limited to local areas, reaching equilibrium when the scarp slope angle is reduced to 1:1 or angle of repose. Therefore, volume of material detached during retrogression would be relatively small.
- Structural and weathering condition of rock at lateral scarp.
- Weather (wetting/drying cycles, sustained precipitation, snowpack/melt, freeze/thaw).
- Ground motions and forces associated with significant seismic events could cause rockfall and displacement of over-steepened slopes such as the lateral scarp area.
- Erosion (root wedging, tree jacking).
- Strength and moisture content of remnant slide debris.
- Effect of groundwater on remnant slide mass.

The lateral scarps of the 2020 slide have exposed rock with some blocks on the order of 10 to 15 feet in maximum dimension. These rocks will likely become dislodged with time due to the inflated nature of the material and the continued erosional and environmental processes that will occur on the slope. Rock debris in the slide, specifically the middle boulder field, include blocks on the order of 10 to 20 feet in maximum dimension. These boulder materials will likely attenuate (i.e., slow down and stop) rockfall that may generate from the lateral scarps. Should rockfall debris have sufficient energy to mobilize past the middle boulder field, it is estimated the loose (i.e., soft) nature of the lower debris flow materials would further slow and stop dislodged rock blocks.

This rockfall scenario would have a very low likelihood to reach developed properties and infrastructure. This scenario would have a very low consequence due to the likely attenuation from the middle boulder field and lower debris flow materials. The risk of this scenario would be considered low.

6.2.11 Debris Flow Runouts

This scenario is based on the potential for a range of fluid flows due to liquefied conditions, likely originating on or slightly upslope of the Mt. Riley (mid-slope) benches. Fluid runout flows and debris flows may occur due to artesian groundwater pressures as a result of significant rainfall events that cause colluvial soils to liquefy. The ground geomorphology indicates that debris flows have occurred throughout the hillside where colluvium deposits and groundwater seepage (springs) exist, resulting in the formation of debris fan deposits. Flow runout modeling and simulations described in Section 5 indicates a potential range of flow runout paths and extents for small and large flow events. Factors that could influence this flow runout scenario include:

- Weather (rainfall, snowpack/melt, runoff).
- Artesian groundwater pressures and groundwater recharge potential.
- Steepness of slopes.
- Drainage paths.
- Liquefiable colluvium thickness and extent.

Mobilization of debris flows that originate from within the landslide debris is discussed separately in the scenario of a catastrophic reactivation of the 2020 landslide debris in Section 6.2.1.

Debris flows could occur as evidenced by the small debris flow slide west of the main landslide. These may have similar runout characteristics and flow path/extents as was observed during the 2020 storm event. However, based on runout modeling simulations presented in Section 5.4 and Appendix C, depending on colluvium extent/depths and artesian groundwater pressures, there is a possibility that greater amounts of flow may occur. Potentially larger flows may result in longer and wider flow paths potentially reaching the Beach Road area. These simulations are rough approximations to identify a range of potential hazards.

For hillside areas within the AOC, but outside the landslide, the interpreted likelihood of reaching developed properties and infrastructure for a small flow runout would be very low to low, and the interpreted likelihood for a large runout would be very low. The potential consequence to public safety and infrastructure (i.e., road, properties, and other infrastructure) for a small flow runout that does not reach developed areas would be low. Whereas the potential consequence for a large flow runout that extends to developed areas could be moderate to high.

In our opinion, the relative risk for flow runouts in hillside areas on either side of the landslide would be considered low to high, depending on the severity and extent of the flows. There is uncertainty in making these assessments due to the uncertainty in the modeled larger debris flow extents, as based on the limited available data.

7 CONCLUSIONS, MITIGATION CONCEPTS AND RECOMMENDATIONS

The following conclusions, mitigation concepts and recommendations are based on the work completed, monitoring data available, and geotechnical interpretations & opinions

7.1 Conclusions

The catastrophic 2020 landslide occurred due to a combination of factors in this localized section of the Mt. Riley hillside, including: upper zone of displaced fractured weathered bedrock (Rock 3: tilted, deformed, crushed, inflated), concentrated surface water, 'thick' accumulation of liquefiable fine-grained colluvium, strong groundwater recharge, and artesian groundwater.

The small debris flow slide located west of the 2020 landslide occurred due to a few factors, including: concentrated artesian groundwater surge in a narrow swale of shallow colluvium bounded by bedrock. This did not result in a catastrophic slide since the Rock 2 unit appears more competent (i.e., less weathered/fractured/deformed) than the Rock 3 unit in the landslide area.

Elsewhere within the AOC, the slopes may have experienced erosion, particularly in swales and drainages, but did not experience landslides or liquefied flows. The bedrock appears more competent (i.e., less weathered/fractured/deformed) than in the landslide area, the mid-slope colluvium was of insufficient thickness, and/or the groundwater did not rise to liquefiable artesian levels.

Geomorphic features indicate that degradation of the bedrock materials has resulted in rockfalls and the formation of colluvium and debris fans. In addition, debris flows have occurred in the past, resulting in accumulations of debris fans in the Mt. Riley mid-slope bench, the lower slope, and across Beach Road.

The remnant slide mass of the catastrophic 2020 landslide is marginally-stable during normal groundwater conditions, but may experience movement during increased groundwater levels during moderate to large storms.

If large slump blocks are displaced from the headscarp area, which could be caused by large storms or earthquakes, the materials would collapse into the headscarp and onto the landslide mass below. The likely result would be a decrease in landslide stability. Mobilization of remnant slide mass would likely not occur until a sufficient surcharge mass accumulates and/or the groundwater pressures are elevated due to large storms.

Rockfall from the headscarp and upper lateral scarps is likely, but would generally be localized and result in very small loading onto the landslide mass. This would have negligible and imperceptible changes in landslide stability and not cause remnant slide mass movement. Boulders that are displaced will likely not travel far downslope due to the roughness and softness of the landslide debris surface. Displaced boulders will likely not reach Beach Road due to the gentle ground slopes in the lower landslide debris flow area.

Elsewhere within the AOC, it is anticipated that the slopes on both sides of the landslide will continue to experience erosion, particularly in swales and drainages. The Rock 2 bedrock will continue to weather and deform in-place, producing more rockfall and colluvium. Localized debris flows, slumps, and creep of colluvium slopes may occur. Large deep-seated landslides in the bedrock slope are the least likely type of landslide hazard to occur. Slides may occur in colluvial deposits on the hillside

slopes, particularly during significant storms that cause high increases in groundwater levels and artesian pressures.

Earthquakes can trigger movement of the landslide, slope displacements outside of the landslide, and rockfall events. Slope stability could be further reduced if seismic events occur during significant precipitation events. Should a magnitude 6 earthquake occur along the Denali Fault 5 kilometers away (i.e., 1,000-year return interval event), the landslide and surrounding slopes would likely become unstable. When considering a magnitude 5.3 earthquake (modeled as a 500-year return interval event), the landslide and surrounding slopes would likely be marginally stable. The upper slump block east of the headscarp of the landslide (represented in geologic cross section 1A) could become unstable even with relatively small earthquake events.

Fluid runout flows and debris flows may occur due to artesian groundwater pressures as a result of significant rainfall events that cause colluvial soils to liquefy. There is ground surface evidence that debris flows have occurred in the past in various locations in the north-facing hillside resulting in the formation of debris fan deposits that extend beneath Beach Road and to the shoreline. A range of debris flow runout extents are possible, as described in Section 5. Extensive and catastrophic flow runouts could occur as witnessed by the runout associated with the December 2, 2020 landslide event. Smaller, more limited debris flows could occur as evidenced by the small debris flow slide west of the main landslide. These debris flow areas may experience similar runout characteristics and flow path/extents as was observed previously. However, there is a possibility that greater amounts of flow may occur, depending on colluvium extent/depth and amount of artesian groundwater pressures. Larger flows may result in longer and wider flow paths potentially reaching the Beach Road area. Refer to various modeled flow runout simulations presented in this report (i.e., Section 5.4 and Appendix C). The analyses and interpretations presented in this report are rough approximations due to the uncertainty in the modeled larger debris flow extents based the limited available data.

7.2 Mitigation Concepts

There are several approaches to deal with landslides and marginally-stable slopes, including: 1) stabilization, 2) avoidance, 3) management, 4) maintenance, and 5) partial mitigation.

Stabilization consists of constructing measures to achieve slope stability by increasing resistance or reducing driving forces, or both, to achieve suitable levels of stability Factor of Safety. Stabilization of large complex landslides, such as the Beach Road Landslide, can be very challenging to design and construct. The landslide blocks are located on the steep hillside, increasing the challenges of construction. In our opinion, full stabilization of the Beach Road Landslide would be prohibitively expensive and thus infeasible.

Avoidance includes avoiding habitable buildings within the active limits of the landslide due to high hazard. The Public may also be advised to avoid this area during extreme rain events.

Management of the landside and geologic hazards in the vicinity can be performed to reduce risks to the public. Caution signs can be used to warn visitors of geologic hazard risks in the north-facing hillside in the AOC. Management could also be used to limit or restrict use of this area during extreme precipitation when the risk of geologic hazards increases.

With the completion of the subsurface instrumentation program, the Borough now has access to on-going monitoring data. Monitoring of geotechnical conditions and weather instruments could be undertaken. The data monitoring systems could be maintained and could be made available to the public for risk awareness and planning activities.

Maintenance of infrastructure could include the preparedness to repair the road and/or utility poles as needed. Ground displacement might occur due to environmental factors, stormwater runoff, debris flows, slide movement/creep, etc.

Drainage mitigation measures could be considered to reduce the risk of liquefaction, runout flows, and slope instability by limiting potential increases in groundwater pressure surges (particularly artesian pressures) during large storms and snowmelt. Horizontal drains and/or trench drains constructed in Colluvium 3 materials at the Mt. Riley mid-slope benches may achieve partial mitigation. Horizontal drains are installed by drilling nearly-horizontal holes into the hillside, approximately 200 to 300 feet long to create depressurizing drainage paths within Colluvium 3 materials. Slotted drain pipes are installed in the drilled holes to collect groundwater and provide a path for the water to discharge. Trench drains could be constructed by hydraulic excavators to depths about 10 to 15 feet and filled with free-draining gravel. Trench drains should be oriented so that they daylight downslope to discharge by gravity. For either of these drainage measures, the collected water should be controlled in piped discharge systems to avoid infiltrating back into the slope or causing erosion or slope instability. Drainage measures would require permission from agencies, which would likely require additional specific review of risks, consequences, and environmental impacts.

Other partial mitigation measures could be used to reduce risks due to small debris flows and rockfall, such as the construction of catchment areas, diversion berms and/or rockfall/debris flow barriers. However, such mitigation measures would not likely stop catastrophic flows like that experienced December 2020.

7.3 Recommendations

Monitoring geotechnical and weather instruments should be continued to establish baseline conditions and to further improve the understanding of the effects weather and groundwater have on the site. This may require retaining specialists to continue data acquisition, maintain the instrumentation, and interpret the results. A long-term goal would be to develop correlations between weather events, groundwater pressures, and ground movements. Threshold values to warn residents of potentially hazardous conditions may be determined once baselines and trends are established and used to evaluate the effects of weather and groundwater on slope stability.

Changes across the AOC and areas surrounding the AOC could be understood if periodic lidar data is collected. Change detection analyses could be performed using the lidar data to monitor changes in slope conditions on the north-facing hillside and to assist in identifying potential unstable conditions that may develop or have occurred. Monitoring could be conducted periodically, initially on an annual basis and decreased to a five-year period or longer should baseline comparisons show consistent conditions.

We recommend preparing a plan for maintenance of infrastructure (i.e., roadway and utilities). Items to consider when preparing a plan could include environmental factors, storm water runoff, debris flows, and slide movement/creep.

Consider the construction of partial mitigation subsurface drainage measures to limit the buildup of groundwater pressures to reduce the risk of liquefaction, runout flows, and slope instability.

Due to the high likelihood of hazard associated with the landslide area, we recommend avoiding construction of buildings within the active landslide limits, possibly including a buffer zone along the boundaries of the landslide or a hazard overlay where there is uncertainty whether the landslide may widen and whether debris flow paths/extent may run beyond the existing landslide impact area. Limiting activities within the landslide area during periods of significant precipitation is also recommended. Caution signs could be maintained to warn visitors of geologic hazard risks along the north-facing hillside of the AOC. Consideration of options would also likely include increased public awareness.

A subsequent work phase could develop recommendations and details for the mitigation and/or management approaches the Borough wants to pursue.

8 REFERENCES

Alaska Department of Natural Resources Division of Geological & Geophysical Survey (DGGS). (2020, December 4 - 13). Photos and Videos of Reconnaissance's by Daanen, R., Wikstrom Jones, K., Hubbard, T., and Willingham, A., Beach Road Landslide.

Alaska Department of Natural Resources Division of Geological & Geophysical Survey (DGGS). (2021, February 11). Haines Landslide Response. Presentation.

Alaska Department of Natural Resources Division of Geological & Geophysical Survey (DGGS). (2021). High-resolution Lidar data for Haines, Southcentral Alaska. December 8-12, 2020. Fairbanks, AK.

Alaska Department of Natural Resources Division of Geological & Geophysical Survey (DGGS). (2021, February 9). Report of Activities - DGGS Haines Landslide Response.

Anderson, N. (2020, December 19; 2021, January 9). Videos of Artesian Flow from Andersons' Well.

Brew, D., & Ford, A. (1994). The Coast Mountains Plutonic-Metamorphic Complex and Related Rocks between Haines, Alaska, and Fraser, British Columbia - Tectonic and Geologic Sketches and Klondike Highway Road Log. Open File Report 94-268. United States Geological Survey.

Buxton, C. (2021, January 11). 2020 Beach Road Mass Wasting Event. Geo-Notes PowerPoint.

Buxton, C. (2021, January 8). Compilation of geologically relevant info from the Beach Road Residents. Phone and email conversations.

Claessens, L., Heuvelink, G., Schoorl, J., & Veldkamp, A. (2005). DEM resolution effects on shallow landslide hazard and soil redistribution modelling. *Earth Surface Processes and Landforms*, 461-477.

Cornforth, D. H., (2005). Landslides In Practice: Investigation, Analysis, and Remedial/Preventative Options In Soils, Wiley.

Dietrich, W., Wilson, C., Montgomery, D., & McKean, J. (1993). Analysis of erosion thresholds, channel networks and landscape morphology using a digital terrain model. *Journal of Geology*, 259-278.

Duncan, J.M., Wright, S.G., and Brandon, T.L. (2014). Soil Strength and Slope Stability. 2nd Edition. Chapter 13 – Factors of Safety and Reliability. Wiley.

Elevate UAS. (2020, December). Aerial Photography and Videos.

Gehrels, G., & Berg, H. (1992). Geologic Map of Southeastern Alaska. Miscellaneous Investigations Series Map 1867. United States Geological Survey.

Genevois, R. and Romeo, R.W. (2003). Probability of Failure Occurrence and Recurrence in Rock Slopes Stability Analysis. ASCE International Journal of Geomechanics. Vol. 3, Issue 1.

Himmelberg, G., & Loney, R. (1995). Characteristics and Petrogenesis of Alaskan-Type Ultramafic-Mafic Intrusions, Southeastern Alaska. Professional Paper 1546. United States Geological Survey.

Hoek, E., 2007 ed. Practical Rock Engineering, RocScience.

Hoek, E. and Brown, E.T., (2019). "The Hoek-Brown Failure Criterion and GSI – 2018 Edition", Journal of Rock Mechanics and Geotechnical Engineering.

Hoek, E., Carranza-Torres, C., Corkum, B., 2002. Hoek-Brown Failure Criterion - 2002 Edition. Rocscience

Hoek, E., Carter, T.G., and Diederichs, M.S., (2013). "Quantification of the Geological Strength Index Chart", 47th US Rock Mechanics/Geomechanics Symposium, San Francisco, CA, USA June 23-26.

Holcomb, D. (2021, February 25). Eyewitness Account. Personal communication.

Holmgren, P. (1994). Multiple flow direction algorithms for runoff modelling in grid based elevation models: An empirical evaluation. *Hydrological Processes*, 327-334.

Horton, P., Jaboyedoff, M., Rudaz, B., & Zimmermann, M. (2013). Flow-R, a model for susceptibility mapping of debris flows and other gravitational hazards at a regional scale. *Natural Hazards and Earth System Sciences*, 869-885.

Jacobs, A. (2021a). Haines Flood, Slide Weather Data Summary/Extremes. December 1-7, 2020. Juneau, AK: National Weather Service.

Jacobs, A. (2021b). Haines Weather/Data Summary for Debris Flows, Landslides, Flooding Event. December 1-8, 2020. Juneau, AK: National Weather Service.

Kirkaldie, L. (1988). Rock Classification Systems for Engineering Purposes. ASTM SPT 984. American Society for Testing and Materials.

Larsen, C., Motyka, R., Freymueller, J., Echelmeyer, K., & Ivins, E. (2005). Rapid Viscoelastic Uplift in Southeast Alaska Caused by Post-Little Ice Age Glacial Retreat. Earth and Planetary Science Letters.

Lemke, R., & Yehle, L. (1972). Reconnaissance Engineering Geology of the Haines Area, Alaska, with Emphasis on Evaluation of Earthquake and Other Geologic Hazards. Open File Report 72-229. United States Geological Survey.

Miller, J.F., 1963; Probable Maximum Precipitation and Rainfall-Frequency Data for Alaska, Technical Paper No. 47, U.S. Department of Commerce, Weather Bureau

Quantum Spatial. (2014, July 24). Skagway, Haines, and Petersburg Lidar. Technical Data Report. Fairbanks, AK.

Quinn, P., Beven, K., Chevallier, P., & Planchon, O. (1991). The prediction of hillslope flow paths for distributed hydrological modelling using digital terrain models. *Hydrological Processes*, 59-79.

Schnabel, R. (2021, February 21, 26). Personal Communication. Southeast Roadbuilders.

Silva, F., Lambe, T.W., and Marr, W.A. (2008). Probability and Risk of Slope Failure. Journal of Geotechnical and Geoenvironmental Engineering. 134(12): 1691-1699.

Slate, A. (2020, December 2). Video of Landslide Second Flow Runout.

Slate, A. (2021, February 19). Eyewitness Account. Personal communication.

Smith, D. (2021, January 27). Beach Rd. Slide Recap. Survey Monitoring. Juneau, AK: Southeast Roadbuilders.

Source? (2020, December 2). Video of Post-Slide Condition from Beach Road (Post Slide Video 1).

Source? (2020, December 2). Videos of Stormwater Runoff along Beach Road, Pre-Landslide (Pre-Slide Videos 1, 2, 3).

Villano, S. (2020, December 2). Video of Stormwater Runoff along Beach Road, above Hollenbeck Property.

Well Log. (2003, March 5). Chilkoot Inlet Sub Block#1 Lot #7, Well #1 (Miller/Simmons Property). Channel Drilling Company.

Well Log. (2013, June 25). Chilkoot Inlet Sub Lot AB5 (Hollenbeck Property). Alaska Department of Natural Resources.

Willingham, A. (2020, December 29). Notes about rocks from Beach Road slide area. Alaska Department of Natural Resources Division of Geological & Geophysical Survey (DGGS).

Wishstar, S. (2021, January 10). Memory of sound events during Beach Road Slide (for Geo Team). Email.

LIMITATIONS IN THE USE AND INTERPRETATIONS OF THIS REPORT

Our professional services were performed, our findings obtained, and our recommendations prepared in accordance with generally accepted engineering principles and practices. This warranty is in lieu of all other warranties, either expressed or implied.

The geotechnical report was prepared for the use of the Owner in the design of the subject facility and should be made available to potential contractors and/or the Contractor for information on factual data only. This report should not be used for contractual purposes as a warranty of interpreted subsurface conditions such as those indicated by the interpretive boring and test pit logs, cross-sections, or discussion of subsurface conditions contained herein.

The analyses, conclusions and recommendations contained in the report are based on site conditions as they presently exist and assume that the exploratory borings, test pits, and/or probes are representative of the subsurface conditions of the site. If, during construction, subsurface conditions are found which are significantly different from those observed in the exploratory borings and test pits, or assumed to exist in the excavations, we should be advised at once so that we can review these conditions and reconsider our recommendations where necessary. If there is a substantial lapse of time between the submission of this report and the start of work at the site, or if conditions have changed due to natural causes or construction operations at or adjacent to the site, this report should be reviewed to determine the applicability of the conclusions and recommendations considering the changed conditions and time lapse.

The Summary Boring Logs are our opinion of the subsurface conditions revealed by periodic sampling of the ground as the borings progressed. The soil descriptions and interfaces between strata are interpretive and actual changes may be gradual.

The boring logs and related information depict subsurface conditions only at these specific locations and at the particular time designated on the logs. Soil conditions at other locations may differ from conditions occurring at these boring locations. Also, the passage of time may result in a change in the soil conditions at these boring locations.

Groundwater levels often vary seasonally. Groundwater levels reported on the boring logs or in the body of the report are factual data only for the dates shown.

Unanticipated soil conditions are commonly encountered on construction sites and cannot be fully anticipated by merely taking soil samples, borings or test pits. Such unexpected conditions frequently require that additional expenditures be made to attain a properly constructed project. It is recommended that the Owner consider providing a contingency fund to accommodate such potential extra costs.

This firm cannot be responsible for any deviation from the intent of this report including, but not restricted to, any changes to the scheduled time of construction, the nature of the project or the specific construction methods or means indicated in this report; nor can our firm be responsible for any construction activity on sites other than the specific site referred to in this report.

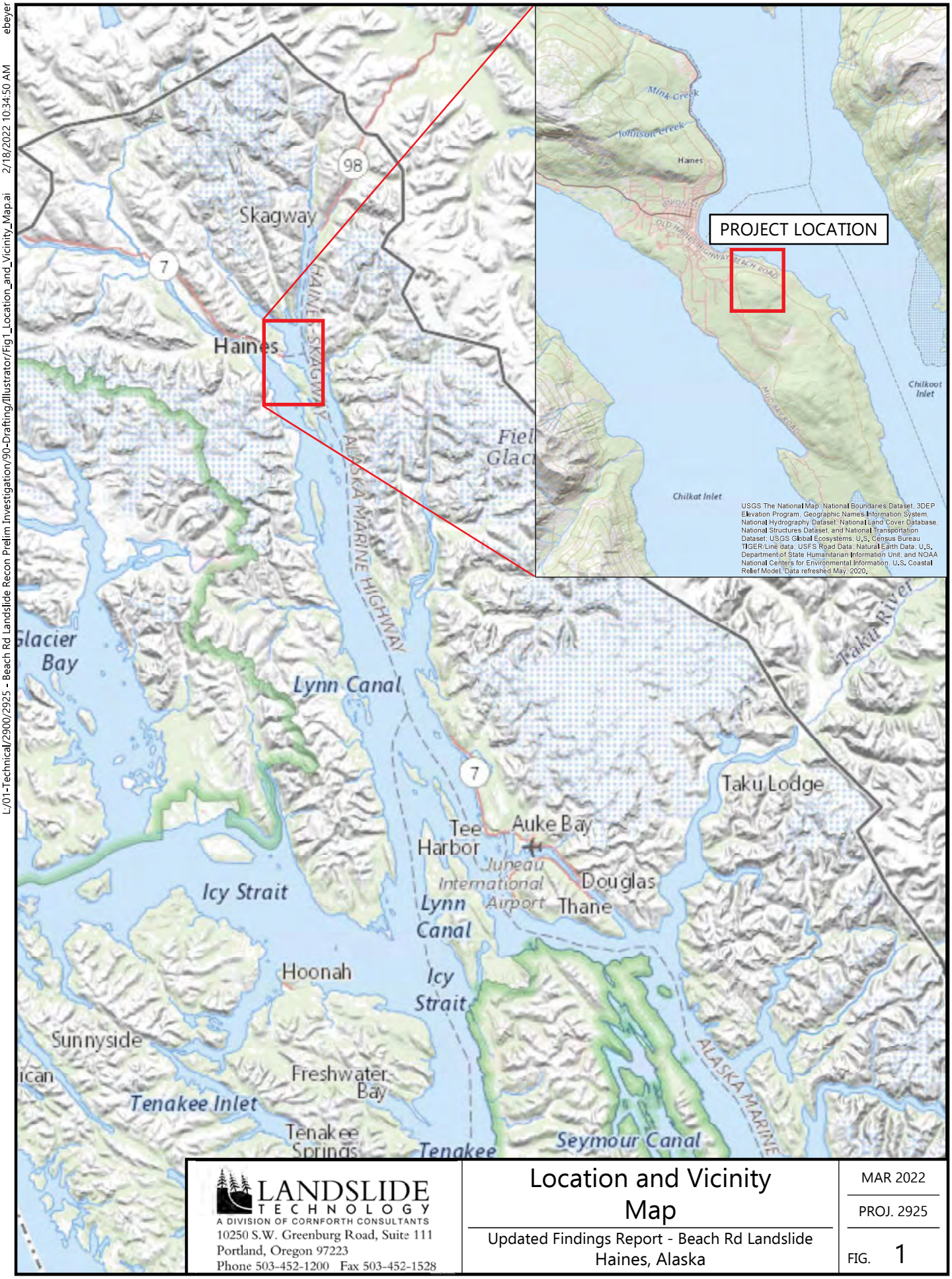

LANDSLIDE TECHNOLOGY
A DIVISION OF CORNFORTH CONSULTANTS
10250 S.W. Greenburg Road, Suite 111
Portland, Oregon 97223
Phone 503-452-1200 Fax 503-452-1528

Location and Vicinity Map

Updated Findings Report - Beach Rd Landslide
Haines, Alaska

MAR 2022

PROJ. 2925

FIG. 1

Notes:
1. Property data obtained from Haines Borough
2. All labeled blocks and lots relate to each parcel's location within the Chilkoot Inlet subdivision
3. Primary aerial photo obtained from Elevate UAS, Dec. 2020
4. Background imagery obtained from ESRI

Legend

- Haines Borough Area of Concern (AOC)
- Parcels (approx.)
  - Developed
  - Undeveloped

CHILKOOT INLET

Beach Road

Mt. Riley Road

Block AB, Lot 2
Block AB, Lot 1
Block 1, Lot 15
Block 1, Lot 14
Block 1, Lot 13
Block 1, Lot 12
Block 1, Lot 11
Block 1, Lot 10
Block 1, Lot 9
Block 1, Lot 8
Block 1, Lot 7
Block 1, Lot 6
Block 1, Lot 5
Block 1, Lot 4
Block 1, Lot 3
Block 1, Lot 2
Block 1, Lot 1
Block 4, Lot 2
Block 4, Lot 1
Block 3, Lot 6C
Block 3, Lot 6B
Block 3, Lot 6A
Block 3, Lot 5
Block 3, Lot 4
Block 3, Lot 3
Block 3, Lot 2
Block 3, Lot 1

Section 1
Section 1A
Section 2
Section 3
Section 4

0 150 300 600 Feet

LANDSLIDE TECHNOLOGY A DIVISION OF CORNFORTH CONSULTANTS 10250 S.W. Greenburg Road, Suite 111 Portland, Oregon 97223 Phone 503-452-1200 Fax 503-452-1528	December 2020 Aerial Photo Map Updated Findings Report - Beach Rd Landslide Haines, Alaska	MAR 2022 PROJ. 2925 FIG. 2

L:\01-Technical\2900\2925 - Beach Rd Landslide Recon Prelim Investigation\92 - GIS\MXD\Updates 20220217\Haines Report Figure 2_2020 Aerial Photo.mxd - JCM

GEOLOGIC MAP OF SOUTHEASTERN ALASKA

BY GEORGE E. GEHRELS AND HENRY C. BERG, 1992

136°00′

0 6 12

SCALE IN MILES

NORTH

DEFINITION OF MAP UNITS

(See footnotes in Correlation of Map Units for restrictions on age designations)

- ŦOsv — Sedimentary and volcanic rocks, undivided (Triassic to Ordovician)
- pTmsv — Metasedimentary and metavolcanic rocks (pre-Tertiary)
- Ŧb — Basaltic rocks (Triassic)
- Tg — Granodiorite (Eocene)
- Tgt — Granodiorite and tonalite (Paleocene)
- TKt — Tonalite (Paleocene and Cretaceous
- TKg — Granodiorite (Paleocene and Cretaceous)
- Kgt — Granodiorite and tonalite (Cretaceous)
- Kdb — Diorite and gabbro (Cretaceous)
- Kum — Ultramafic rocks (Cretaceous)
- Qs — Surficial Sedimentary deposits (Quaternary)

Contact—Approximately located; dotted where concealed; queried where inferred

Fault—Dashed where approximately located or where interpreted; dotted where concealed. Arrows indicate sense of strike-slip displacement. Amounts of displacement from Hudson and others (1982) (Chatham Strait fault) and from Gehrels and others (1987) (Clarence Strait fault)

Thrust fault—Dashed where approximately located or where interpreted; dotted where concealed. Sawteeth on upper plate

Normal fault—Dotted where concealed. Hachures on down-dropped block

Coast Range megalineament—Topographic and structural lineament (as described by Brew and Ford, 1978)

Undifferentiated intrusive and stratified rocks—Map unit symbol or color in stippled area indicates predominant lithic unit

Ice or permanent snow

DENALI FAULT

Chilkat R

Unmapped

Glacier

Skagway

Klukwan

KLUKWAN IND RES

Chilkat Lake

SANDSTUCK IND RES

Port Chilkoot

Haines

Meade Glacier

Unmapped

Auer Glacier

Carroll Glacier

SLIDE LOCATION

LANDSLIDE TECHNOLOGY
A DIVISION OF CORNFORTH CONSULTANTS
10250 S.W. Greenburg Road, Suite 111
Portland, Oregon 97223
Phone 503-452-1200 Fax 503-452-1528

Regional Geologic Map

Updated Findings Report - Beach Rd Landslide
Haines, Alaska

MAR 2022

PROJ. 2925

FIG. 3

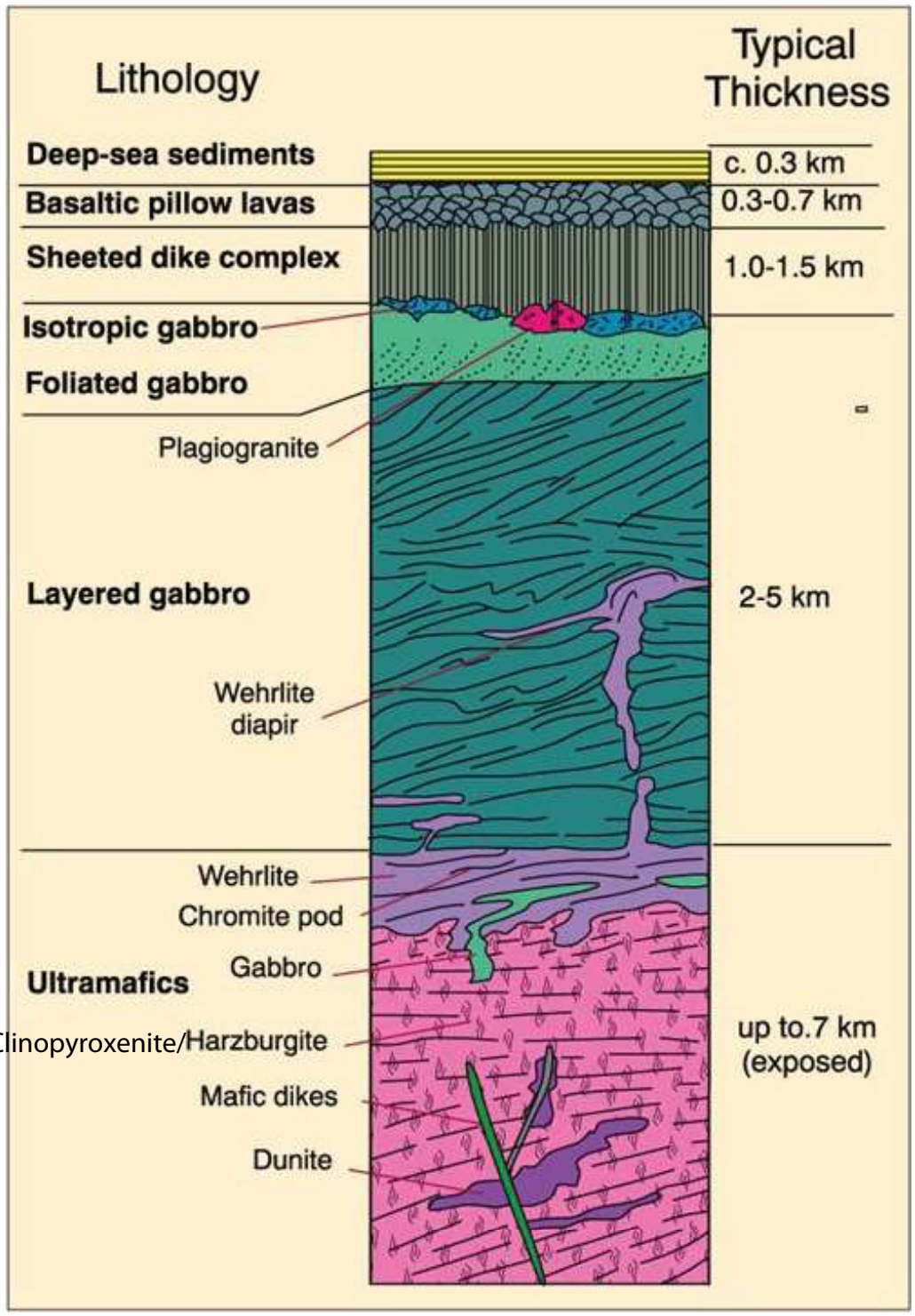

Source: Modified from Boudier and Nicolas (1985) Earth Planet. Sci. Lett., 76, 84-92.

LANDSLIDE TECHNOLOGY
A DIVISION OF CORNFORTH CONSULTANTS
10250 S.W. Greenburg Road, Suite 111
Portland, Oregon 97223
Phone 503-452-1200 Fax 503-452-1528

Typical Ophiolite Sequence

Updated Findings Report - Beach Rd Landslide
Haines, Alaska

MAR 2022
PROJ. 2925
FIG. 4

L:\01-Technical\2900\2925 - Beach Rd Landslide Recon Prelim Investigation\92 - GIS\MXD\Updates_20220217\Haines Report Figure 5_2014 Topo Map.mxd - JCM

CHILKOOT
INLET

Beach Road

Mt. Riley
Road

Contour Interval: 5ft
0 150 300 600
Feet

Note: Topographic lines derived from 2014 lidar data provided by DGGS, acquired May 2014.

Legend

Haines Borough Area of Concern (AOC)

LANDSLIDE TECHNOLOGY
A DIVISION OF CORNFORTH CONSULTANTS
10250 S.W. Greenburg Road, Suite 111
Portland, Oregon 97223
Phone 503-452-1200 Fax 503-452-1528

2014 Topographic Map

Updated Findings Report - Beach Rd Landslide
Haines, Alaska

MAR 2022
PROJ. 2925
FIG. 5

L:\01-Technical\2900\2925 - Beach Rd Landslide Recon Prelim Investigation\92 - GIS\MXD\Updates_20220217\Haines Report Figure 6_2014 Slope Map.mxd - JCM

CHILKOOT
INLET

Beach Road

Riley Road

Legend

Haines Borough Area of Concern (AOC)

0 150 300 600
Feet

Note: Surface Slope raster derived from 2014 lidar data provided by DGGS, acquired May 2014.

LANDSLIDE TECHNOLOGY
A DIVISION OF CORNFORTH CONSULTANTS
10250 S.W. Greenburg Road, Suite 111
Portland, Oregon 97223
Phone 503-452-1200 Fax 503-452-1528

2014 Slope Shade Map

Updated Findings Report - Beach Rd Landslide
Haines, Alaska

MAR 2022

PROJ. 2925

FIG. 6

L:\01-Technical\2900\2925 - Beach Rd Landslide Recon Prelim Investigation\92 - GIS\MXD\Updates_2022021?\Haines Report Figure 7_Obliques.mxd - JCM

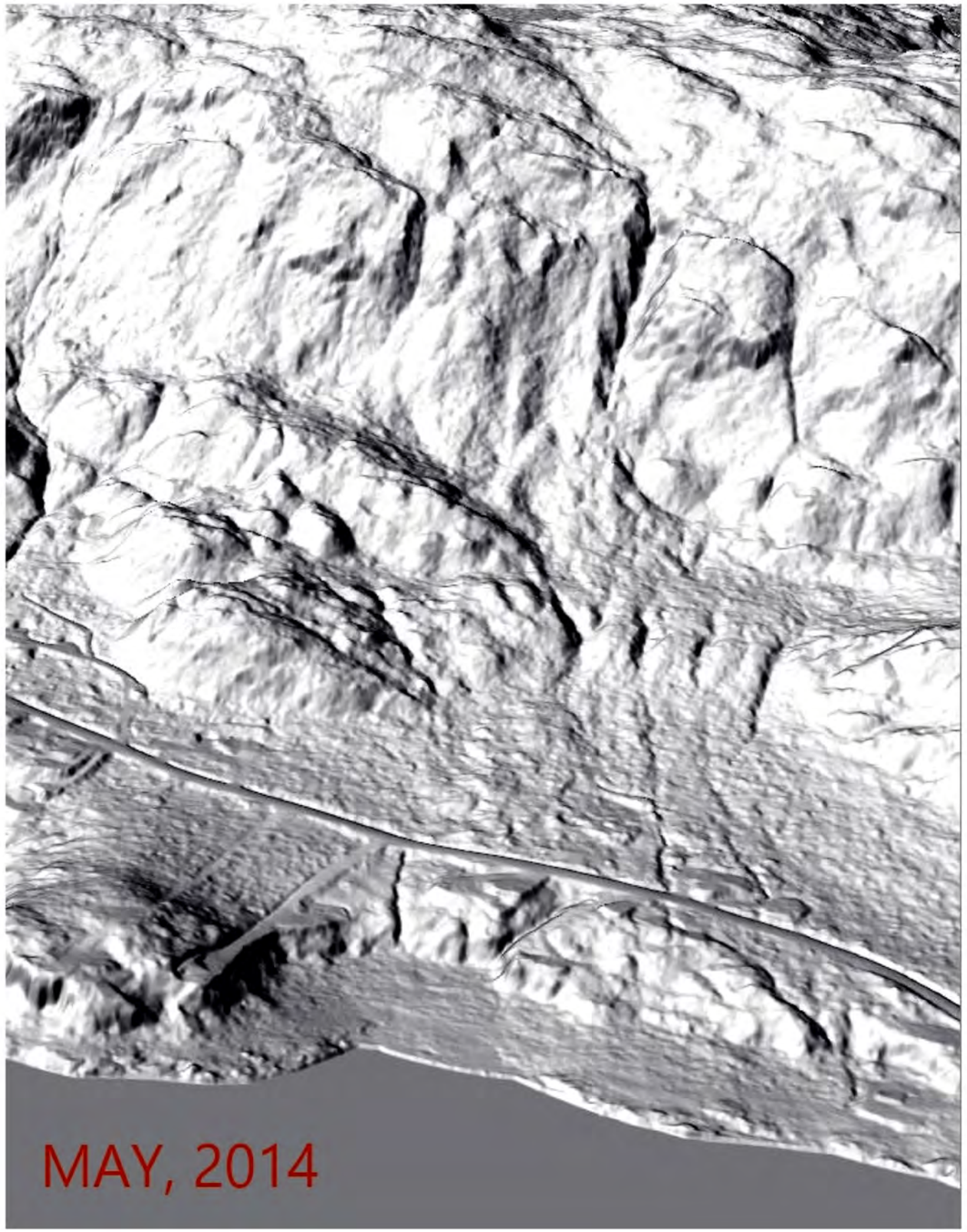

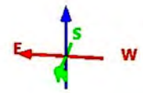

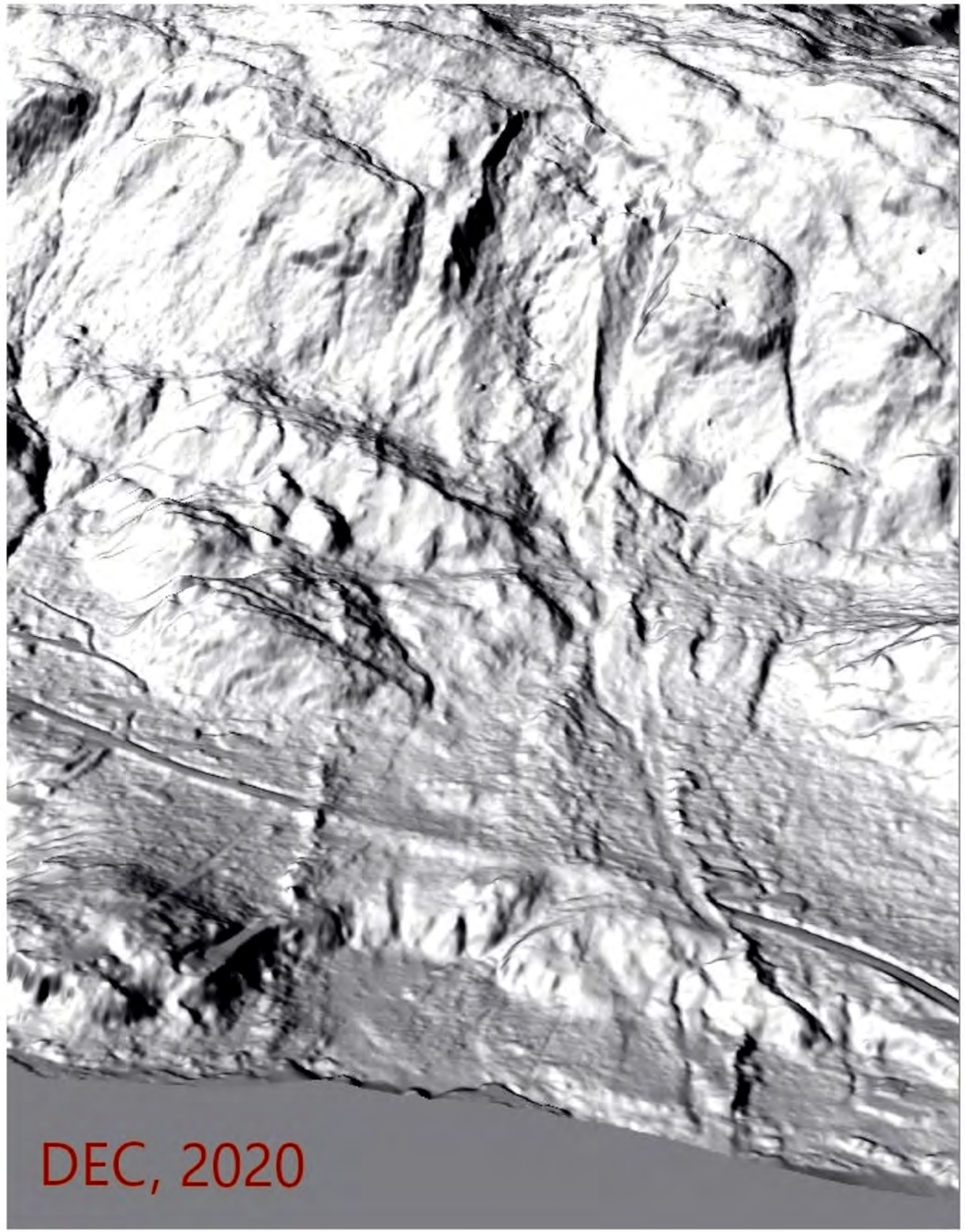

LANDSLIDE TECHNOLOGY
A DIVISION OF CORNFORTH CONSULTANTS
10250 S.W. Greenburg Road, Suite 111
Portland, Oregon 97223
Phone 503-452-1200 Fax 503-452-1528

Oblique Hillshade Views

Updated Findings Report - Beach Rd Landslide
Haines, Alaska

MAR 2022

PROJ. 2925

FIG. 7

L:\01-Technical\2900\2925 - Beach Rd Landslide Recon Prelim Investigation\92 - GIS\MXD\Updates_20220217\Haines Report Figure 8a Change Detection Topo.mxd - JCM

CHILKOOT
INLET

Beach Road

Mt. Riley Road

Legend

Haines Borough Area of Concern (AOC)

Elevation Change (ft)

- -55' to -20'
- -20' to -7'
- -7' to -3'
- -3' to -1'
- -1' to 1'
- 1' to 5'
- 5' to 8'
- 8' to 19'

Contour Interval: 5ft

0 150 300 600 Feet

Note: Difference raster derived from 2014 and 2020 lidar data provided by-DGGS. Topographic lines derived from 2020 lidar.

LANDSLIDE TECHNOLOGY
A DIVISION OF CORNFORTH CONSULTANTS
10250 S.W. Greenburg Road, Suite 111
Portland, Oregon 97223
Phone 503-452-1200 Fax 503-452-1528

Vertical Change Detection

Updated Findings Report - Beach Rd Landslide
Haines, Alaska

MAR 2022

PROJ. 2925

FIG. 8

CHILKOOT INLET

Beach Road

Mt. Riley Road

LT-1
LT-2
LT-3
LT-4
LT-5
LT-6
LT-7
LT-8
LT-9
LT-10
LT-11
LT-12

Section 1
Section 1A
Section 2
Section 3
Section 4

Legend

- 2021 Boring Locations
- Debris Flow Fan Slope
- Deep-Seated Creep Slope
- Haines Borough Area of Concern

Colluvium/ Bedrock Units

- Rock 1
- Rock 2
- Rock 3
- Overburden Sediments, Colluvium, Etc

Contour Interval: 5ft

0 150 300 600 Feet

Note: Topographic lines derived from 2014 lidar data provided by DGGS, acquired May 2014.

LANDSLIDE TECHNOLOGY
A DIVISION OF CORNFORTH CONSULTANTS
10250 S.W. Greenburg Road, Suite 111
Portland, Oregon 97223
Phone 503-452-1200 Fax 503-452-1528

2014 Geomorphic Interpretation Map

Updated Findings Report - Beach Rd Landslide
Haines, Alaska

MAR 2022
PROJ. 2925
FIG. 9

L:\01-Technical\2900\2925 - Beach Rd Landslide Recon Prelim Investigation\92 - GIS\MXD\Updates_20220217\Haines Report Figure 10_2020 Geomorph.mxd - JCM

CHILKOOT INLET

Beach Road

Mt. Riley Road

LT-1
LT-2
LT-3
LT-4
LT-5
LT-6
LT-7
LT-8
LT-9
LT-10
LT-11
LT-12

Section 1
Section 2
Section 3
Section 4
Section 1A

EASTERN TENSION CRACK

WESTERN TENSION CRACK

Legend

- 2021 Boring Locations
- Seepage
- Debris Flow Fan Slope
- Deep-Seated Creep Slope
- Haines Borough Area of Concern (AOC)

Interpreted Features/Geology

- Tension Crack Outlined Slump
- Upper Rock Slump
- Headscarp and Lateral Rock Scarps
- Soil Scarps
- Middle Boulder Field
- East and West Side of Middle Boulder Field
- Lower Debris Flow
- Debris Flow Lobes

Colluvium/ Bedrock Units

- Rock 1
- Rock 2
- Overburden Sediments, Colluvium, Etc

Contour Interval: 5ft

0 150 300 600 Feet

Note: Topographic contours are derived from 2020 lidar data provided by DGGS, acquired December 2020.

LANDSLIDE TECHNOLOGY
A DIVISION OF CORNFORTH CONSULTANTS
10250 S.W. Greenburg Road, Suite 111
Portland, Oregon 97223
Phone 503-452-1200 Fax 503-452-1528

2020 Geomorphic Interpretation Map

Updated Findings Report - Beach Rd Landslide
Haines, Alaska

MAR 2022
PROJ. 2925
FIG. 10

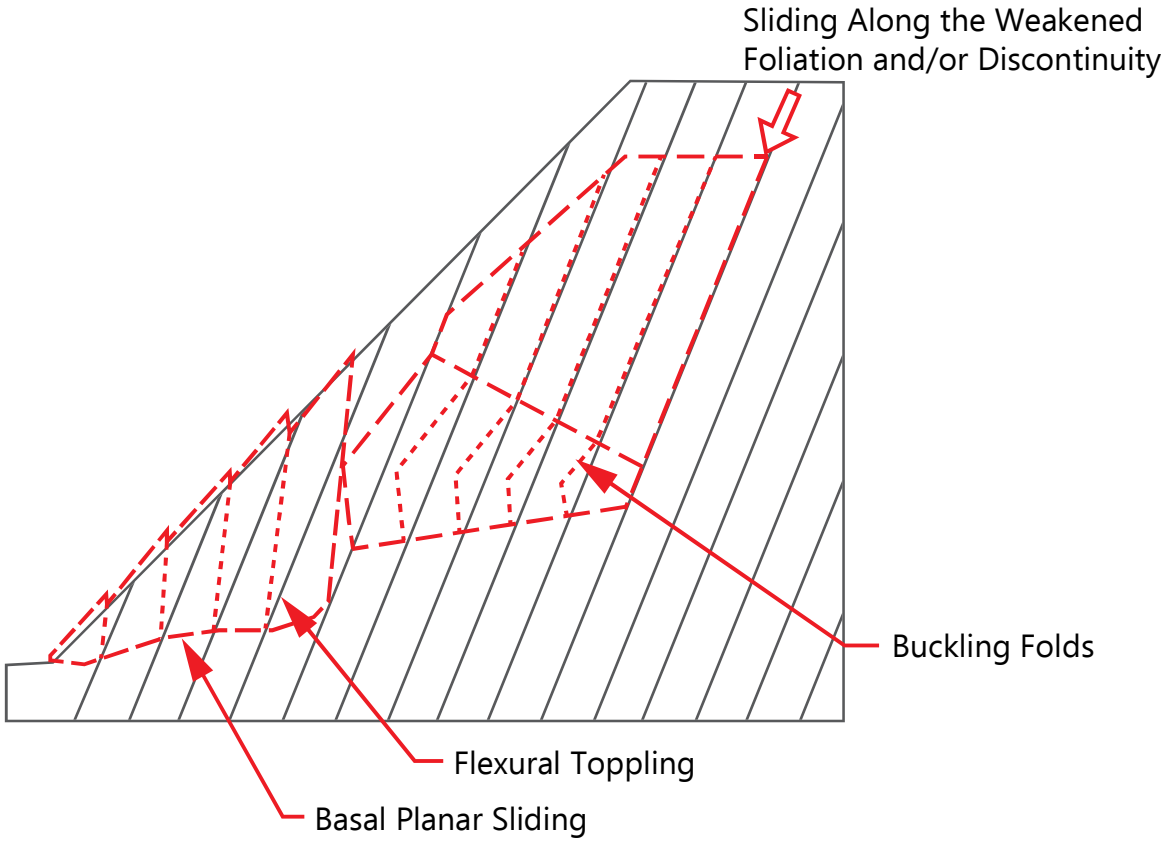

Note: Schematic after scielo.org

LANDSLIDE TECHNOLOGY
A DIVISION OF CORNFORTH CONSULTANTS
10250 S.W. Greenburg Road, Suite 111
Portland, Oregon 97223
Phone 503-452-1200 Fax 503-452-1528

Mechanical Inflation and Slope Creep Schematic

Updated Findings Report - Beach Rd Landslide
Haines, Alaska

MAR 2022
PROJ. 2925
FIG. 11

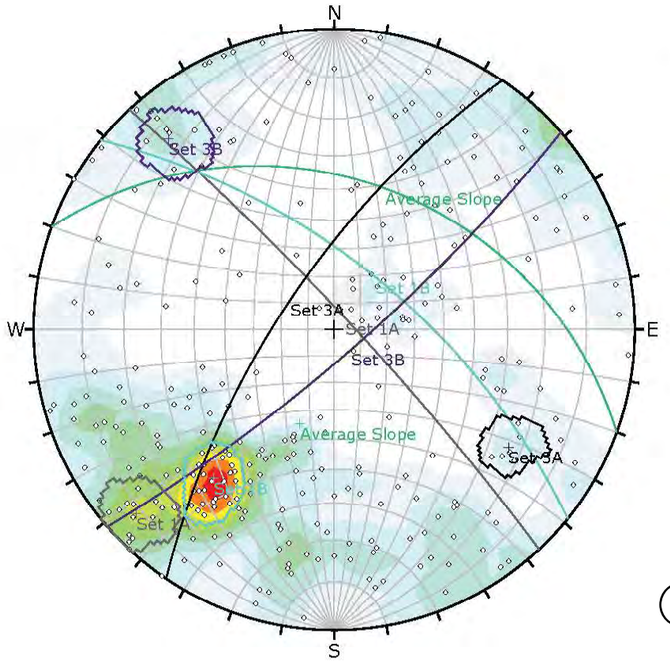

Symbol	Feature
◇	Pole Vectors

Color	Density Concentrations
	0.00 - 0.70
	0.70 - 1.40
	1.40 - 2.10
	2.10 - 2.80
	2.80 - 3.50
	3.50 - 4.20
	4.20 - 4.90
	4.90 - 5.60
	5.60 - 6.30
	6.30 - 7.00

Contour Data	Pole Vectors
Maximum Density	6.92%
Contour Distribution	Fisher
Counting Circle Size	1.0%

	Color	Dip	Dip Direction	Label
User Planes				
1		37	20	Average Slope
Mean Set Planes				
1m		84	47	Set 1A
2m		65	39	Set 1B
3m		70	304	Set 3A
4m		80	139	Set 3B

Plot Mode	Pole Vectors
Vector Count	305 (305 Entries)
Hemisphere	Lower
Projection	Equal Angle

(A) ALL DATA

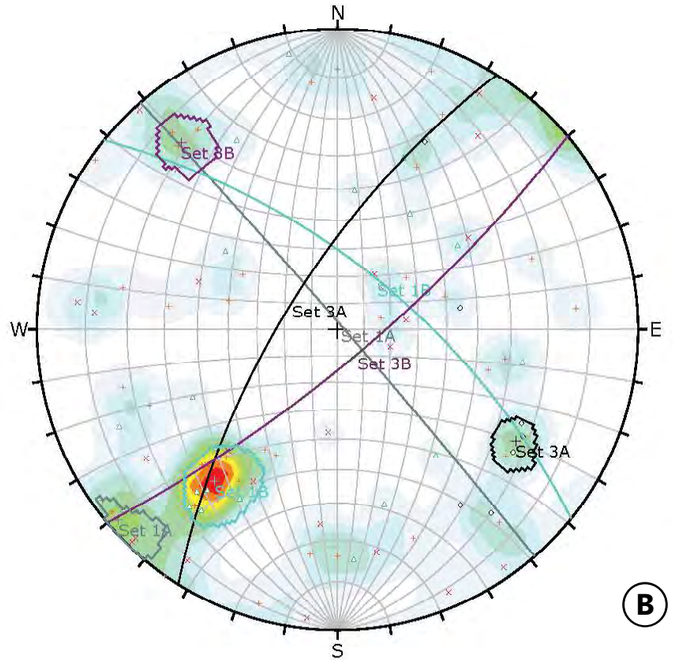

Symbol	ELEVATION	Quantity
◇	BEACH	7
×	HIGH	27
△	LOW	20
+	MIDDLE	37

Color	Density Concentrations
	0.00 - 0.90
	0.90 - 1.80
	1.80 - 2.70
	2.70 - 3.60
	3.60 - 4.50
	4.50 - 5.40
	5.40 - 6.30
	6.30 - 7.20
	7.20 - 8.10
	8.10 - 9.00

Contour Data	Pole Vectors
Maximum Density	8.86%
Contour Distribution	Fisher
Counting Circle Size	1.0%

	Color	Dip	Dip Direction	Label
Mean Set Planes				
1m		88	49	Set 1A
2m		66	39	Set 1B
3m		70	302	Set 3A
4m		78	140	Set 3B

Plot Mode	Pole Vectors
Vector Count	91 (91 Entries)
Hemisphere	Lower
Projection	Equal Angle

(B) WESTERN AREAS

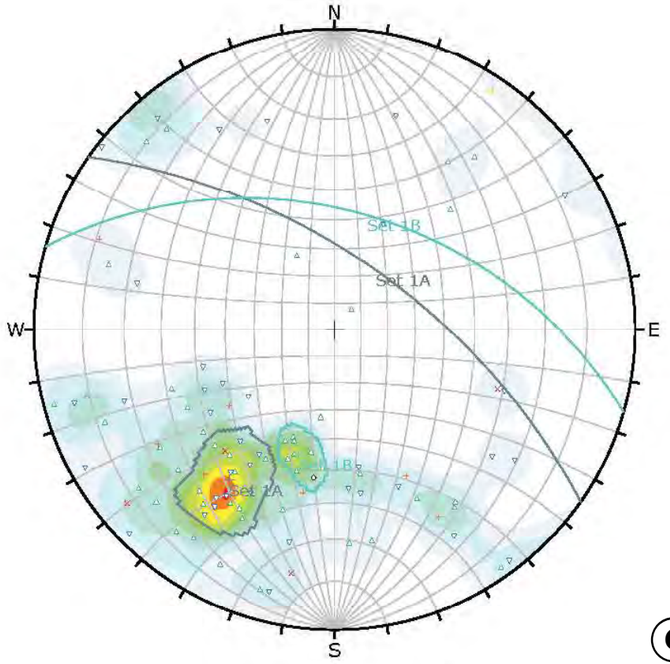

Symbol	ELEVATION	Quantity
◇	Compositional fracture	1
×	EAST LATERAL SCARP	4
△	HEADSCARP/UPPER	48
+	LOW	8
▽	MIDDLE	37
—	Subordante fracture	2

Color	Density Concentrations
	0.00 - 1.10
	1.10 - 2.20
	2.20 - 3.30
	3.30 - 4.40
	4.40 - 5.50
	5.50 - 6.60
	6.60 - 7.70
	7.70 - 8.80
	8.80 - 9.90
	9.90 - 11.00

Contour Data	Pole Vectors
Maximum Density	10.14%
Contour Distribution	Fisher
Counting Circle Size	1.0%

	Color	Dip	Dip Direction	Label
Mean Set Planes				
1m		63	35	Set 1A
2m		47	16	Set 1B

Plot Mode	Pole Vectors
Vector Count	100 (100 Entries)
Hemisphere	Lower
Projection	Equal Angle

(C) SLIDE AREA

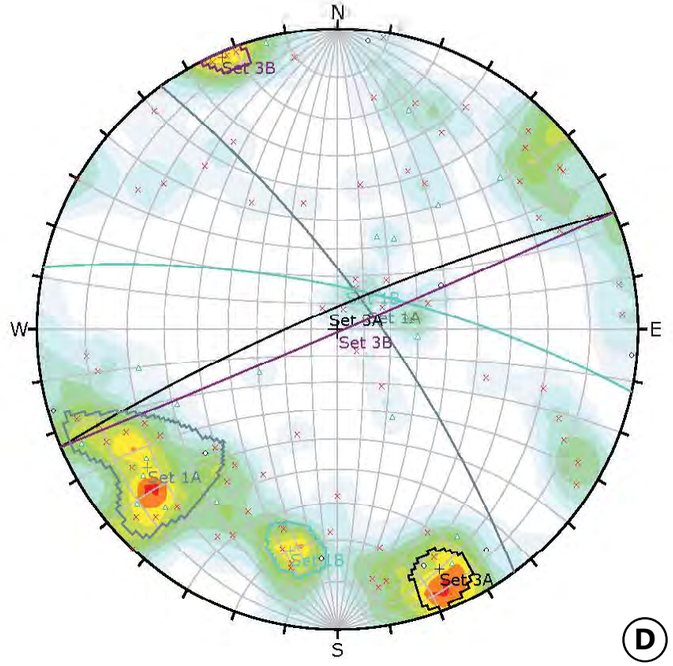

Symbol	ELEVATION - SIMPLE	Quantity
◇	BEACH	8
×	EAST UPPER BLOCKS	83
△	LOW	23

Color	Density Concentrations
	0.00 - 0.65
	0.65 - 1.30
	1.30 - 1.95
	1.95 - 2.60
	2.60 - 3.25
	3.25 - 3.90
	3.90 - 4.55
	4.55 - 5.20
	5.20 - 5.85
	5.85 - 6.50

Contour Data	Pole Vectors
Maximum Density	6.04%
Contour Distribution	Fisher
Counting Circle Size	1.0%

	Color	Dip	Dip Direction	Label
Mean Set Planes				
1m		76	54	Set 1A
2m		74	12	Set 1B
3m		82	337	Set 3A
4m		89	157	Set 3B

Plot Mode	Pole Vectors
Vector Count	114 (114 Entries)
Hemisphere	Lower
Projection	Equal Angle

(D) EASTERN AREAS

LANDSLIDE TECHNOLOGY
A DIVISION OF CORNFORTH CONSULTANTS
10250 S.W. Greenburg Road, Suite 111
Portland, Oregon 97223
Phone 503-452-1200 Fax 503-452-1528

Discontinuity Stereonets Surface Hand Measurements

Updated Findings Report - Beach Rd Landslide
Haines, Alaska

MAR 2022
PROJ. 2925
FIG. 12

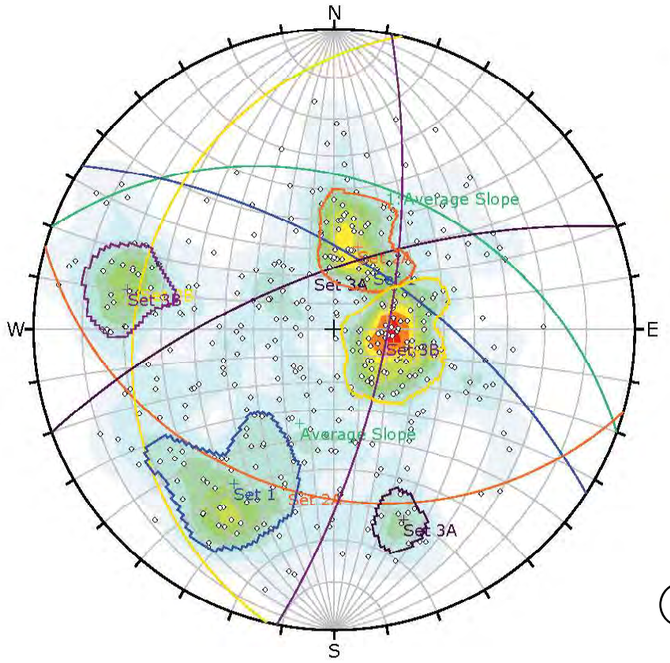

Symbol	Feature
◇	Pole Vectors

Color	Density Concentrations
	0.00 - 0.50
	0.50 - 1.00
	1.00 - 1.50
	1.50 - 2.00
	2.00 - 2.50
	2.50 - 3.00
	3.00 - 3.50
	3.50 - 4.00
	4.00 - 4.50
	4.50 - 5.00

Contour Data	Pole Vectors
Maximum Density	4.84%
Contour Distribution	Fisher
Counting Circle Size	1.0%

	Color	Dip	Dip Direction	Label
User Planes				
1		37	20	Average Slope
Mean Set Planes				
1m		63	33	Set 1
2m		32	196	Set 2A
3m		23	283	Set 2B
4m		68	340	Set 3A
5m		70	101	Set 3B

Plot Mode	Pole Vectors
Vector Count	385 (385 Entries)
Hemisphere	Lower
Projection	Equal Angle

(A) ALL DATA

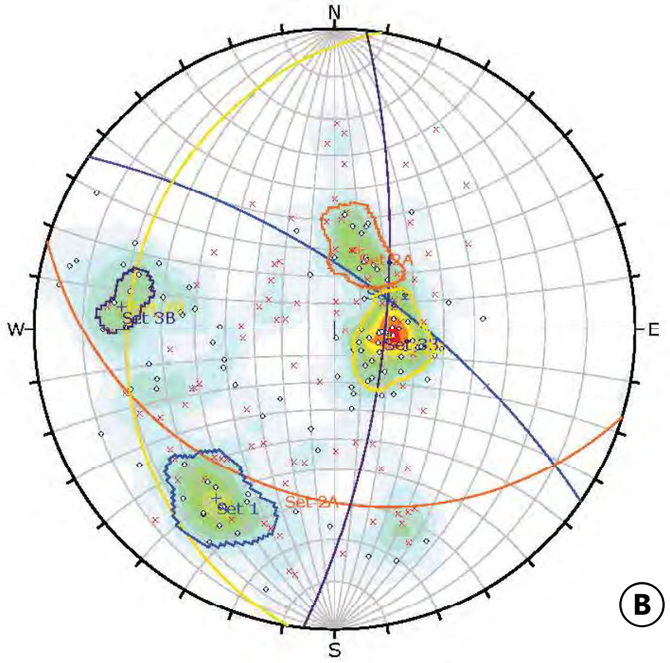

Symbol	BORING	Quantity
◇	LT-10	115
×	LT-9	97

Color	Density Concentrations
	0.00 - 0.70
	0.70 - 1.40
	1.40 - 2.10
	2.10 - 2.80
	2.80 - 3.50
	3.50 - 4.20
	4.20 - 4.90
	4.90 - 5.60
	5.60 - 6.30
	6.30 - 7.00

Contour Data	Pole Vectors
Maximum Density	6.80%
Contour Distribution	Fisher
Counting Circle Size	1.0%

	Color	Dip	Dip Direction	Label
Mean Set Planes				
1m		69	35	Set 1
2m		31	197	Set 2A
3m		21	279	Set 2B
5m		71	96	Set 3B

Plot Mode	Pole Vectors
Vector Count	212 (212 Entries)
Hemisphere	Lower
Projection	Equal Angle

(B) WESTERN AREAS

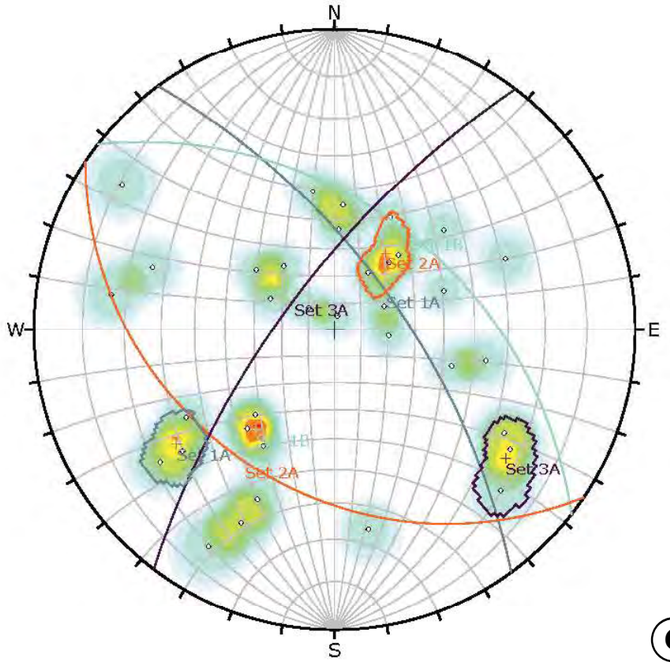

Symbol	BORING	Quantity
◇	LI-8	35

Color	Density Concentrations
	0.00 - 0.80
	0.80 - 1.60
	1.60 - 2.40
	2.40 - 3.20
	3.20 - 4.00
	4.00 - 4.80
	4.80 - 5.60
	5.60 - 6.40
	6.40 - 7.20
	7.20 - 8.00

Contour Data	Pole Vectors
Maximum Density	7.31%
Contour Distribution	Fisher
Counting Circle Size	1.0%

	Color	Dip	Dip Direction	Label
Mean Set Planes				
1m		66	54	Set 1A
2m		46	38	Set 1B
3m		34	214	Set 2A
4m		71	307	Set 3A

Plot Mode	Pole Vectors
Vector Count	35 (35 Entries)
Hemisphere	Lower
Projection	Equal Angle

(C) SLIDE AREA

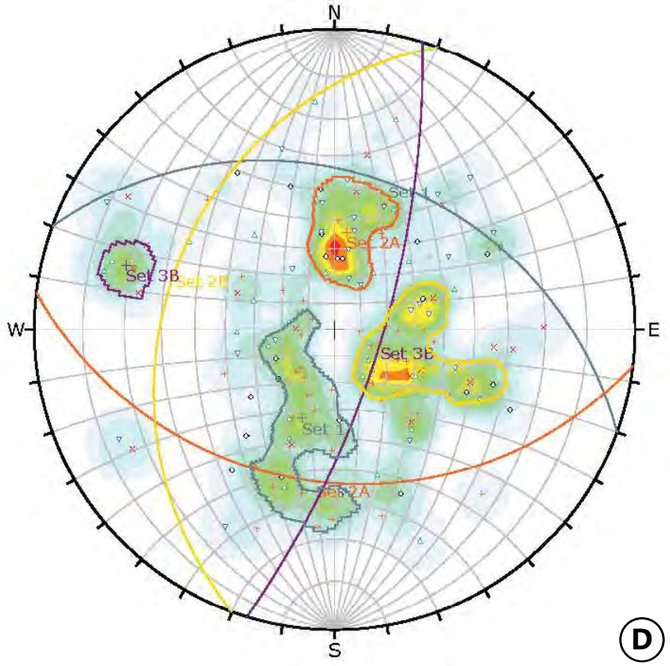

Symbol	BORING	Quantity
◇	LT-1	23
×	LT-2	20
△	LT-3	26
+	LT-4	42
▽	LT-7	27

Color	Density Concentrations
	0.00 - 0.50
	0.50 - 1.00
	1.00 - 1.50
	1.50 - 2.00
	2.00 - 2.50
	2.50 - 3.00
	3.00 - 3.50
	3.50 - 4.00
	4.00 - 4.50
	4.50 - 5.00

Contour Data	Pole Vectors
Maximum Density	4.94%
Contour Distribution	Fisher
Counting Circle Size	1.0%

	Color	Dip	Dip Direction	Label
Mean Set Planes				
1m		35	20	Set 1
2m		36	187	Set 2A
3m		31	290	Set 2B
4m		72	107	Set 3B

Plot Mode	Pole Vectors
Vector Count	138 (138 Entries)
Hemisphere	Lower
Projection	Equal Angle

(D) EASTERN AREAS

LANDSLIDE TECHNOLOGY
A DIVISION OF CORNFORTH CONSULTANTS
10250 S.W. Greenburg Road, Suite 111
Portland, Oregon 97223
Phone 503-452-1200 Fax 503-452-1528

Discontinuity Stereonets Upper Rock Unit Measurements

Updated Findings Report - Beach Rd Landslide
Haines, Alaska

MAR 2022
PROJ. 2925
FIG. 13

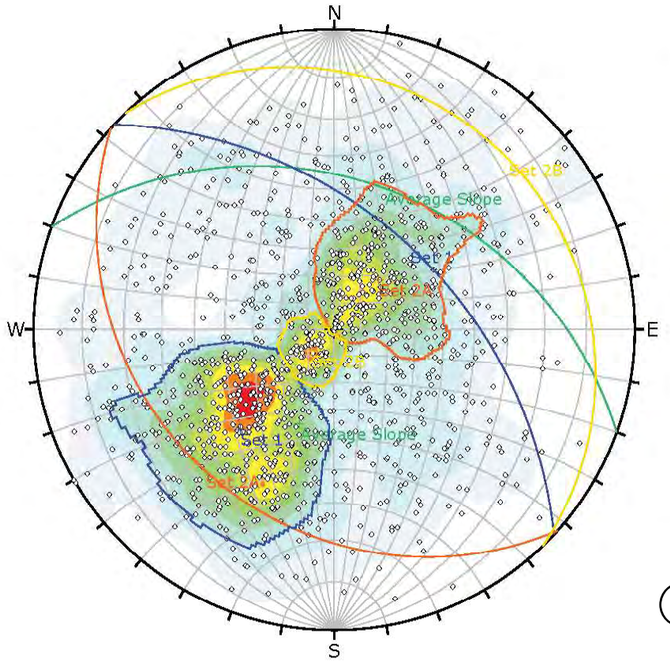

Symbol	Feature
◇	Pole Vectors

Color	Density Concentrations
	0.00 - 0.40
	0.40 - 0.80
	0.80 - 1.20
	1.20 - 1.60
	1.60 - 2.00
	2.00 - 2.40
	2.40 - 2.80
	2.80 - 3.20
	3.20 - 3.60
	3.60 - 4.00

Contour Data	Pole Vectors
Maximum Density	3.92%
Contour Distribution	Fisher
Counting Circle Size	1.0%

	Color	Dip	Dip Direction	Label
User Planes				
1		37	20	Average Slope
Mean Set Planes				
1m		49	43	Set 1
2m		25	222	Set 2A
3m		12	46	Set 2B

Plot Mode	Pole Vectors
Vector Count	1227 (1227 Entries)
Hemisphere	Lower
Projection	Equal Angle

(A) ALL DATA

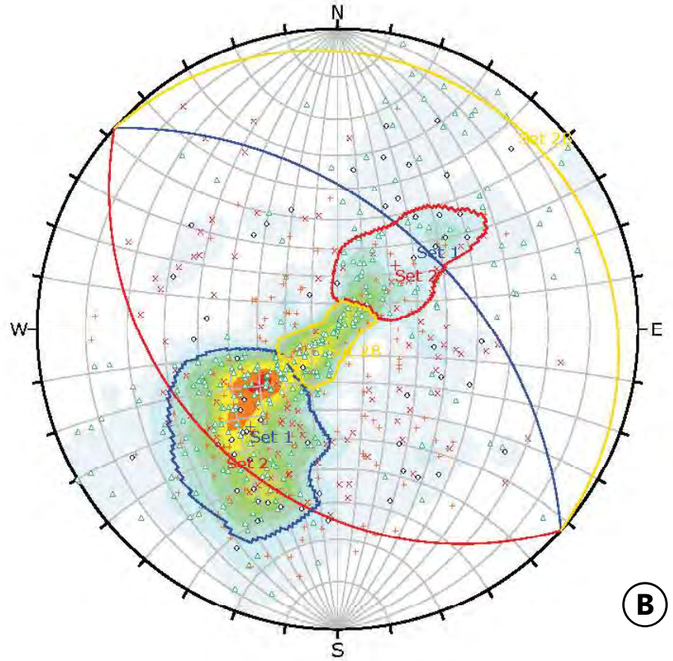

Symbol	BORING	Quantity
◇	LT-12	59
×	LT-5	101
△	LT-6	305
+	LT-8	127

Color	Density Concentrations
	0.00 - 0.60
	0.60 - 1.20
	1.20 - 1.80
	1.80 - 2.40
	2.40 - 3.00
	3.00 - 3.60
	3.60 - 4.20
	4.20 - 4.80
	4.80 - 5.40
	5.40 - 6.00

Contour Data	Pole Vectors
Maximum Density	5.65%
Contour Distribution	Fisher
Counting Circle Size	1.0%

	Color	Dip	Dip Direction	Label
Mean Set Planes				
1m		47	42	Set 1
2m		32	222	Set 2
3m		6	42	Set 2B

Plot Mode	Pole Vectors
Vector Count	592 (592 Entries)
Hemisphere	Lower
Projection	Equal Angle

(B) WESTERN AREAS

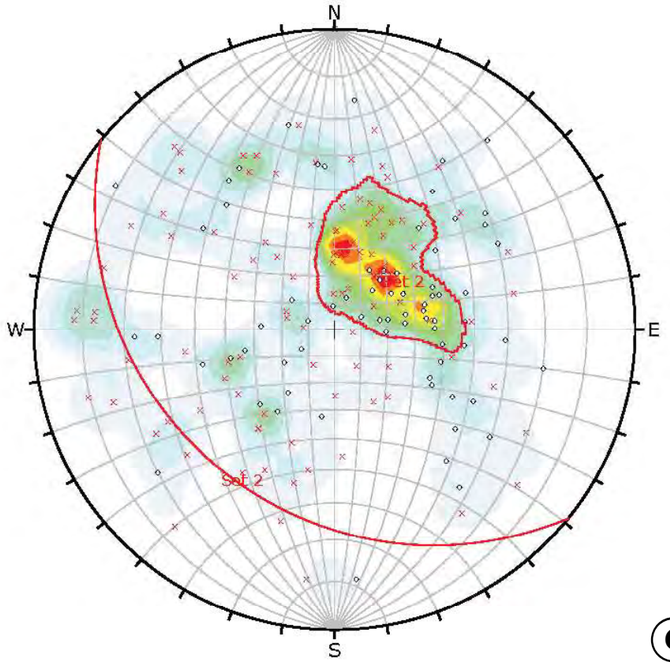

Symbol	BORING	Quantity
◇	LT-10	72
×	LT-9	108

Color	Density Concentrations
	0.00 - 0.60
	0.60 - 1.20
	1.20 - 1.80
	1.80 - 2.40
	2.40 - 3.00
	3.00 - 3.60
	3.60 - 4.20
	4.20 - 4.80
	4.80 - 5.40
	5.40 - 6.00

Contour Data	Pole Vectors
Maximum Density	5.94%
Contour Distribution	Fisher
Counting Circle Size	1.0%

	Color	Dip	Dip Direction	Label
Mean Set Planes				
1m		28	219	Set 2

Plot Mode	Pole Vectors
Vector Count	180 (180 Entries)
Hemisphere	Lower
Projection	Equal Angle

(C) SLIDE AREA

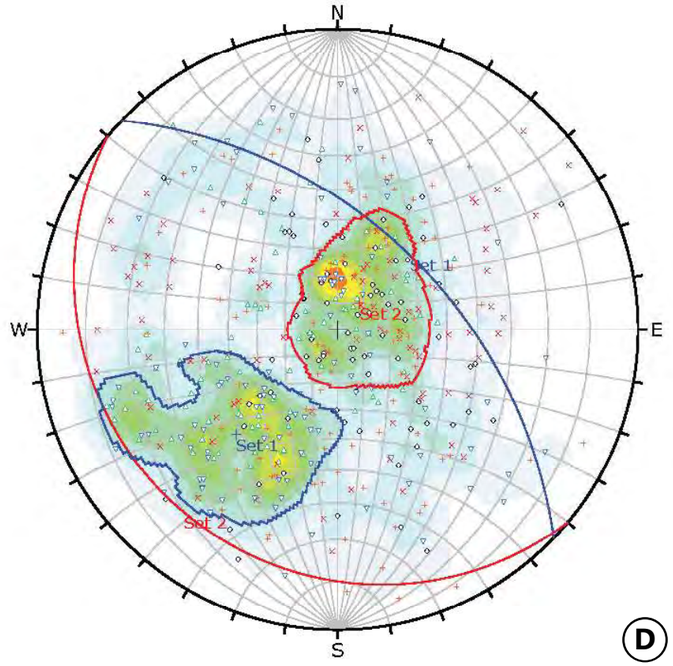

Symbol	BORING	Quantity
◇	LT-1	84
×	LT-2	90
△	LT-3	82
+	LT-4	102
▽	LT-7	97

Color	Density Concentrations
	0.00 - 0.45
	0.45 - 0.90
	0.90 - 1.35
	1.35 - 1.80
	1.80 - 2.25
	2.25 - 2.70
	2.70 - 3.15
	3.15 - 3.60
	3.60 - 4.05
	4.05 - 4.50

Contour Data	Pole Vectors
Maximum Density	4.00%
Contour Distribution	Fisher
Counting Circle Size	1.0%

	Color	Dip	Dip Direction	Label
Mean Set Planes				
1m		52	44	Set 1
2m		13	220	Set 2

Plot Mode	Pole Vectors
Vector Count	455 (455 Entries)
Hemisphere	Lower
Projection	Equal Angle

(D) EASTERN AREAS

LANDSLIDE TECHNOLOGY
A DIVISION OF CORNFORTH CONSULTANTS
10250 S.W. Greenburg Road, Suite 111
Portland, Oregon 97223
Phone 503-452-1200 Fax 503-452-1528

Discontinuity Stereonets Lower Rock Unit Measurements

Updated Findings Report - Beach Rd Landslide
Haines, Alaska

MAR 2022
PROJ. 2925
FIG. 14

L:\01-Technical\2900\2925 - Beach Rd Landslide Recon Prelim Investigation\90-Drafting\uStation\Design\DGN\Working\Surfaces.dgn :: Fig15 3/8/2022 12:34:11 PM DSparby

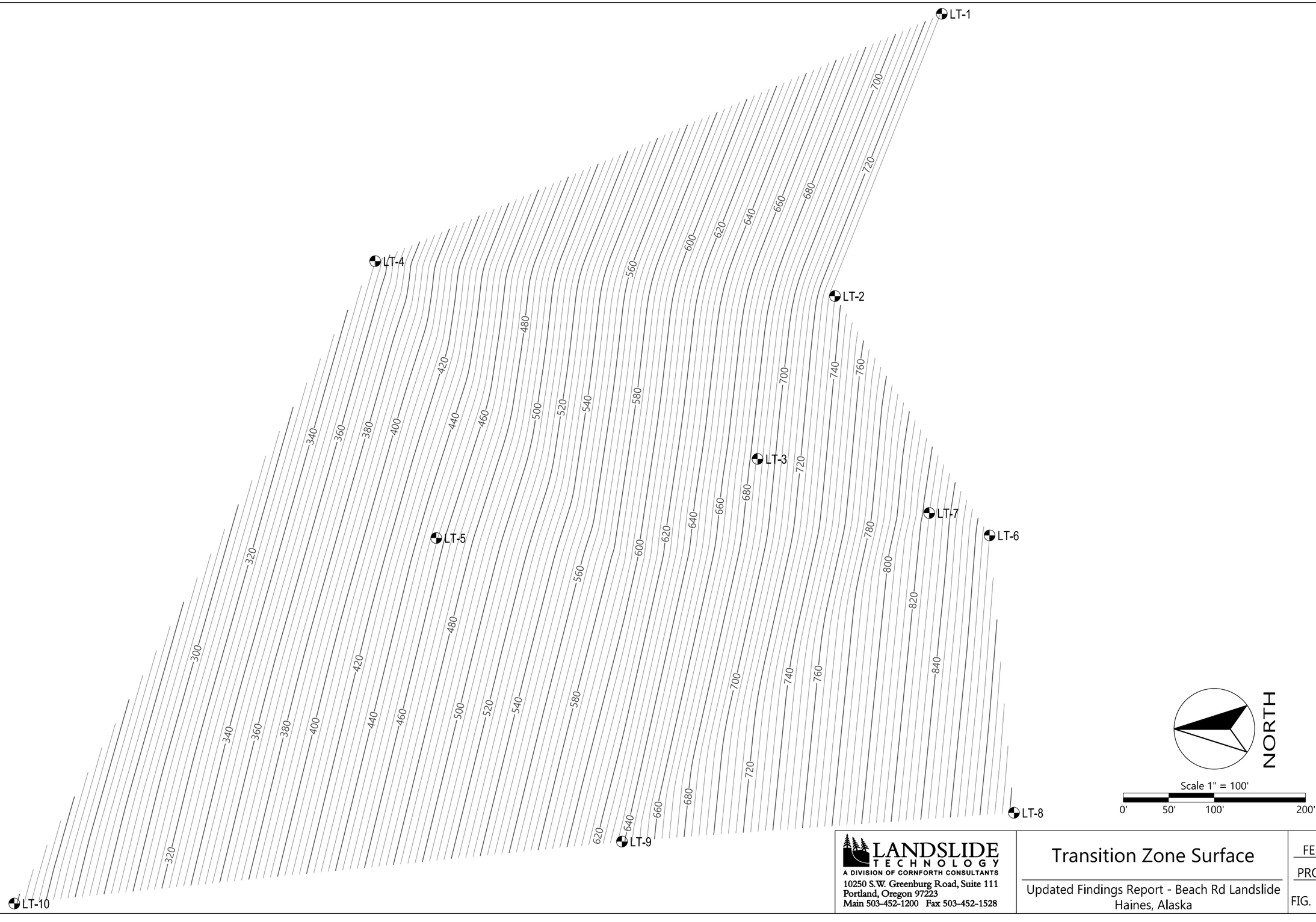

LANDSLIDE TECHNOLOGY
A DIVISION OF CORNFORTH CONSULTANTS
10250 S.W. Greenburg Road, Suite 111
Portland, Oregon 97223
Main 503-452-1200 Fax 503-452-1528

Transition Zone Surface

Updated Findings Report - Beach Rd Landslide
Haines, Alaska

FEB 2022
PROJ. 2925
FIG. 15

LEGEND:

- Rock 1 - Low Stress-Relief, In-place, Uninflated
- Rock 2 - Moderate to High Stress-Relief, Inflated
- Rock 3 - Moderate to High Stress-Relief, Inflated and Displaced
- Colluvium 1 - Weathered in-Place
- Colluvium 2 - Talus Deposits
- Colluvium 3 - Slumped and Flow Deposits
- Colluvium 4 - Debris Flow and Flood Deposits

- 2014 Ground Surface
- Groundwater Pressure Surface

Piezometer Pressures: LT-10 — Unit contact, typical; Upper Piezometer; Lower Piezometer

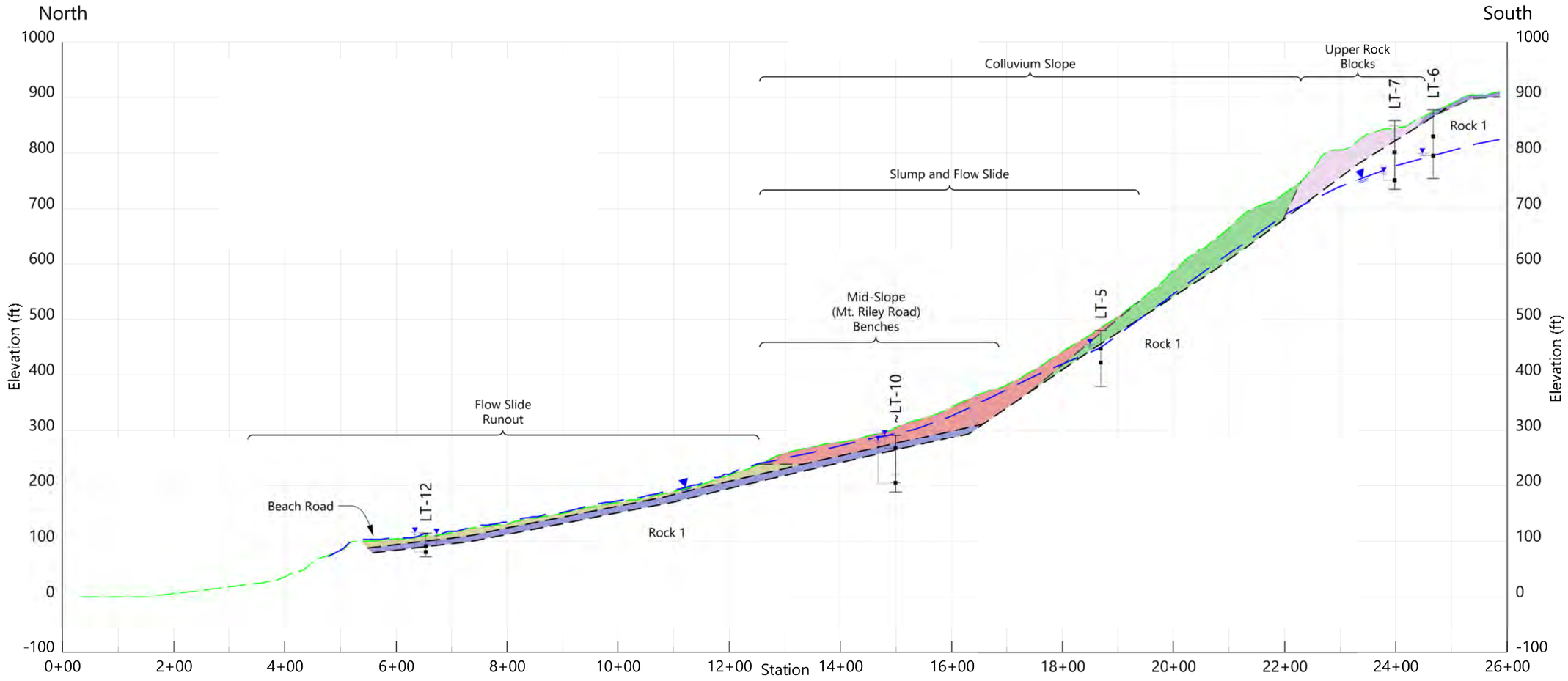

Source: Ground surface derived from May 2014 lidar data provided by DGGS.

LANDSLIDE TECHNOLOGY
A DIVISION OF CORNFORTH CONSULTANTS
10250 S.W. Greenburg Road, Suite 111
Portland, Oregon 97223
Main 503-452-1200 Fax 503-452-1528

Interpreted 2014 Section 1

Updated Findings Report - Beach Rd Landslide
Haines, Alaska

MAR 2022
PROJ. 2925
FIG. 16

LEGEND:

- Rock 1 - Low Stress-Relief, In-place, Uninflated
- Rock 2 - Moderate to High Stress-Relief, Inflated
- Rock 3 - Moderate to High Stress-Relief, Inflated and Displaced
- Colluvium 1 - Weathered in-Place
- Colluvium 2 - Talus Deposits
- Colluvium 3 - Slumped and Flow Deposits
- Colluvium 4 - Debris Flow and Flood Deposits

- 2020 Ground Surface
- Groundwater Pressure Surface
- Piezometer Pressures
- LT-10
- Unit contact, typical
- Upper Piezometer
- Lower Piezometer

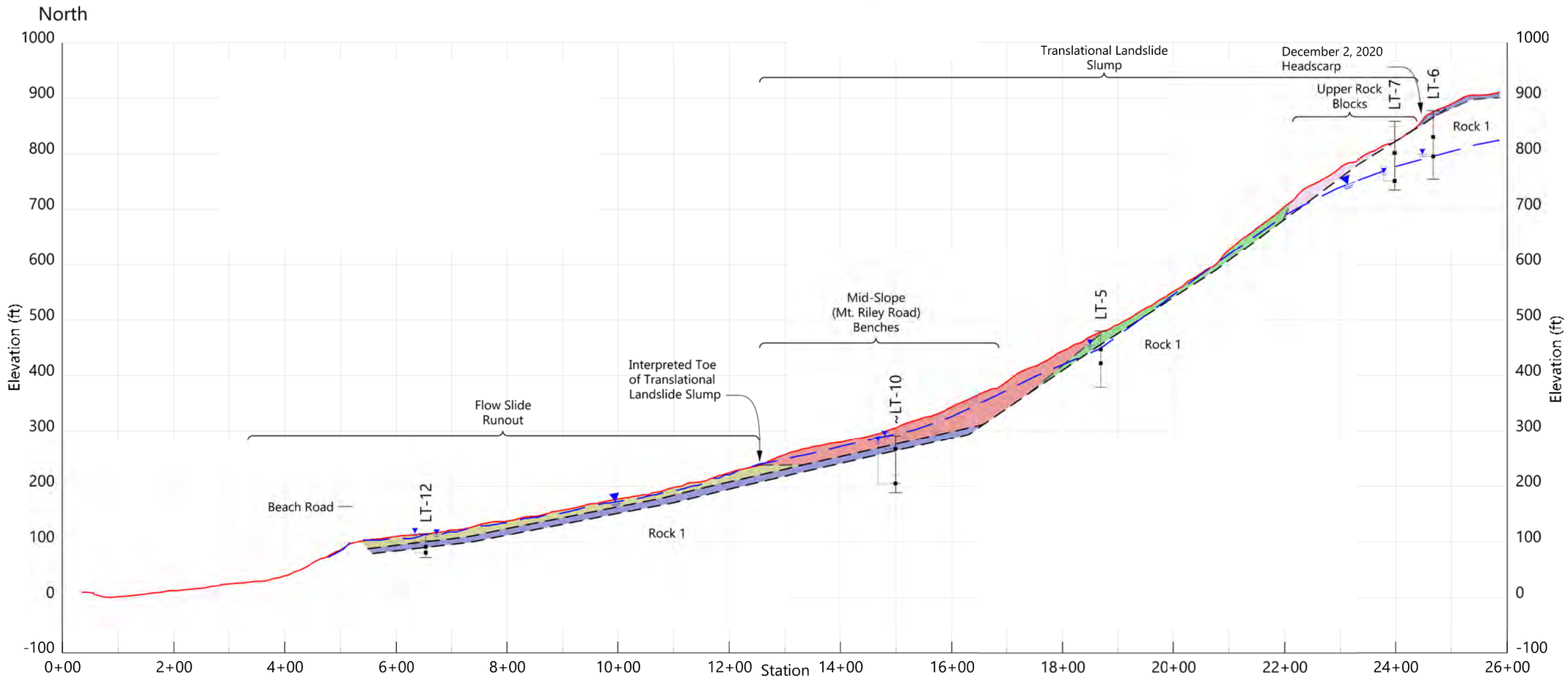

Source: Ground surface derived from December 2020 lidar data provided by DGGS.

LANDSLIDE TECHNOLOGY
A DIVISION OF CORNFORTH CONSULTANTS
10250 S.W. Greenburg Road, Suite 111
Portland, Oregon 97223
Main 503-452-1200 Fax 503-452-1528

Interpreted 2020 Section 1

Updated Findings Report - Beach Rd Landslide
Haines, Alaska

MAR 2022
PROJ. 2925
FIG. 17

LEGEND:

- Rock 1 - Low Stress-Relief, In-place, Uninflated
- Rock 2 - Moderate to High Stress-Relief, Inflated
- Rock 3 - Moderate to High Stress-Relief, Inflated and Displaced
- Colluvium 1 - Weathered in-Place
- Colluvium 2 - Talus Deposits
- Colluvium 3 - Slumped and Flow Deposits
- Colluvium 4 - Debris Flow and Flood Deposits

2014 Ground Surface

Groundwater Pressure Surface

LT-10

Piezometer Pressures

Unit contact, typical

Upper Piezometer

Lower Piezometer

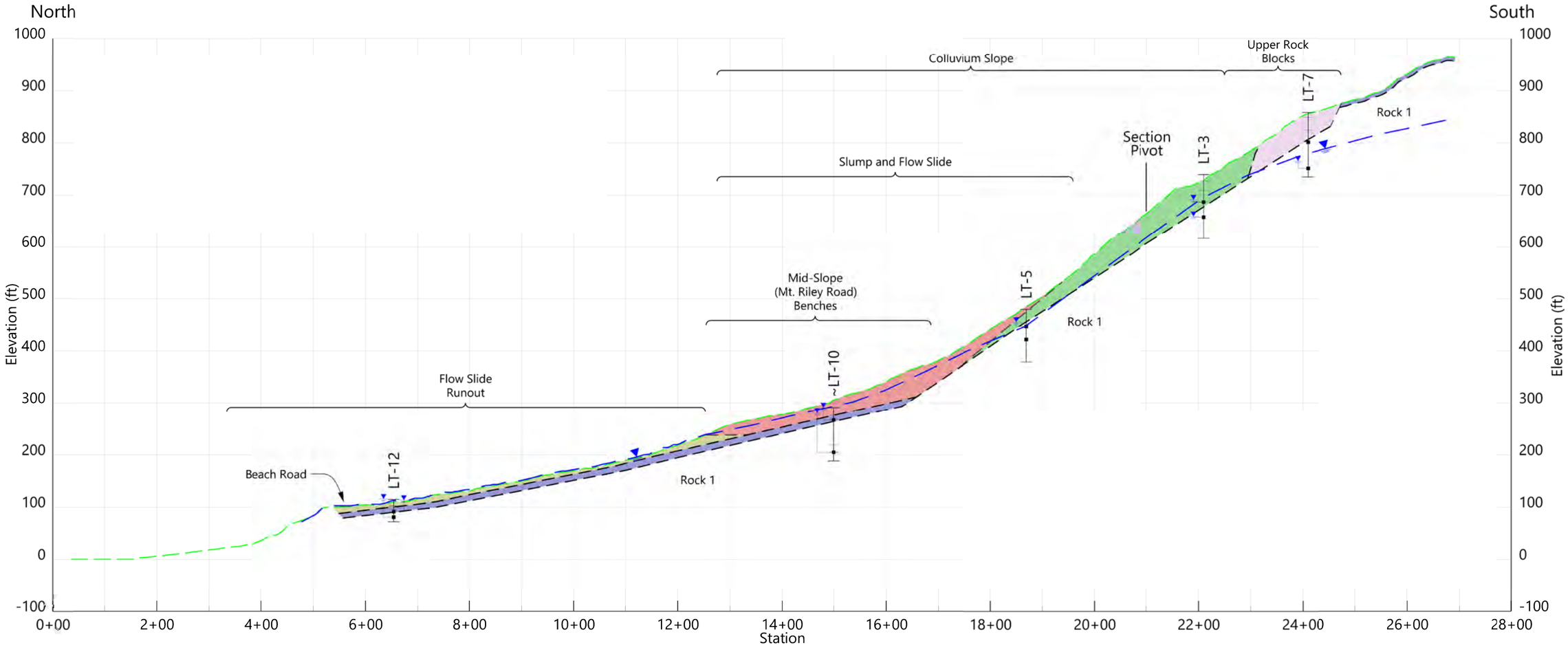

Source: Ground surface derived from May 2014 lidar data provided by DGGS.

LANDSLIDE TECHNOLOGY
A DIVISION OF CORNFORTH CONSULTANTS
10250 S.W. Greenburg Road, Suite 111
Portland, Oregon 97223
Main 503-452-1200 Fax 503-452-1528

Interpreted 2014 Section 1A

Updated Findings Report - Beach Rd Landslide
Haines, Alaska

MAR 2022

PROJ. 2925

FIG. 18

LEGEND:

- Rock 1 - Low Stress-Relief, In-place, Uninflated
- Rock 2 - Moderate to High Stress-Relief, Inflated
- Rock 3 - Moderate to High Stress-Relief, Inflated and Displaced
- Colluvium 1 - Weathered in-Place
- Colluvium 2 - Talus Deposits
- Colluvium 3 - Slumped and Flow Deposits
- Colluvium 4 - Debris Flow and Flood Deposits

- 2020 Ground Surface
- Groundwater Pressure Surface
- LT-10 Piezometer Pressures
- Unit contact, typical
- Upper Piezometer
- Lower Piezometer

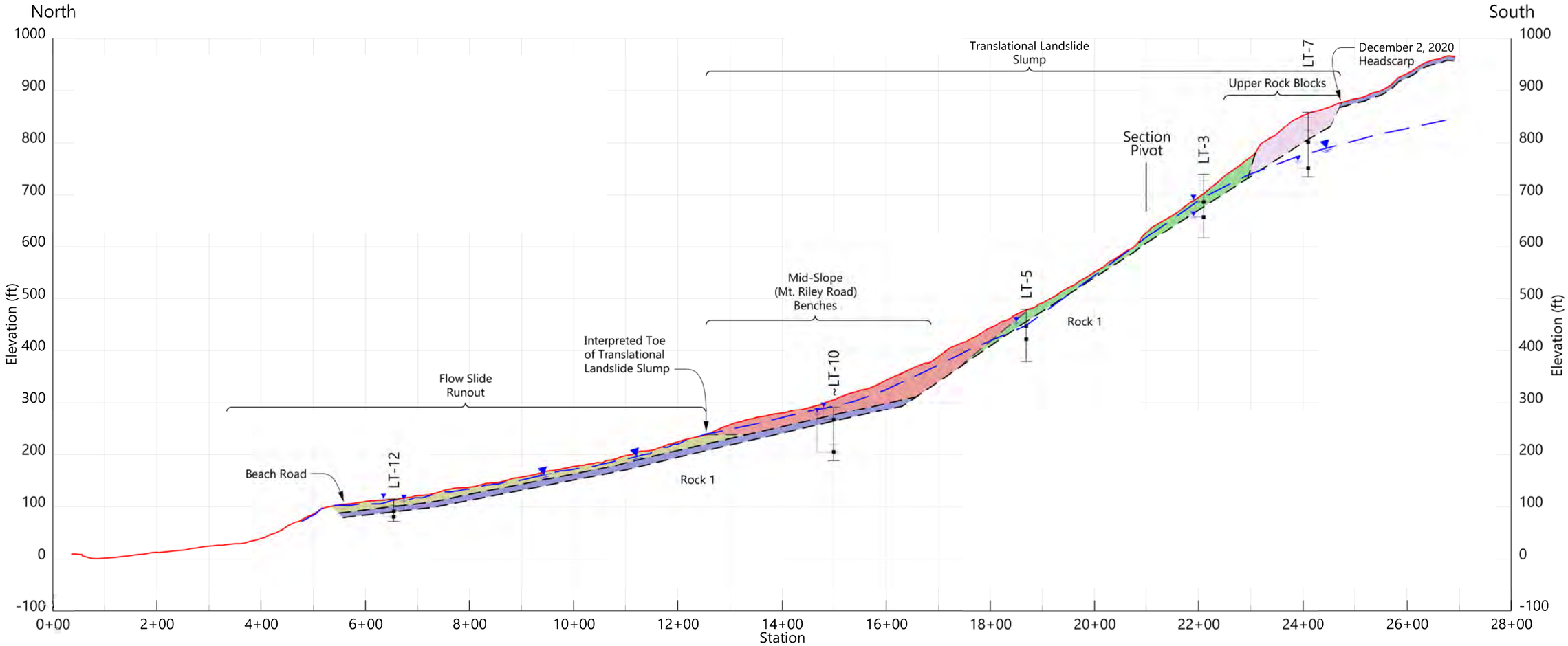

Source: Ground surface derived from December 2020 lidar data provided by DGGS.

LANDSLIDE TECHNOLOGY
A DIVISION OF CORNFORTH CONSULTANTS
10250 S.W. Greenburg Road, Suite 111
Portland, Oregon 97223
Main 503-452-1200 Fax 503-452-1528

Interpreted 2020 Section 1A

Updated Findings Report - Beach Rd Landslide
Haines, Alaska

MAR 2022
PROJ. 2925
FIG. 19

LEGEND:

- Rock 1 - Low Stress-Relief, In-place, Uninflated
- Rock 2 - Moderate to High Stress-Relief, Inflated
- Rock 3 - Moderate to High Stress-Relief, Inflated and Displaced
- Colluvium 1 - Weathered in-Place
- Colluvium 2 - Talus Deposits
- Colluvium 3 - Slumped and Flow Deposits
- Colluvium 4 - Debris Flow and Flood Deposits

- 2014 Ground Surface
- 2020 Ground Surface
- Groundwater Pressure Surface

Piezometer Pressures — LT-10
- Unit contact, typical
- Upper Piezometer
- Lower Piezometer

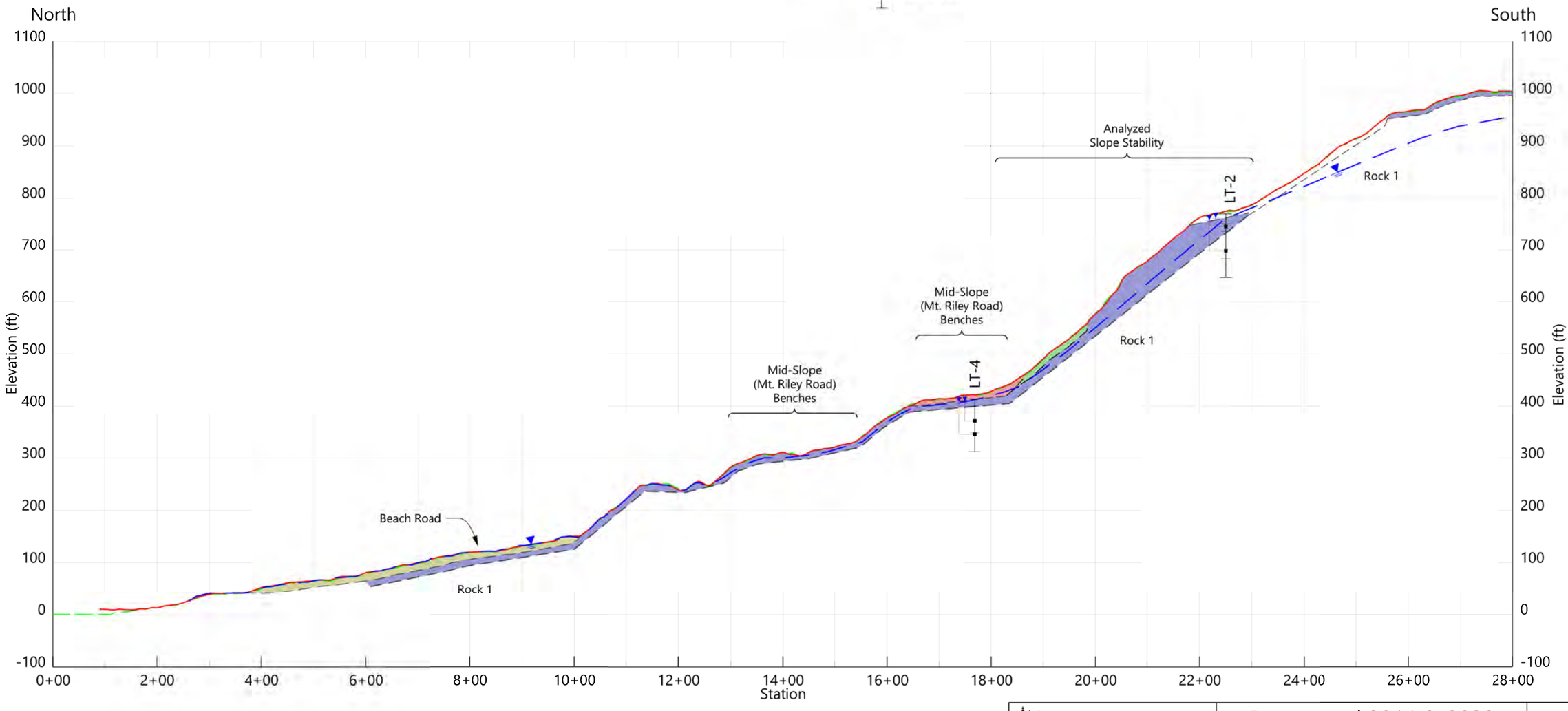

Source: Ground surface derived from 2014 and 2020 lidar data provided by DGGS.

LANDSLIDE TECHNOLOGY
A DIVISION OF CORNFORTH CONSULTANTS
10250 S.W. Greenburg Road, Suite 111
Portland, Oregon 97223
Main 503-452-1200 Fax 503-452-1528

Interpreted 2014 & 2020 Section 2

Updated Findings Report - Beach Rd Landslide
Haines, Alaska

MAR 2022
PROJ. 2925
FIG. 20

LEGEND:

- Rock 1 - Low Stress-Relief, In-place, Uninflated
- Rock 2 - Moderate to High Stress-Relief, Inflated
- Rock 3 - Moderate to High Stress-Relief, Inflated and Displaced
- Colluvium 1 - Weathered in-Place
- Colluvium 2 - Talus Deposits
- Colluvium 3 - Slumped and Flow Deposits
- Colluvium 4 - Debris Flow and Flood Deposits

- 2014 Ground Surface
- 2020 Ground Surface
- Groundwater Pressure Surface

Piezometer Pressures — LT-10
- Unit contact, typical
- Upper Piezometer
- Lower Piezometer

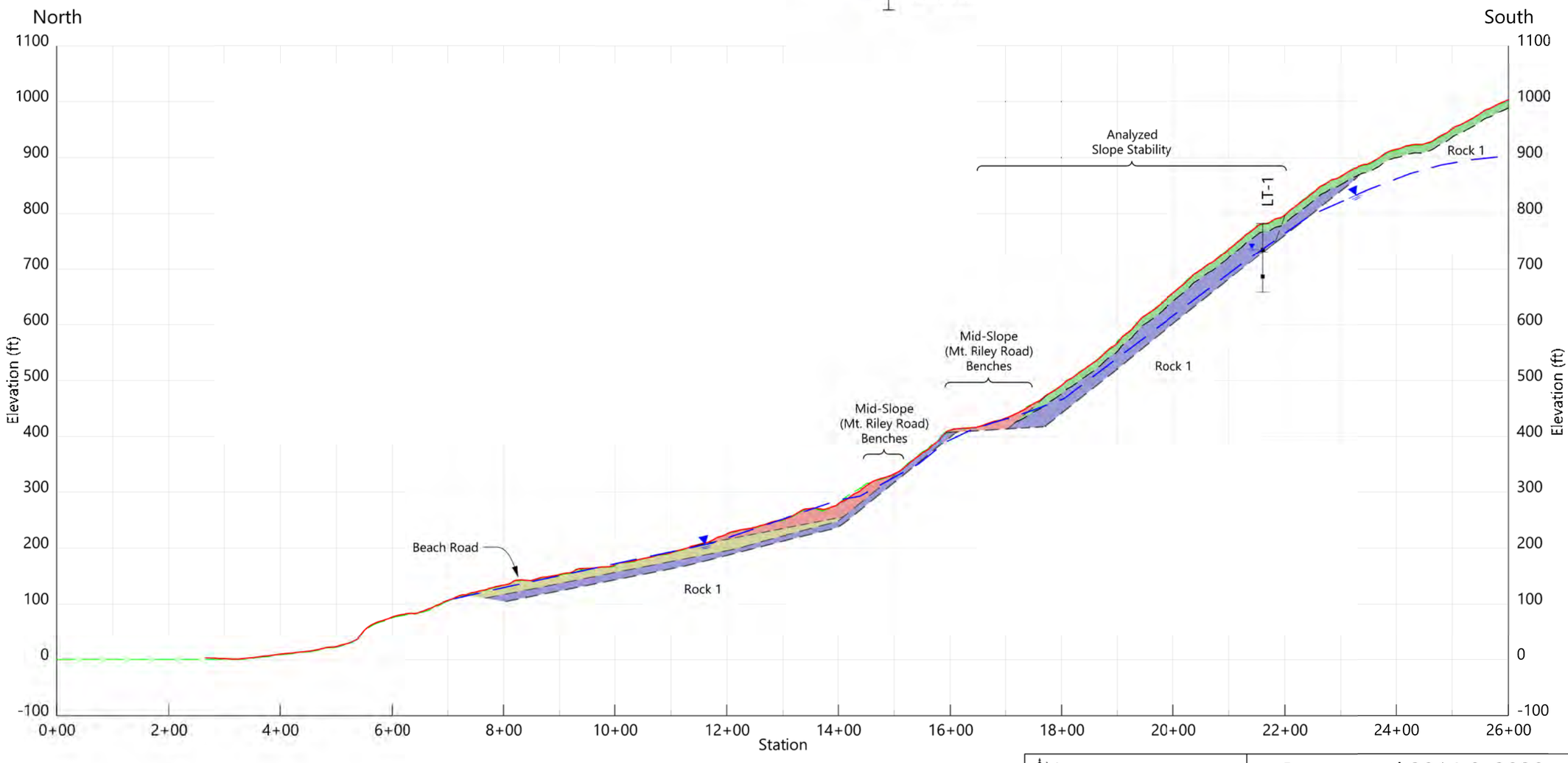

Source: Ground surface derived from 2014 and 2020 lidar data provided by DGGS.

LANDSLIDE TECHNOLOGY
A DIVISION OF CORNFORTH CONSULTANTS
10250 S.W. Greenburg Road, Suite 111
Portland, Oregon 97223
Main 503-452-1200 Fax 503-452-1528

Interpreted 2014 & 2020 Section 3

Updated Findings Report - Beach Rd Landslide
Haines, Alaska

MAR 2022
PROJ. 2925
FIG. 21

LEGEND:

- Rock 1 - Low Stress-Relief, In-place, Uninflated
- Rock 2 - Moderate to High Stress-Relief, Inflated
- Rock 3 - Moderate to High Stress-Relief, Inflated and Displaced
- Colluvium 1 - Weathered in-Place
- Colluvium 2 - Talus Deposits
- Colluvium 3 - Slumped and Flow Deposits
- Colluvium 4 - Debris Flow and Flood Deposits

- 2014 Ground Surface
- 2020 Ground Surface
- Groundwater Pressure Surface

Piezometer Pressures — LT-10
- Unit contact, typical
- Upper Piezometer
- Lower Piezometer

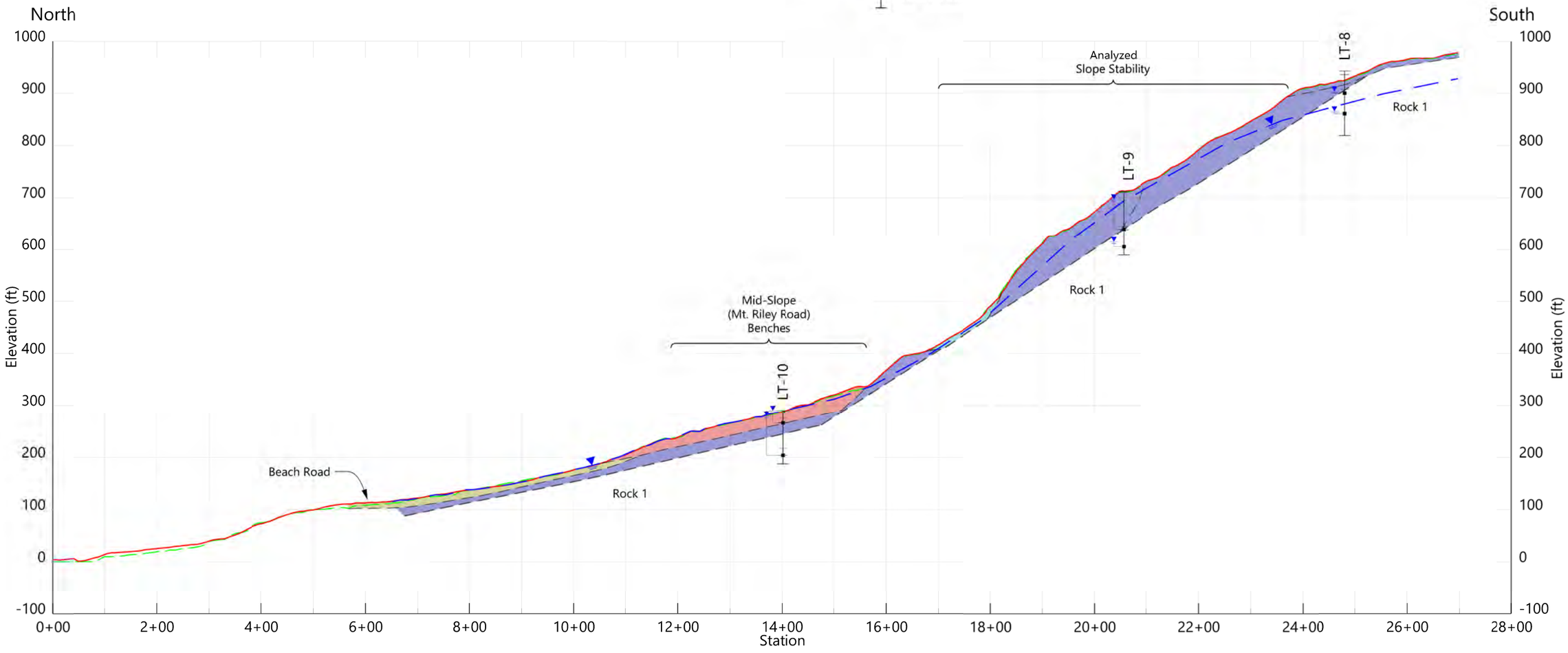

Source: Ground surface derived from 2014 and 2020 lidar data provided by DGGS.

LANDSLIDE TECHNOLOGY
A DIVISION OF CORNFORTH CONSULTANTS
10250 S.W. Greenburg Road, Suite 111
Portland, Oregon 97223
Main 503-452-1200 Fax 503-452-1528

Interpreted 2014 & 2020 Section 4

Updated Findings Report - Beach Rd Landslide
Haines, Alaska

MAR 2022
PROJ. 2925
FIG. 22

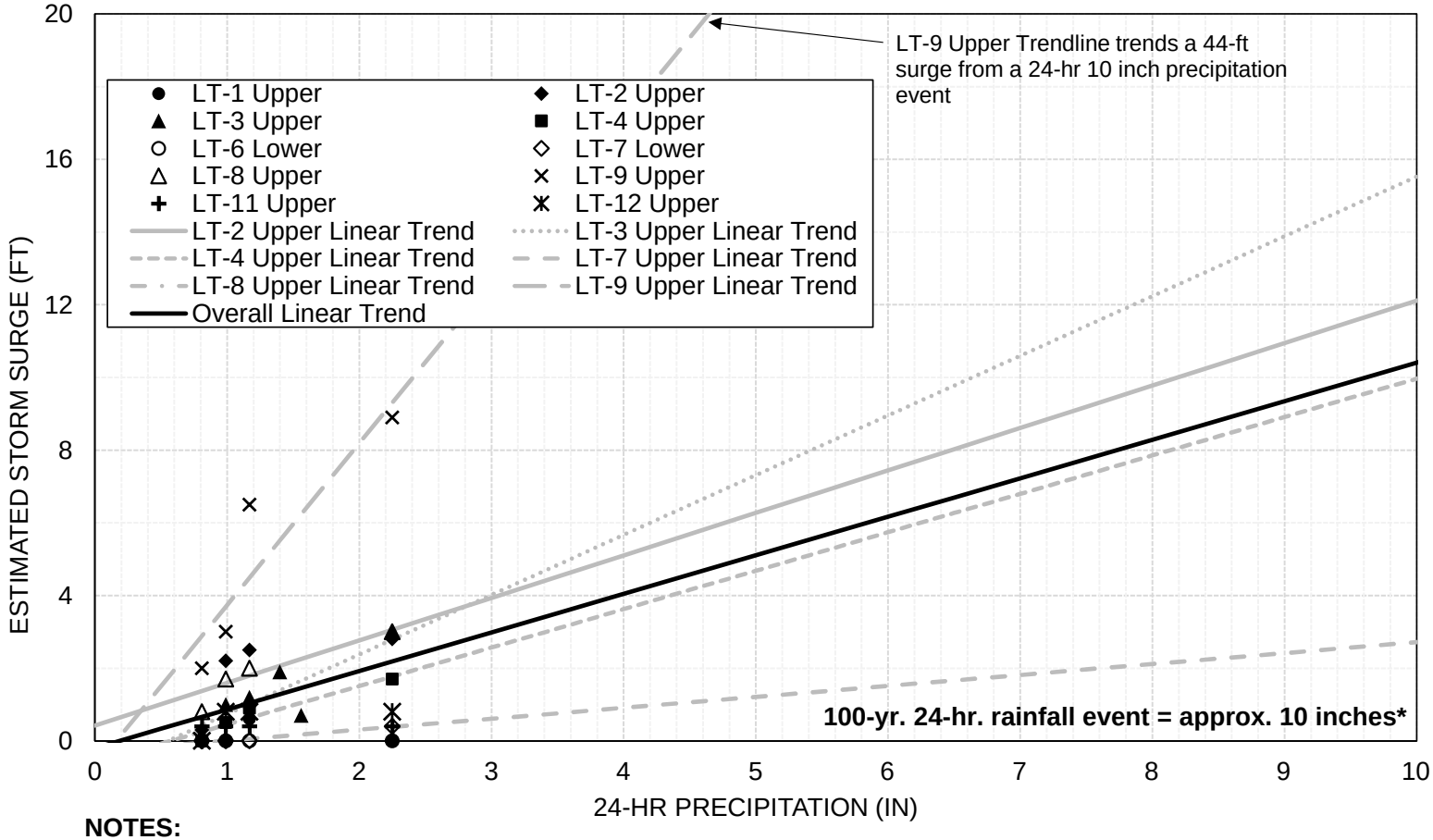

NOTES:

- A 24-hr period is denoted as one calendar day in the Haines, AK time zone
- Linear trendlines were developed from estimated increase in groundwater levels from a 24-hr precipitation event greater than 0.8 inches from October 01, 2021 to February 22, 2022
- The overall trendline was developed from all groundwater surge estimates
- LT-10 and LT-5 were omitted due to noise in VWP readings

*Figure 3-59: Technical Paper No. 47: Probability Maximum Precipitation and Rainfall-Frequency Data for Alaska (1963)

LANDSLIDE TECHNOLOGY
A DIVISION OF CORNFORTH CONSULTANTS
10250 S.W. Greenburg Road, Suite 111
Portland, Oregon 97223
Phone 503-452-1200 Fax 503-452-1528

24-Hr Precipitation Groundwater Surge Estimation

Updated Findings Report - Beach Rd Landslide
Haines, Alaska

MAR 2022
PROJ. 2925
FIG. 23

LEGEND:

- Rock 1 - Low Stress-Relief, In-place, Uninflated
- Rock 2 - Moderate to High Stress-Relief, Inflated
- Rock 3 - Moderate to High Stress-Relief, Inflated and Displaced
- Colluvium 1 - Weathered in-Place
- Colluvium 2 - Talus Deposits
- Colluvium 3 - Slumped and Flow Deposits
- Colluvium 4 - Debris Flow and Flood Deposits

- 2020 Ground Surface
- Modeled Silp-Surface
- Assumed Groundwater Pressure Surface

Piezometer Pressures — LT-10: Unit contact, typical; Upper Piezometer; Lower Piezometer

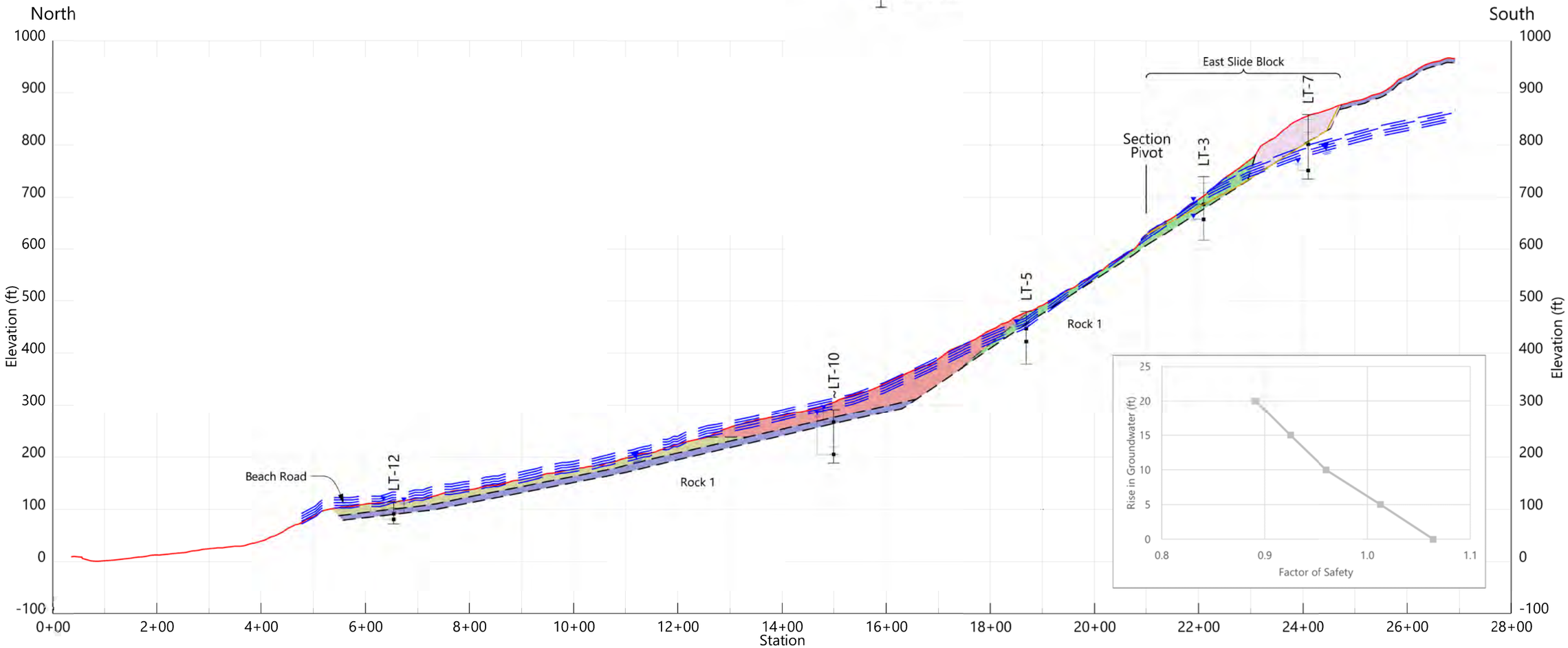

Source: Ground surface derived from December 2020 lidar data provided by DGGS.

LANDSLIDE TECHNOLOGY
A DIVISION OF CORNFORTH CONSULTANTS
10250 S.W. Greenburg Road, Suite 111
Portland, Oregon 97223
Main 503-452-1200 Fax 503-452-1528

Section 1A Back Analysis

Updated Findings Report - Beach Rd Landslide
Haines, Alaska

MAR 2022
PROJ. 2925
FIG. 24

LEGEND:

- Rock 1 - Low Stress-Relief, In-place, Uninflated
- Rock 2 - Moderate to High Stress-Relief, Inflated
- Rock 3 - Moderate to High Stress-Relief, Inflated and Displaced
- Colluvium 1 - Weathered in-Place
- Colluvium 2 - Talus Deposits
- Colluvium 3 - Slumped and Flow Deposits
- Colluvium 4 - Debris Flow and Flood Deposits

- 2014 Ground Surface
- Modeled Silp-Surface
- Assumed Groundwater Pressure Surface

Piezometer Pressures
- LT-10
- Unit contact, typical
- Upper Piezometer
- Lower Piezometer

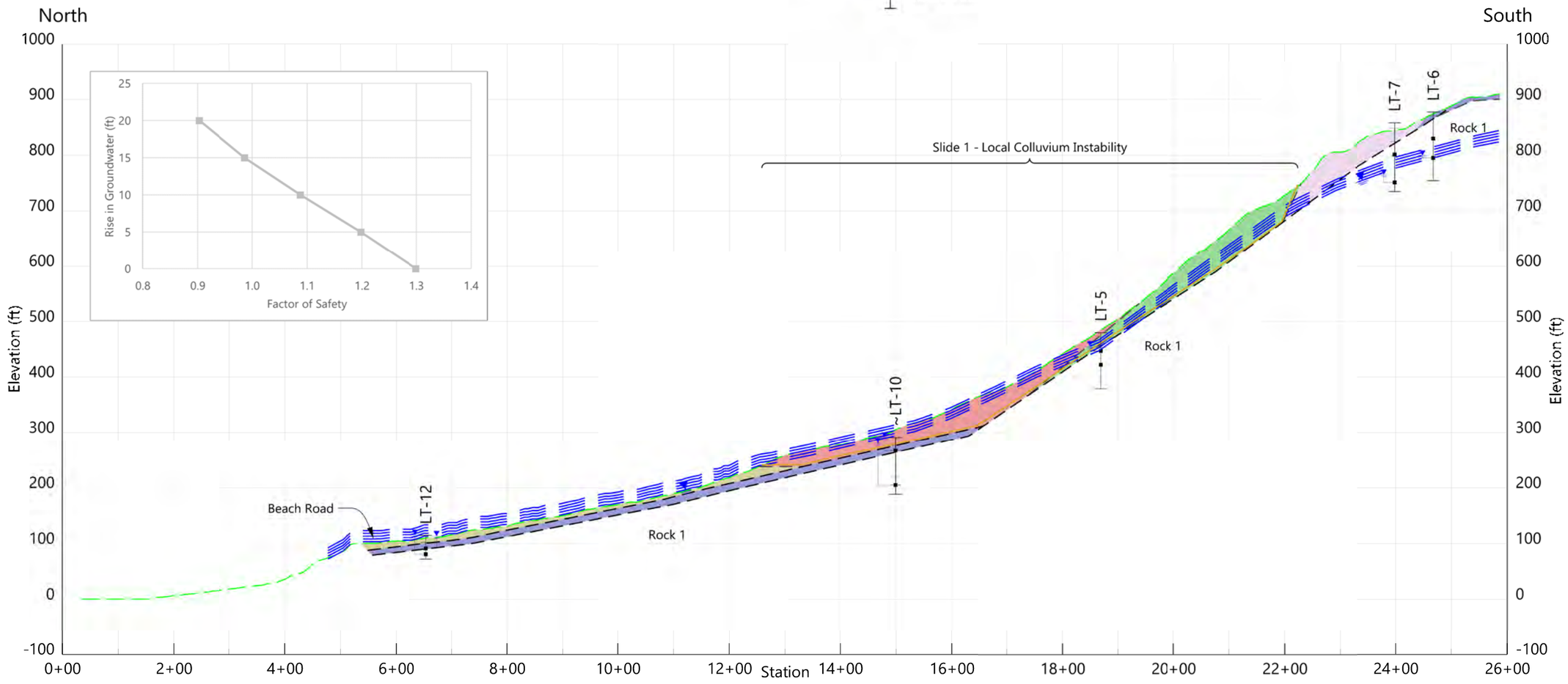

Source: Ground surface derived from December 2020 lidar data provided by DGGS.

LANDSLIDE TECHNOLOGY
A DIVISION OF CORNFORTH CONSULTANTS
10250 S.W. Greenburg Road, Suite 111
Portland, Oregon 97223
Main 503-452-1200 Fax 503-452-1528

Section 1
Slide 1 Analysis (Pre-Failure)

Updated Findings Report - Beach Rd Landslide
Haines, Alaska

MAR 2022
PROJ. 2925
FIG. 25

LEGEND:

- Rock 1 - Low Stress-Relief, In-place, Uninflated
- Rock 2 - Moderate to High Stress-Relief, Inflated
- Rock 3 - Moderate to High Stress-Relief, Inflated and Displaced
- Colluvium 1 - Weathered in-Place
- Colluvium 2 - Talus Deposits
- Colluvium 3 - Slumped and Flow Deposits
- Colluvium 4 - Debris Flow and Flood Deposits

- 2014 Ground Surface
- 2020 Ground Surface
- Modeled Silp-Surface
- Assumed Groundwater Pressure Surface

Piezometer Pressures — LT-10
- Unit contact, typical
- Upper Piezometer
- Lower Piezometer

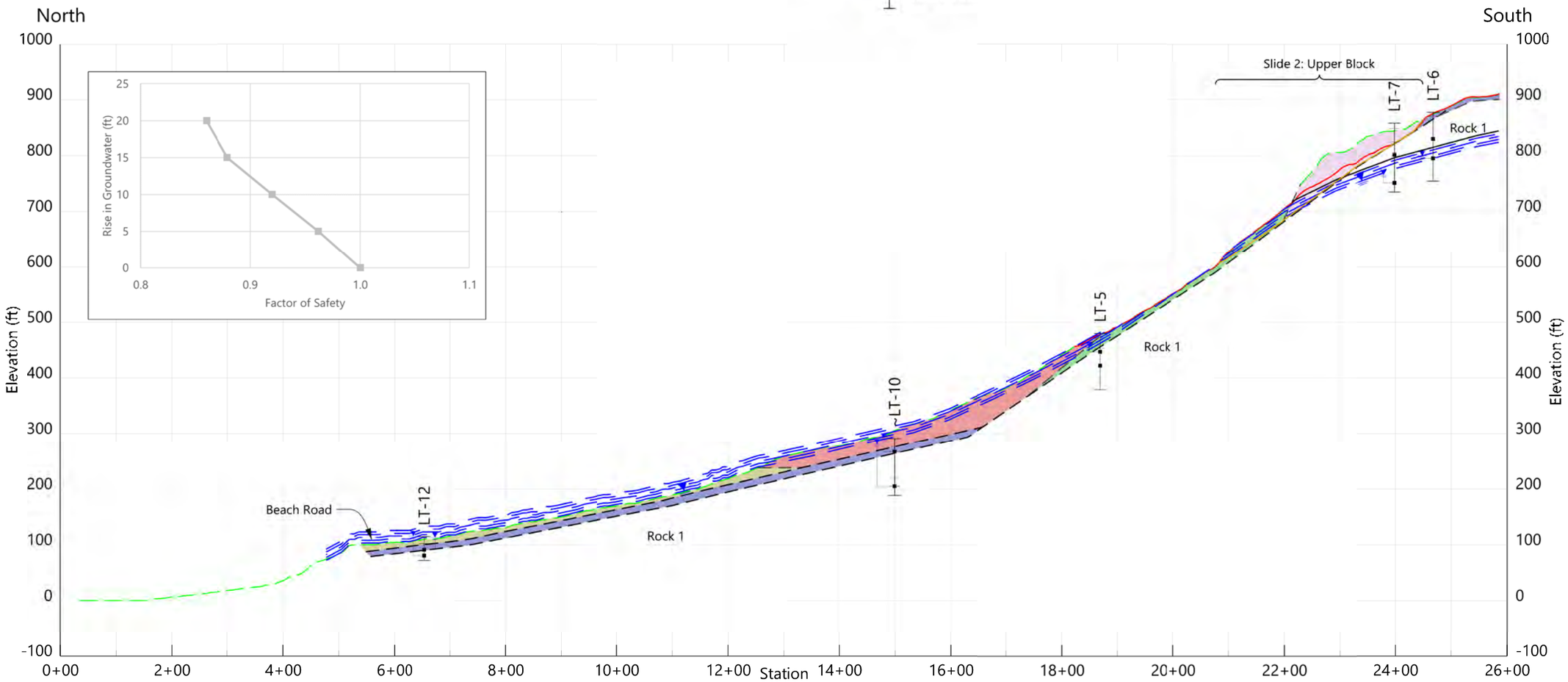

Source: Ground surface derived from December 2020 lidar data provided by DGGS.

LANDSLIDE TECHNOLOGY
A DIVISION OF CORNFORTH CONSULTANTS
10250 S.W. Greenburg Road, Suite 111
Portland, Oregon 97223
Main 503-452-1200 Fax 503-452-1528

Section 1
Slide 2 Analysis (Pre-Failure)

Updated Findings Report - Beach Rd Landslide
Haines, Alaska

MAR 2022
PROJ. 2925
FIG. 26

LEGEND:

- Rock 1 - Low Stress-Relief, In-place, Uninflated
- Rock 2 - Moderate to High Stress-Relief, Inflated
- Rock 3 - Moderate to High Stress-Relief, Inflated and Displaced
- Colluvium 1 - Weathered in-Place
- Colluvium 2 - Talus Deposits
- Colluvium 3 - Slumped and Flow Deposits
- Colluvium 4 - Debris Flow and Flood Deposits

- 2014 Ground Surface
- Modeled Silp-Surface
- Assumed Groundwater Pressure Surface

Piezometer Pressures — LT-10
- Unit contact, typical
- Upper Piezometer
- Lower Piezometer

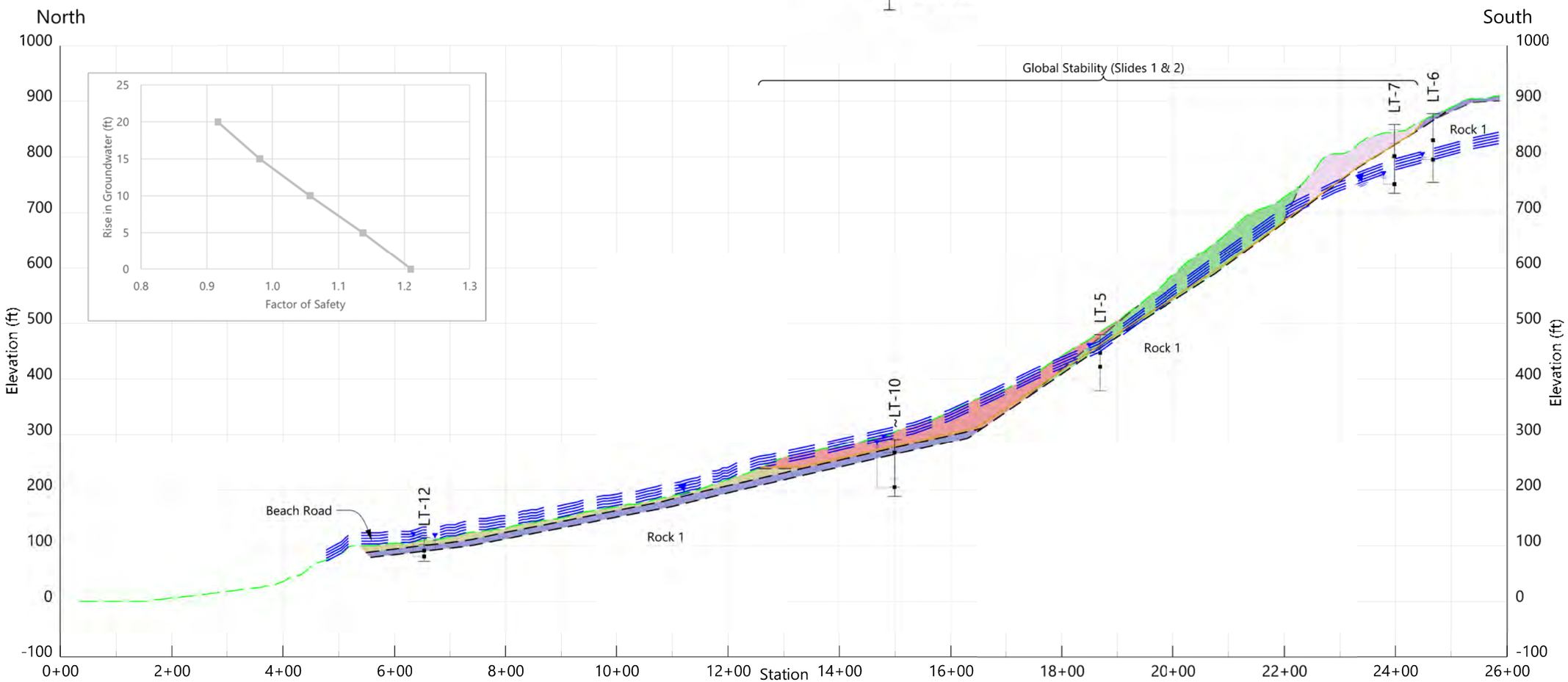

Source: Ground surface derived from December 2020 lidar data provided by DGGS.

LANDSLIDE TECHNOLOGY
A DIVISION OF CORNFORTH CONSULTANTS
10250 S.W. Greenburg Road, Suite 111
Portland, Oregon 97223
Main 503-452-1200 Fax 503-452-1528

Section 1 Global Slide Analysis (Pre-Failure)

Updated Findings Report - Beach Rd Landslide
Haines, Alaska

MAR 2022
PROJ. 2925
FIG. 27

LEGEND:

- Rock 1 - Low Stress-Relief, In-place, Uninflated
- Rock 2 - Moderate to High Stress-Relief, Inflated
- Rock 3 - Moderate to High Stress-Relief, Inflated and Displaced
- Colluvium 1 - Weathered in-Place
- Colluvium 2 - Talus Deposits
- Colluvium 3 - Slumped and Flow Deposits
- Colluvium 4 - Debris Flow and Flood Deposits

- 2014 Ground Surface
- 2020 Ground Surface
- Modeled Silp-Surface
- Assumed Groundwater Pressure Surface

Piezometer Pressures — LT-10 — Unit contact, typical; Upper Piezometer; Lower Piezometer

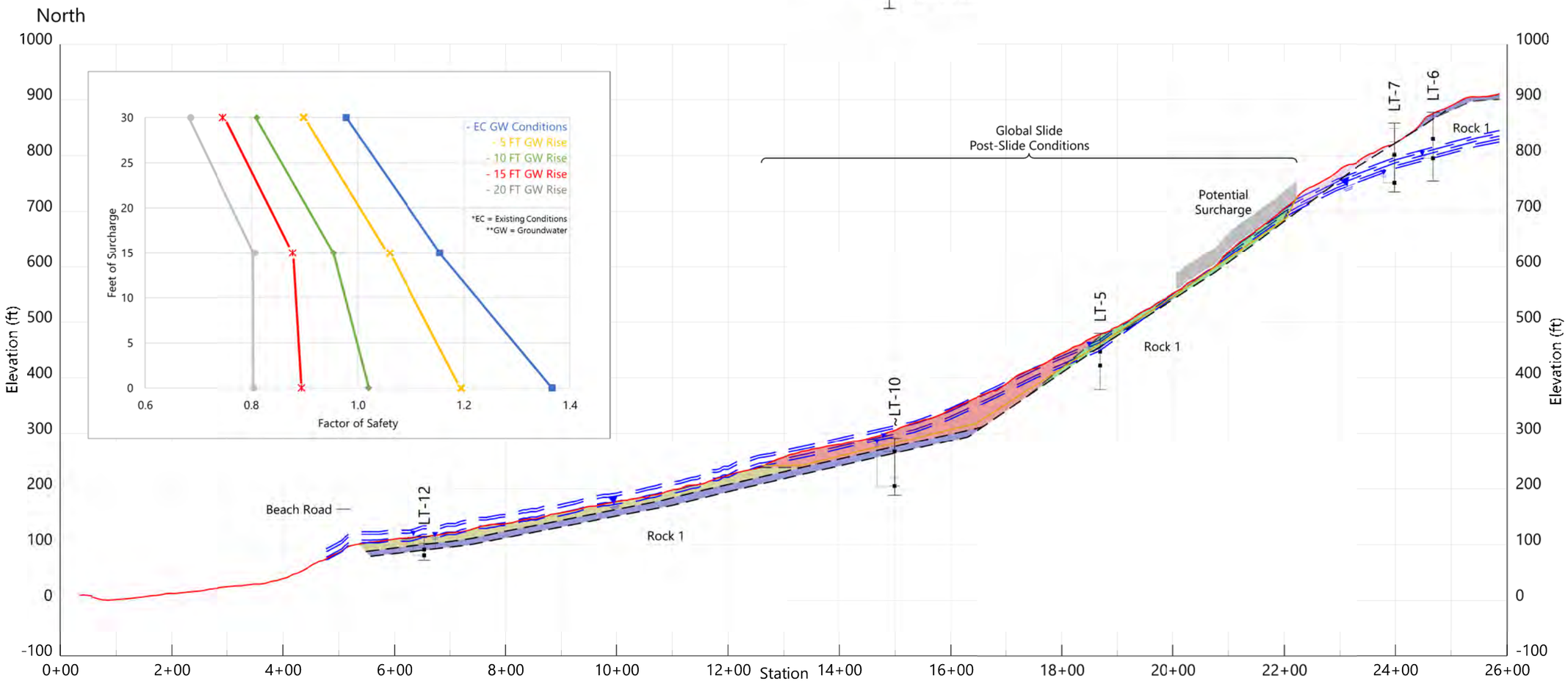

Source: Ground surface derived from December 2020 lidar data provided by DGGS.

LANDSLIDE TECHNOLOGY
A DIVISION OF CORNFORTH CONSULTANTS
10250 S.W. Greenburg Road, Suite 111
Portland, Oregon 97223
Main 503-452-1200 Fax 503-452-1528

Section 1 Global Slide Analysis (Post-Failure)

Updated Findings Report - Beach Rd Landslide
Haines, Alaska

MAR 2022
PROJ. 2925
FIG. 28

LEGEND:

- Rock 1 - Low Stress-Relief, In-place, Uninflated
- Rock 2 - Moderate to High Stress-Relief, Inflated
- Rock 3 - Moderate to High Stress-Relief, Inflated and Displaced
- Colluvium 1 - Weathered in-Place
- Colluvium 2 - Talus Deposits
- Colluvium 3 - Slumped and Flow Deposits
- Colluvium 4 - Debris Flow and Flood Deposits

- 2014 Ground Surface
- 2020 Ground Surface
- Modeled Silp-Surface
- Assumed Groundwater Pressure Surface

Piezometer Pressures — LT-10
- Unit contact, typical
- Upper Piezometer
- Lower Piezometer

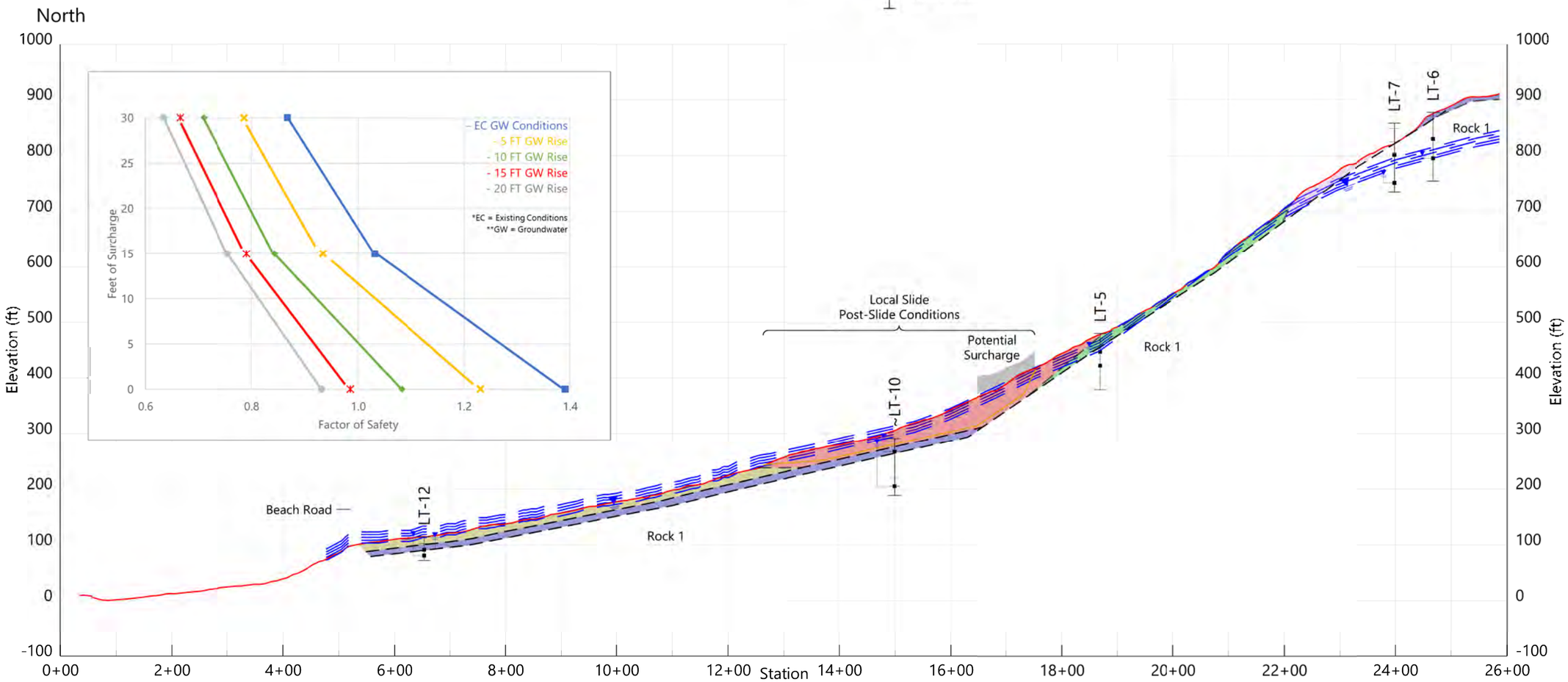

Source: Ground surface derived from December 2020 lidar data provided by DGGS.

LANDSLIDE TECHNOLOGY
A DIVISION OF CORNFORTH CONSULTANTS
10250 S.W. Greenburg Road, Suite 111
Portland, Oregon 97223
Main 503-452-1200 Fax 503-452-1528

Section 1 Local Slide Analysis (Post-Failure)

Updated Findings Report - Beach Rd Landslide
Haines, Alaska

MAR 2022
PROJ. 2925
FIG. 29

LEGEND:

- Rock 1 - Low Stress-Relief, In-place, Uninflated
- Rock 2 - Moderate to High Stress-Relief, Inflated
- Rock 3 - Moderate to High Stress-Relief, Inflated and Displaced
- Colluvium 1 - Weathered in-Place
- Colluvium 2 - Talus Deposits
- Colluvium 3 - Slumped and Flow Deposits
- Colluvium 4 - Debris Flow and Flood Deposits

- 2014 Ground Surface
- 2020 Ground Surface
- Modeled Silp-Surface
- Assumed Groundwater Pressure Surface

Piezometer Pressures — LT-10
- Unit contact, typical
- Upper Piezometer
- Lower Piezometer

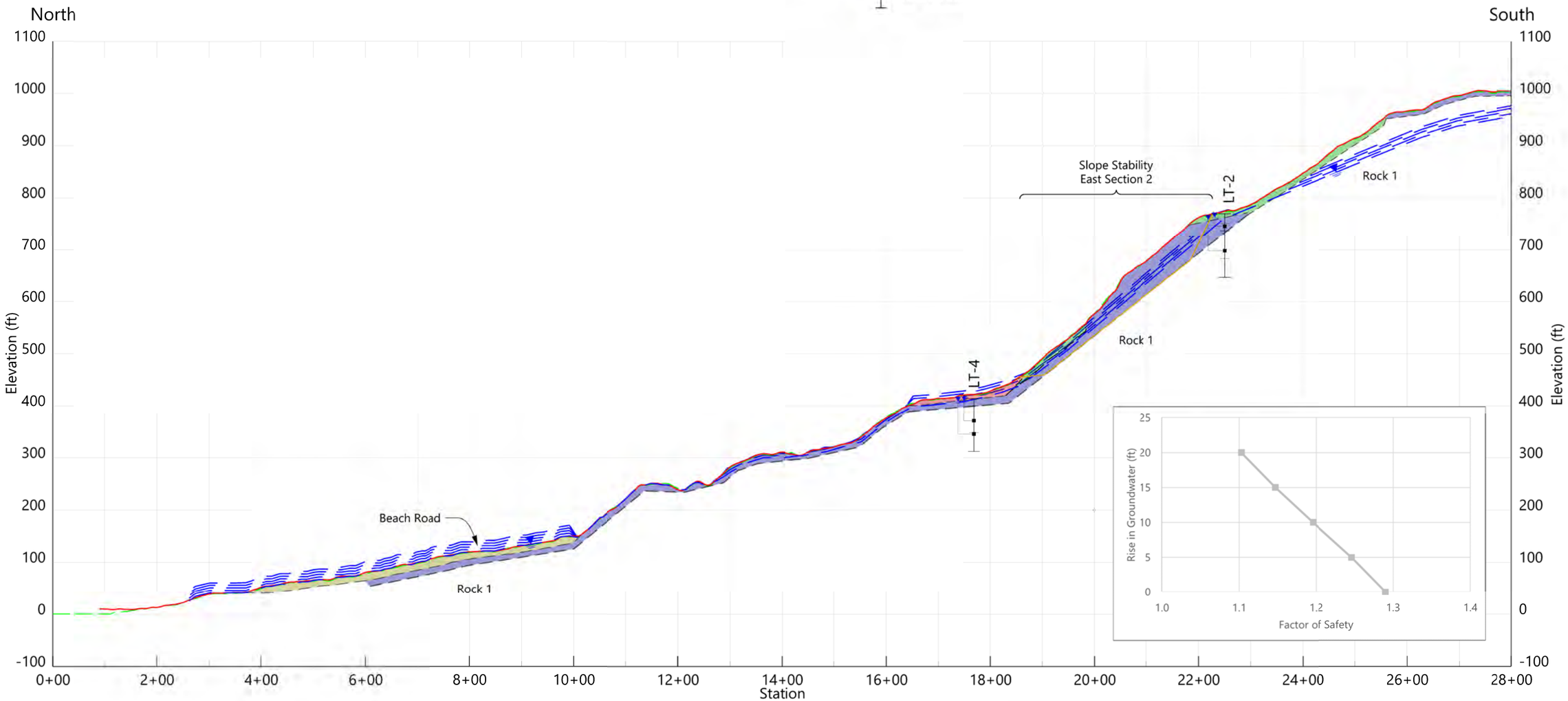

Source: Ground surface derived from 2014 & 2020 lidar data provided by DGGS.

LANDSLIDE TECHNOLOGY
A DIVISION OF CORNFORTH CONSULTANTS
10250 S.W. Greenburg Road, Suite 111
Portland, Oregon 97223
Main 503-452-1200 Fax 503-452-1528

Section 2
Slope Stability Analysis

Updated Findings Report - Beach Rd Landslide
Haines, Alaska

MAR 2022
PROJ. 2925
FIG. 30

LEGEND:

- Rock 1 - Low Stress-Relief, In-place, Uninflated
- Rock 2 - Moderate to High Stress-Relief, Inflated
- Rock 3 - Moderate to High Stress-Relief, Inflated and Displaced
- Colluvium 1 - Weathered in-Place
- Colluvium 2 - Talus Deposits
- Colluvium 3 - Slumped and Flow Deposits
- Colluvium 4 - Debris Flow and Flood Deposits

- 2014 Ground Surface
- 2020 Ground Surface
- Modeled Silp-Surface
- Assumed Groundwater Pressure Surface

Piezometer Pressures — LT-10
- Unit contact, typical
- Upper Piezometer
- Lower Piezometer

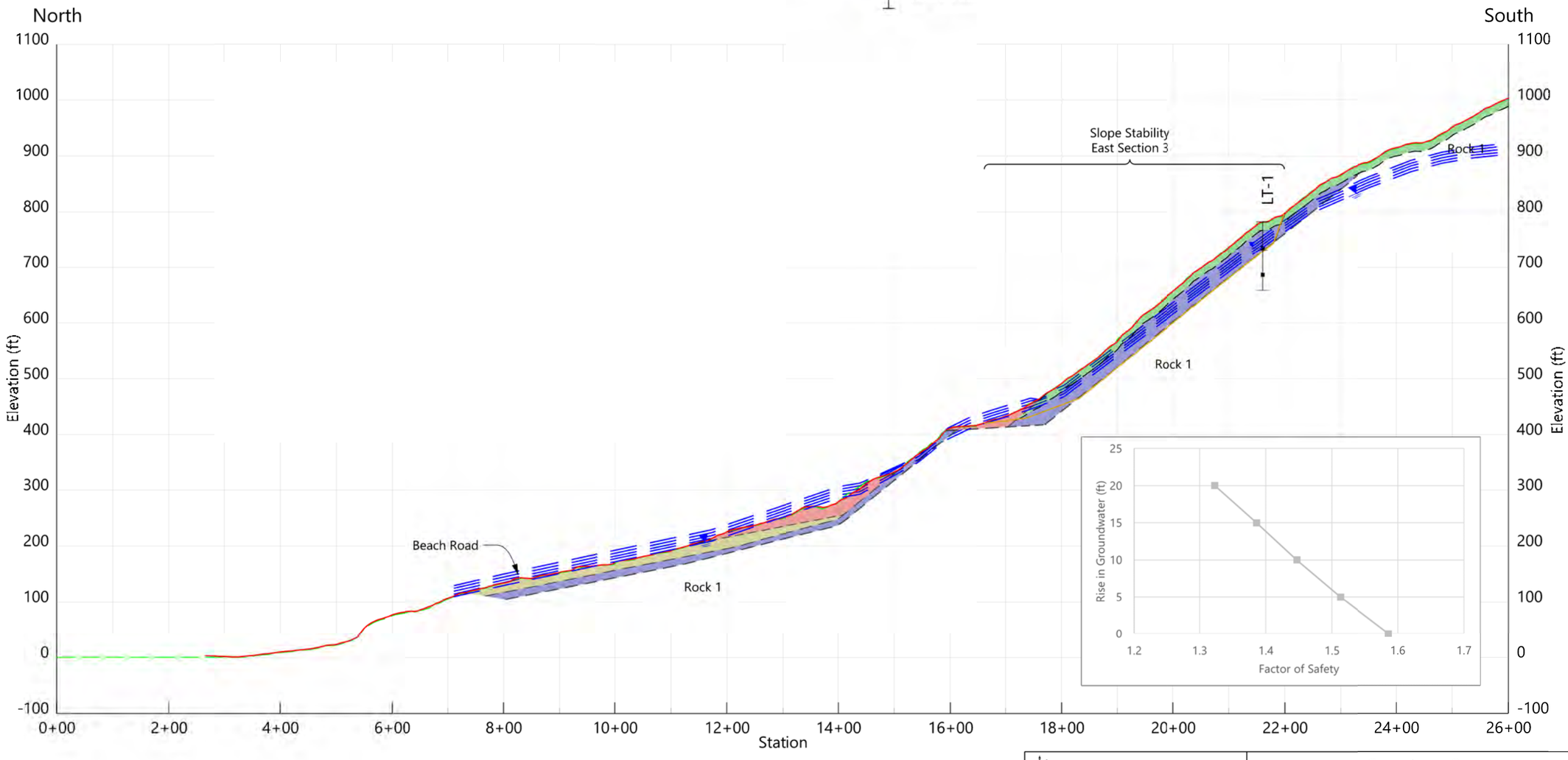

Source: Ground surface derived from 2014 & 2020 lidar data provided by DGGS.

LANDSLIDE TECHNOLOGY
A DIVISION OF CORNFORTH CONSULTANTS
10250 S.W. Greenburg Road, Suite 111
Portland, Oregon 97223
Main 503-452-1200 Fax 503-452-1528

Section 3
Slope Stability Analysis

Updated Findings Report - Beach Rd Landslide
Haines, Alaska

MAR 2022
PROJ. 2925
FIG. 31

LEGEND:

- Rock 1 - Low Stress-Relief, In-place, Uninflated
- Rock 2 - Moderate to High Stress-Relief, Inflated
- Rock 3 - Moderate to High Stress-Relief, Inflated and Displaced
- Colluvium 1 - Weathered in-Place
- Colluvium 2 - Talus Deposits
- Colluvium 3 - Slumped and Flow Deposits
- Colluvium 4 - Debris Flow and Flood Deposits

- 2014 Ground Surface
- 2020 Ground Surface
- Modeled Silp-Surface
- Assumed Groundwater Pressure Surface

Piezometer Pressures — LT-10 — Unit contact, typical; Upper Piezometer; Lower Piezometer

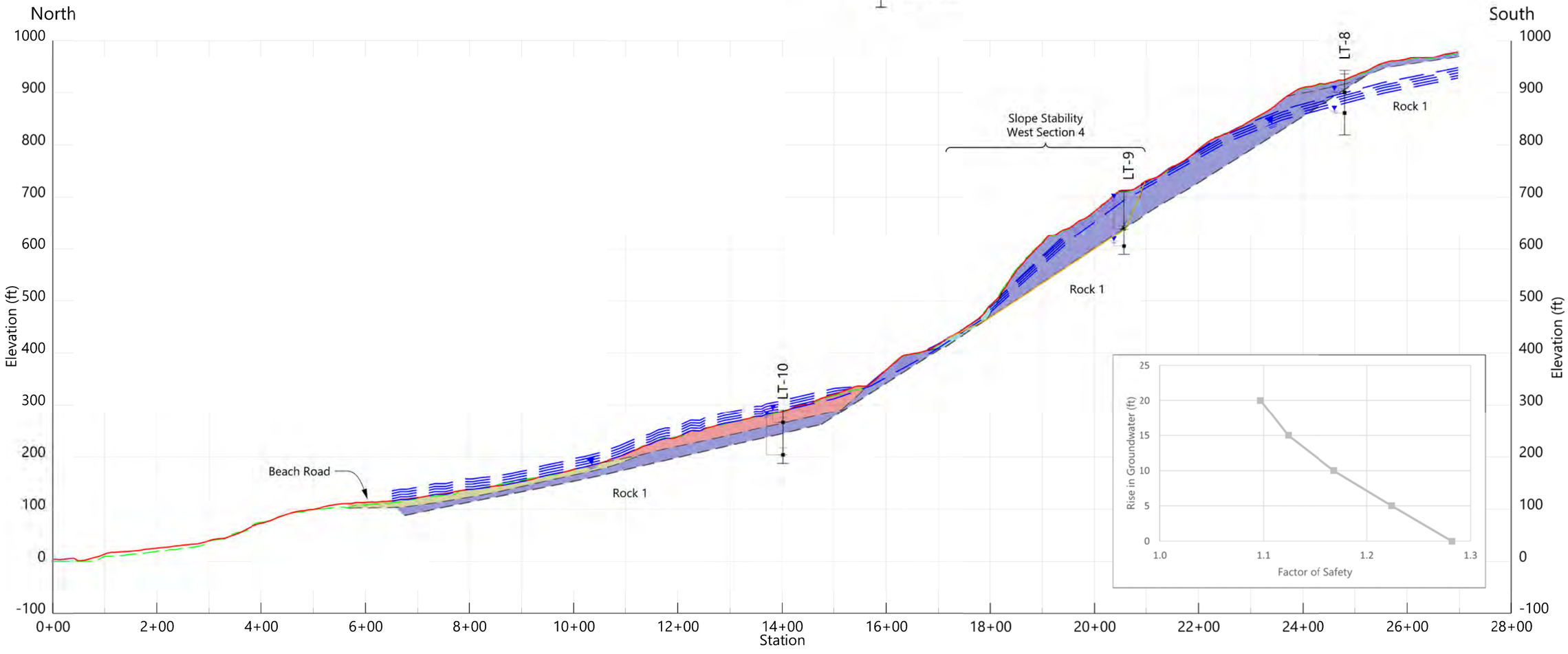

Source: Ground surface derived from 2014 & 2020 lidar data provided by DGGS.

LANDSLIDE TECHNOLOGY
A DIVISION OF CORNFORTH CONSULTANTS
10250 S.W. Greenburg Road, Suite 111
Portland, Oregon 97223
Main 503-452-1200 Fax 503-452-1528

Section 4
Slope Stability Analysis

Updated Findings Report - Beach Rd Landslide
Haines, Alaska

MAR 2022
PROJ. 2925
FIG. 32

Flow-R Source Areas

Haines Borough Area of Concern

Geomorphic Interpretations

Beach Road

Mt. Riley Road

1

2

3

4

5

6

7

0 150 300 600 Feet

Note: Topography derived from 2020 LiDAR data provided by DGGS.

LANDSLIDE TECHNOLOGY
A DIVISION OF CORNFORTH CONSULTANTS
10250 S.W. Greenburg Road, Suite 111
Portland, Oregon 97223
Phone 503-452-1200 Fax 503-452-1528

Source Areas Used for Runout Modeling

Updated Findings Report - Beach Rd Landslide
Haines, Alaska

MAR 2022

PROJ. 2925

FIG. 33

Flow-R Source Areas

Geomorphic Observations

Haines Borough Area of Concern

Likelihood of Flow Paths (%)

0

< 10

10 to 20

20 to 30

30 to 40

40 to 50

> 50

1

2

3

4

5

6

7

0 150 300 600 Feet

Note: Topography derived from 2014 LiDAR data provided by DGGS.

LANDSLIDE TECHNOLOGY
A DIVISION OF CORNFORTH CONSULTANTS
10250 S.W. Greenburg Road, Suite 111
Portland, Oregon 97223
Phone 503-452-1200 Fax 503-452-1528

Back Analysis of 2020 Beach Road Landslide (Model A)

Updated Findings Report - Beach Rd Landslide
Haines, Alaska

MAR 2022

PROJ. 2925

FIG. 34

Flow-R Source Areas

Geomorphic Observations

Haines Borough
Area of Concern

Likelihood of Flow Paths (%)

0

< 10

10 to 20

20 to 30

30 to 40

40 to 50

> 50

1

2

3

4

5

6

7

0 150 300 600 Feet

Note: Topography derived from 2014 LiDAR data provided by DGGS.

LANDSLIDE TECHNOLOGY
A DIVISION OF CORNFORTH CONSULTANTS
10250 S.W. Greenburg Road, Suite 111
Portland, Oregon 97223
Phone 503-452-1200 Fax 503-452-1528

Back Analysis of Debris Flow West of Landslide (Model B)

Updated Findings Report - Beach Rd Landslide
Haines, Alaska

MAR 2022

PROJ. 2925

FIG. 35

Beach Road

Mt. Riley Road

1

2

3

4

5

6

7

N

Flow-R Source Areas

Haines Borough Area of Concern

Geomorphic Interpretations

Likelihood of Flow Paths (%)

0

< 10

10 to 20

20 to 30

30 to 40

40 to 50

> 50

0 150 300 600 Feet

Note: Topography derived from 2020 LiDAR data provided by DGGS.

LANDSLIDE TECHNOLOGY
A DIVISION OF CORNFORTH CONSULTANTS
10250 S.W. Greenburg Road, Suite 111
Portland, Oregon 97223
Phone 503-452-1200 Fax 503-452-1528

Model A Applied to Western Source Areas

Updated Findings Report - Beach Rd Landslide
Haines, Alaska

MAR 2022

PROJ. 2925

FIG. 36

Flow-R Source Areas

Haines Borough Area of Concern

Geomorphic Interpretations

Likelihood of Flow Paths (%)

0

< 10

10 to 20

20 to 30

30 to 40

40 to 50

> 50

Beach Road

Mt. Riley Road

1

2

3

4

5

6

7

0 150 300 600 Feet

Note: Topography derived from 2020 LiDAR data provided by DGGS.

LANDSLIDE TECHNOLOGY
A DIVISION OF CORNFORTH CONSULTANTS
10250 S.W. Greenburg Road, Suite 111
Portland, Oregon 97223
Phone 503-452-1200 Fax 503-452-1528

Model B Applied to Western Source Areas

Updated Findings Report - Beach Rd Landslide
Haines, Alaska

MAR 2022

PROJ. 2925

FIG. 37

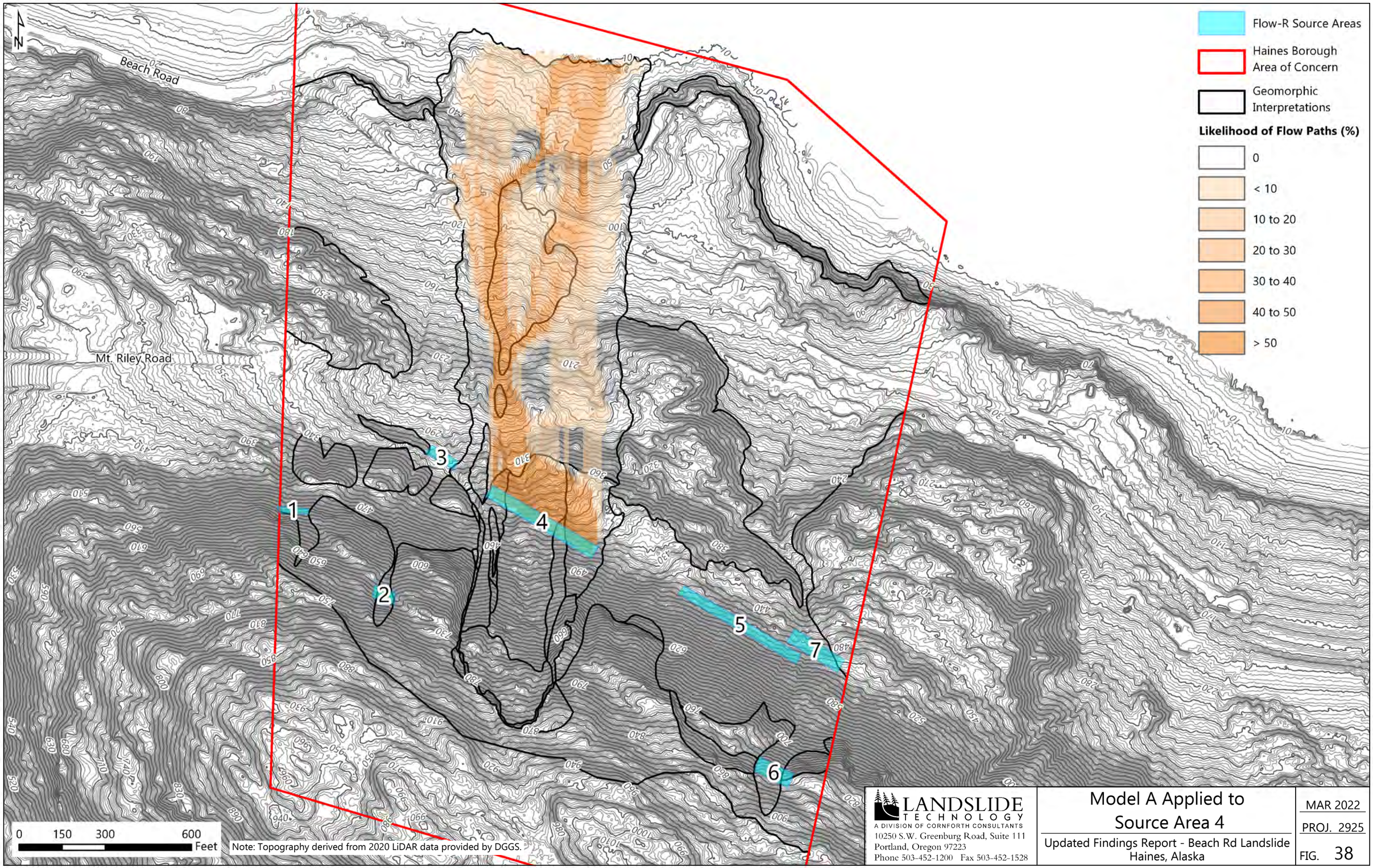

LANDSLIDE TECHNOLOGY
A DIVISION OF CORNFORTH CONSULTANTS
10250 S.W. Greenburg Road, Suite 111
Portland, Oregon 97223
Phone 503-452-1200 Fax 503-452-1528

Model A Applied to Source Area 4

Updated Findings Report - Beach Rd Landslide
Haines, Alaska

MAR 2022
PROJ. 2925
FIG. 38

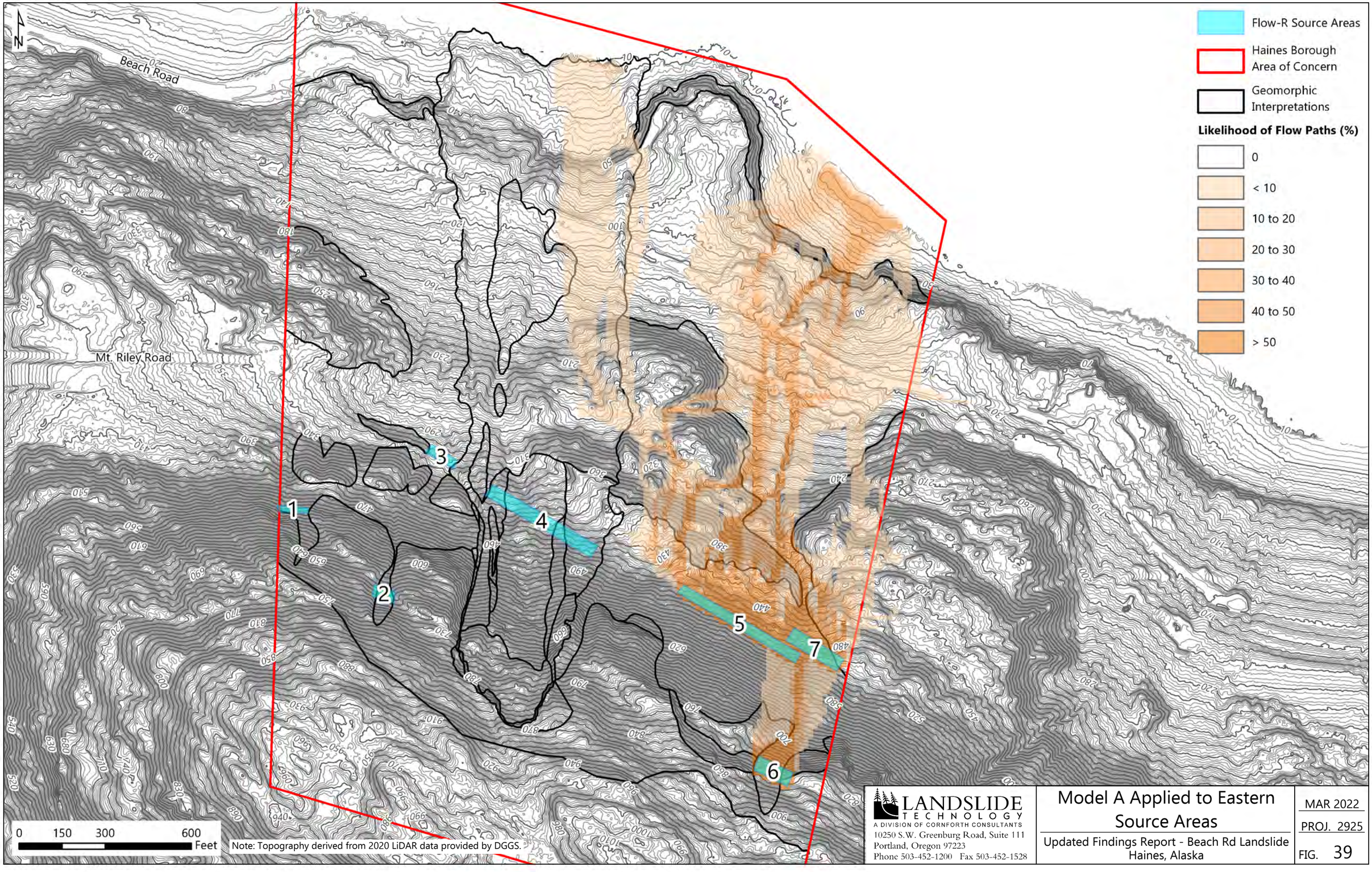

Note: Topography derived from 2020 LiDAR data provided by DGGS.

LANDSLIDE TECHNOLOGY
A DIVISION OF CORNFORTH CONSULTANTS
10250 S.W. Greenburg Road, Suite 111
Portland, Oregon 97223
Phone 503-452-1200 Fax 503-452-1528

Model A Applied to Eastern Source Areas

Updated Findings Report - Beach Rd Landslide
Haines, Alaska

MAR 2022
PROJ. 2925
FIG. 39

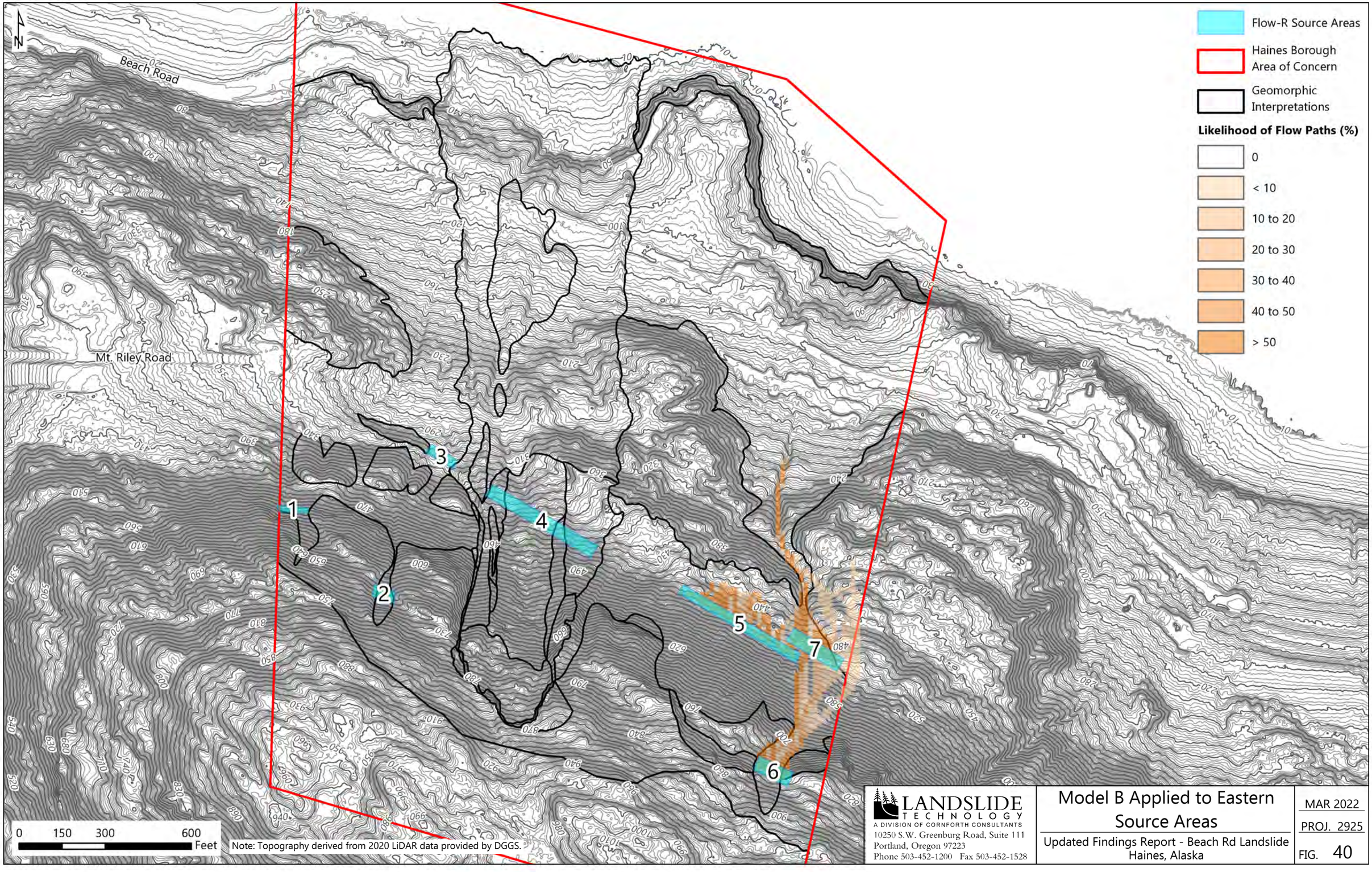

Note: Topography derived from 2020 LiDAR data provided by DGGS.

LANDSLIDE TECHNOLOGY
A DIVISION OF CORNFORTH CONSULTANTS
10250 S.W. Greenburg Road, Suite 111
Portland, Oregon 97223
Phone 503-452-1200 Fax 503-452-1528

Model B Applied to Eastern Source Areas

Updated Findings Report - Beach Rd Landslide
Haines, Alaska

MAR 2022
PROJ. 2925
FIG. 40

GEOLOGIC HAZARD

1. Catastrophic Reactivation of 2020 Landslide Debris (extreme weather)
2. Localized Reactivation of 2020 Landslide Debris (normal weather)
3. Boulders within 2020 Landslide Mass Rolling Downslope
4. Retrogression of 2020 Landslide Over-Steepened Scarps
5. Slump Bounded by Tension Cracks East and West of 2020 Headscarp
6. Global Failure of Bedrock Slopes East and West of 2020 Landslide
7. Global Failure of Colluvial Slopes East and West of 2020 Landslide
8. Weathering/Erosion of Bedrock/Colluvial East and West of 2020 Landslide
9. Seismically Triggered Slope Movements
10. Rockfall from Lateral Scarps
11. Debris Flow Runouts

POTENTIAL IMPACTS

i = Infrastructure (damage to buildings, road, utilities, properties)

p = Public Safety (injury or worse)

NOTE: Risk-informed matrix based on Landslide Technology geologic interpretations and engineering analyses. Refer to Chapter 6 of this *Updated Findings Report* for details of geologic hazards, interpretations and analyses.

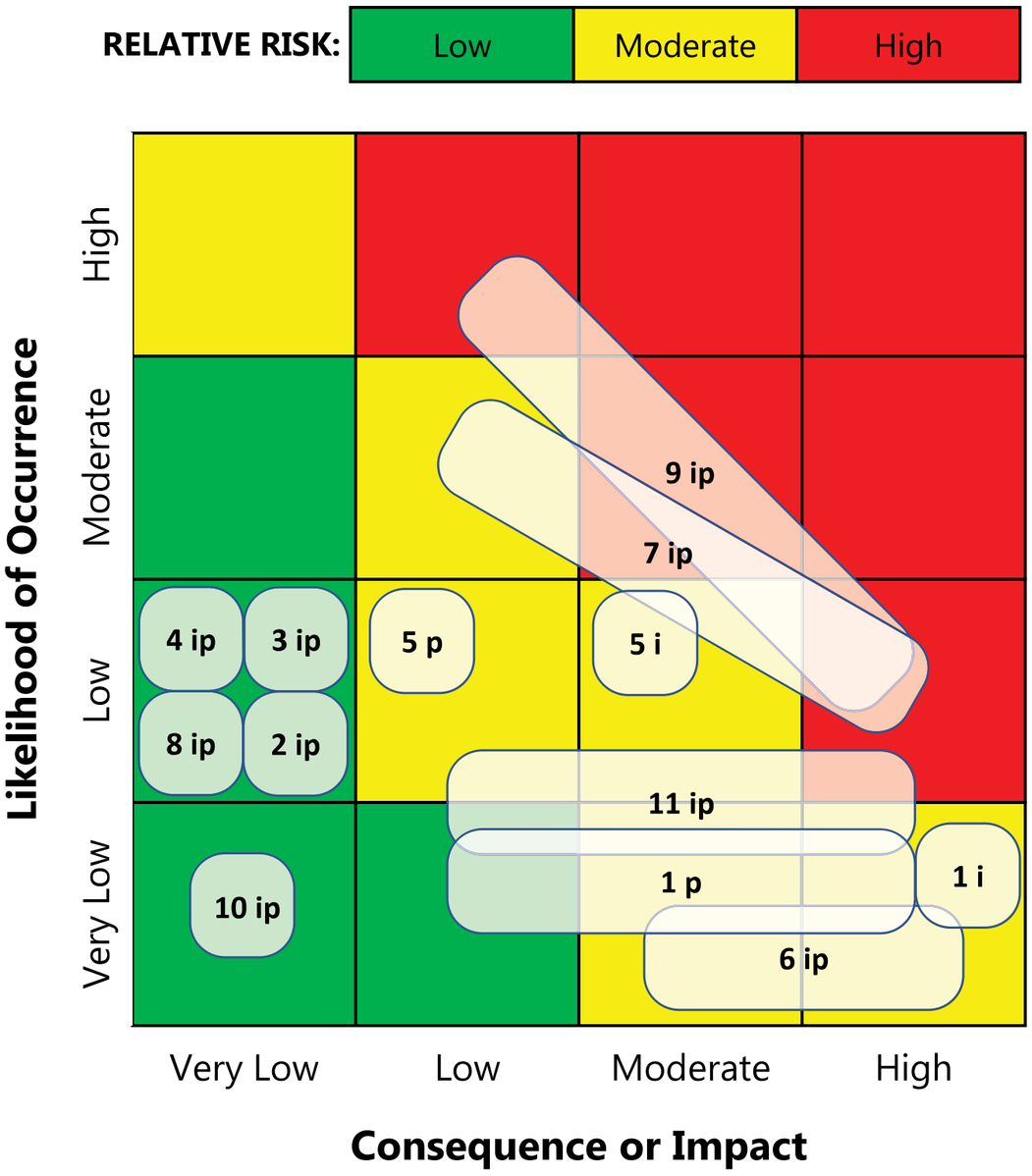

LANDSLIDE TECHNOLOGY
A DIVISION OF CORNFORTH CONSULTANTS
10250 S.W. Greenburg Road, Suite 111
Portland, Oregon 97223
Phone 503-452-1200 Fax 503-452-1528

Risk Informed Decision Matrix

Updated Findings Report - Beach Rd Landslide-Haines, Alaska

MAR 2022

PROJ. 2925

FIG. 41

Appendix A: Photographs – Representative Materials

A: Rock 1 located at elevation 750 feet approximately 1,000 feet east of the 2020 landslide.

B: Rock 2 located at elevation 820-840 feet on the west headscarp of the 2020 landslide.

A: Rock 2 at elevation 600 feet approximately 100 feet west of the 2020 landslide.

B: Rock 3 at elevation 730-750 feet on the West Slump Block, west of the Upper Rock Slump.

A: Rock 3 at elevation 830-840 feet on the East Slump Block, east of the Upper Rock Slump.

B: Colluvium 1 at elevation 650-680 on the West Soil Scarp.

Colluvium 1 at elevation 670-680 on the West Soil Scarp.

Colluvium 1 at elevation 630 feet on the West Soil Scarp.

A: Colluvium 1 at elevation 640 feet on the West Soil Scarp.

B: Colluvium 1 at elevation 620 feet on the West Soil Scarp.

A: Colluvium 2 (newly deposited) at elevation 740-760 feet on the Upper Rock Slump of the 2020 landslide.

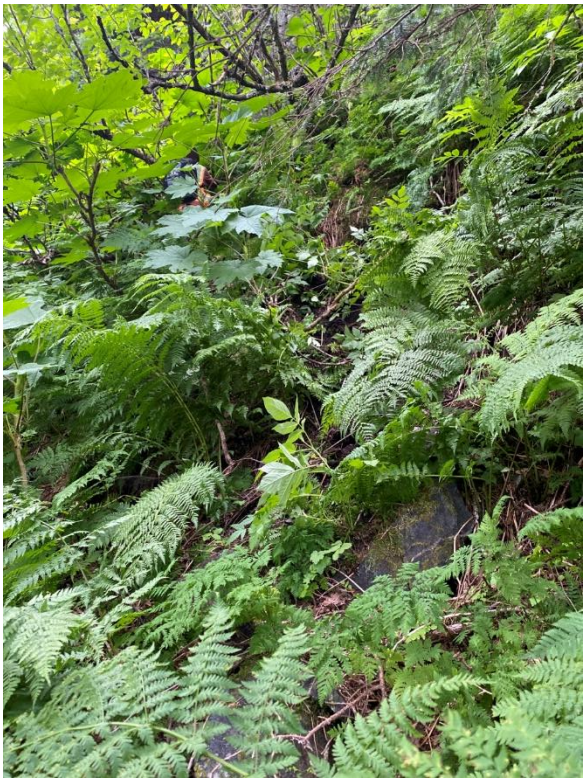

B: Colluvium 2 (overgrown) at elevation 640-660 feet approximately 1,000 feet east of the 2020 landslide

A: Colluvium 3 at elevation 460 feet East Side of Middle Boulder Field.

B: Colluvium 3 at Test Pit No. 27 (elevation 300 feet).

Colluvium 4 at elevation 160 feet on the west side of the Lower Debris Flow.

Appendix B: Transition Zone Imagery

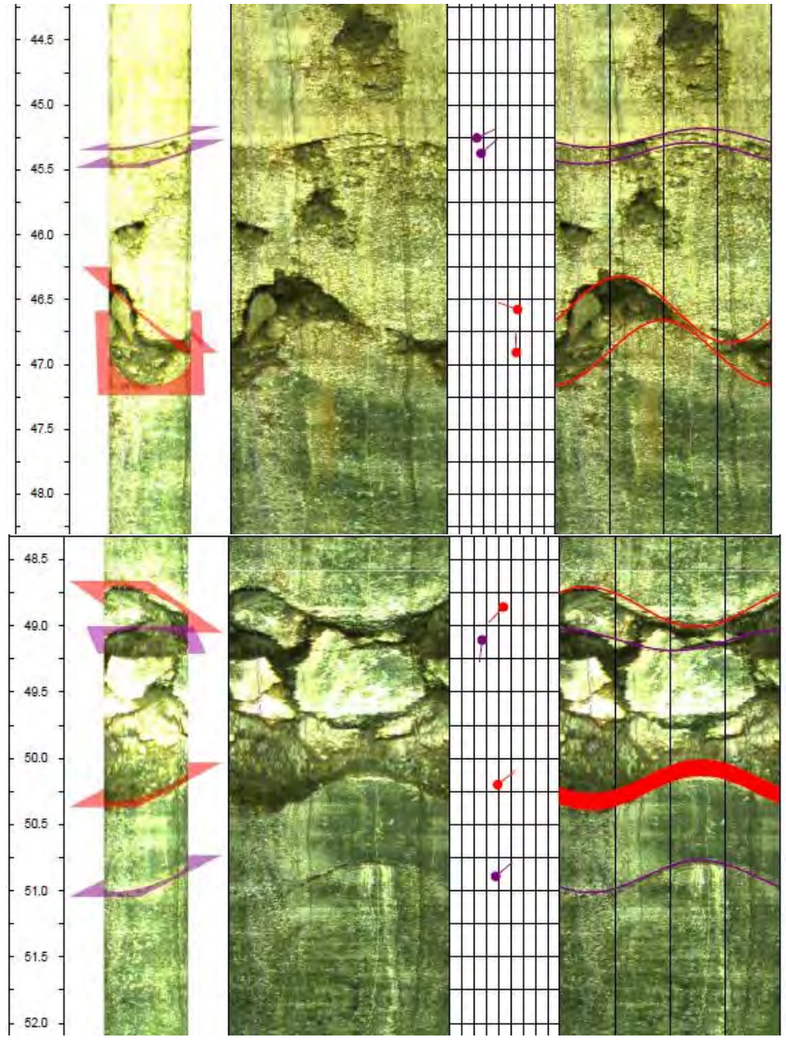

LT-1 transition at 50.8 ft

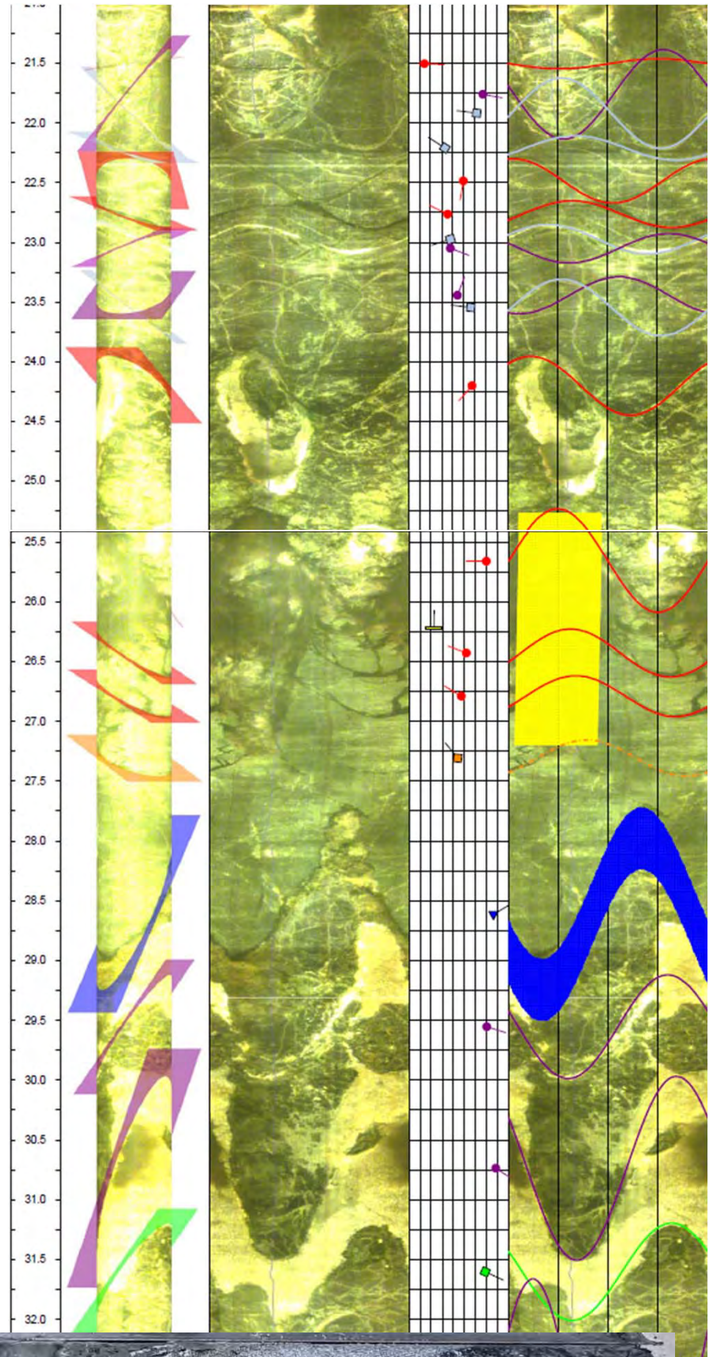

LT-2 transition at 32.8

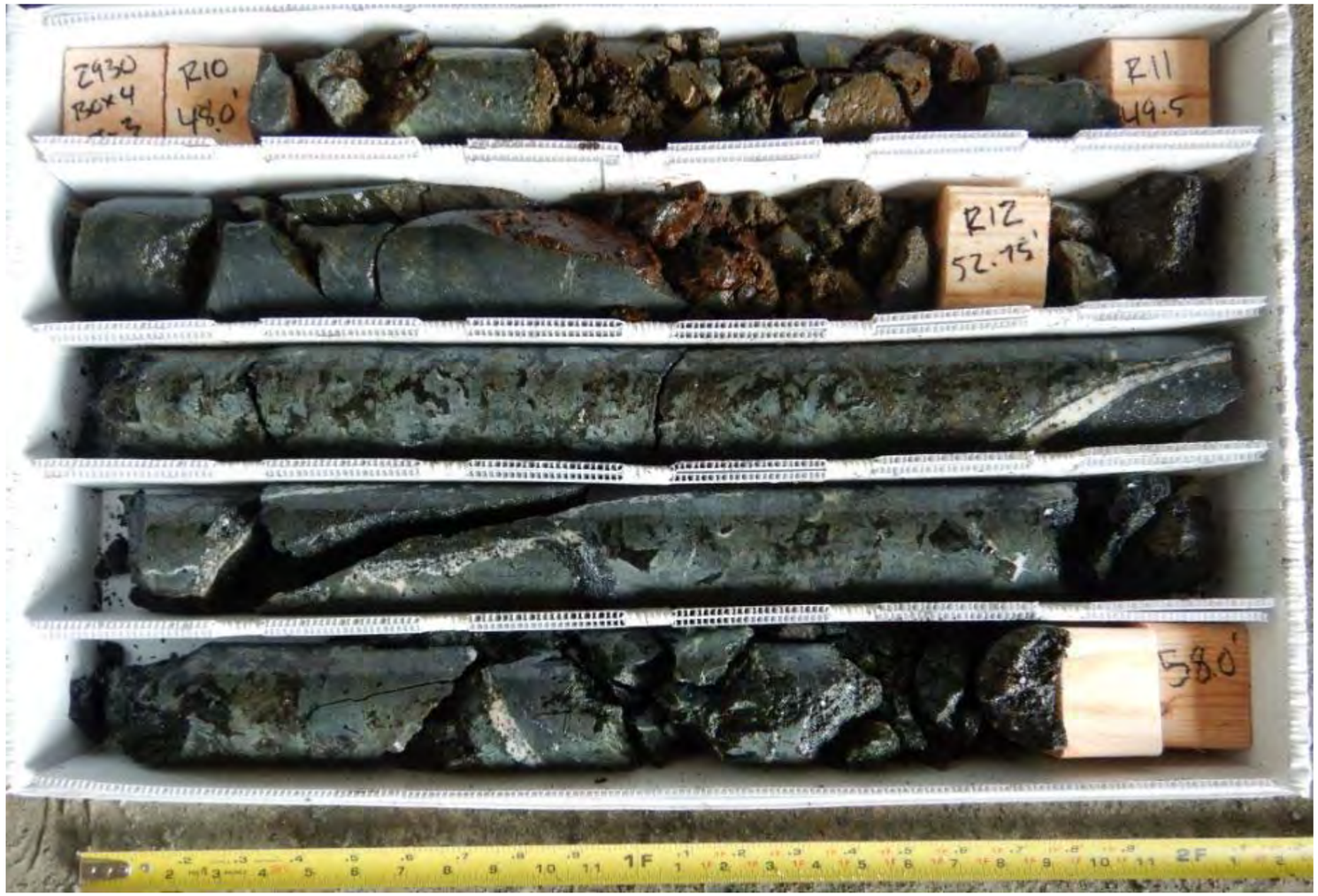

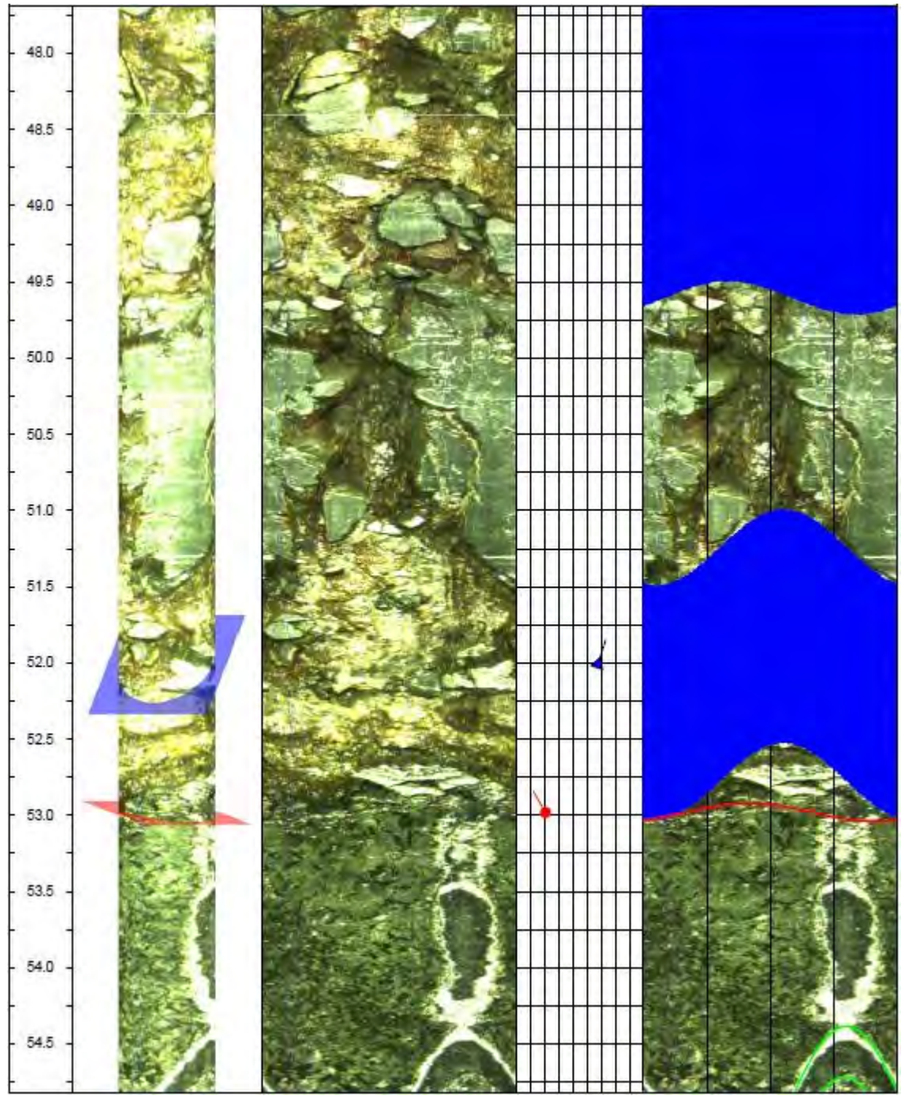

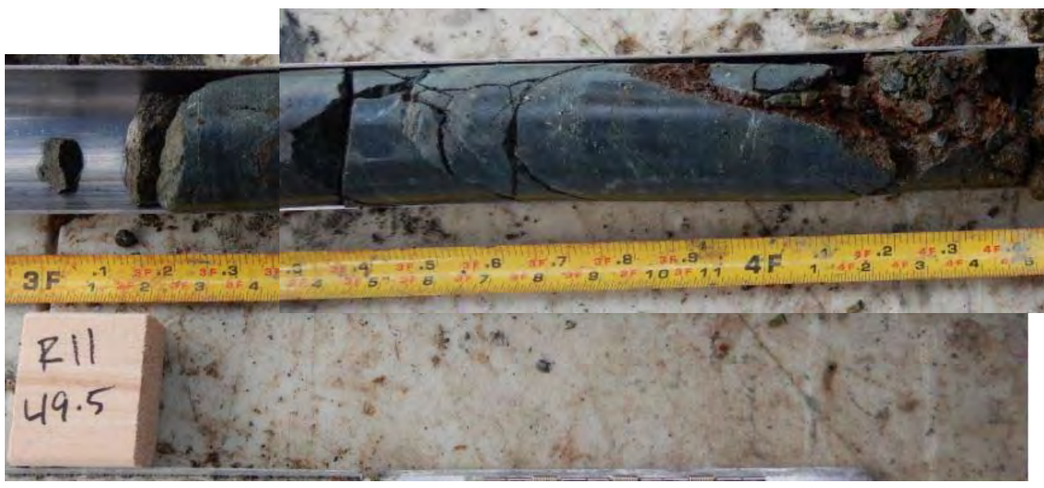

LT-3 transition at 52.9 ft

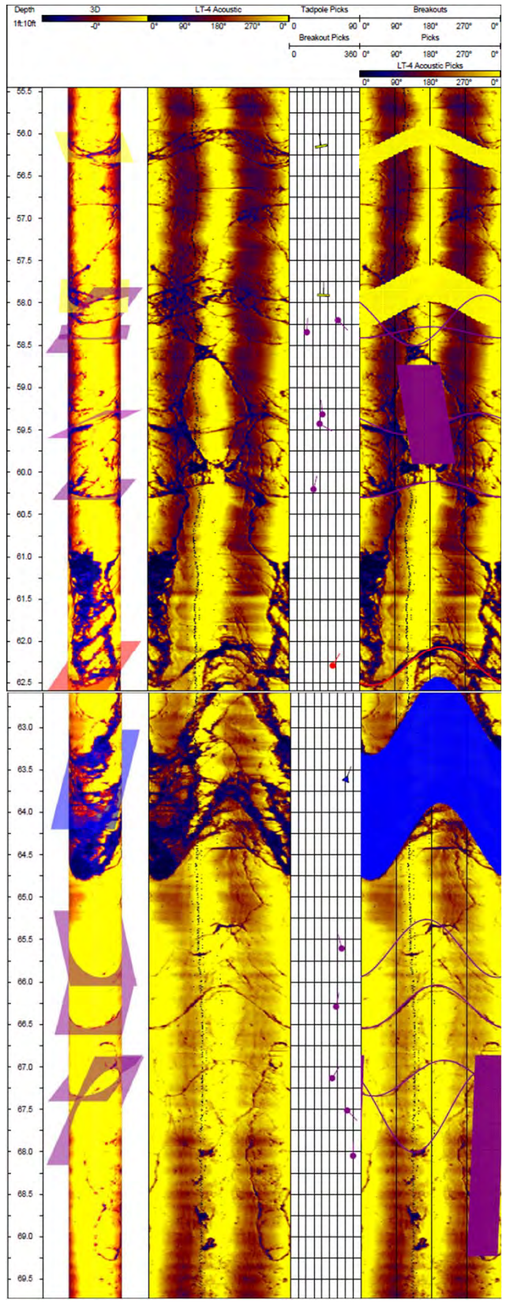

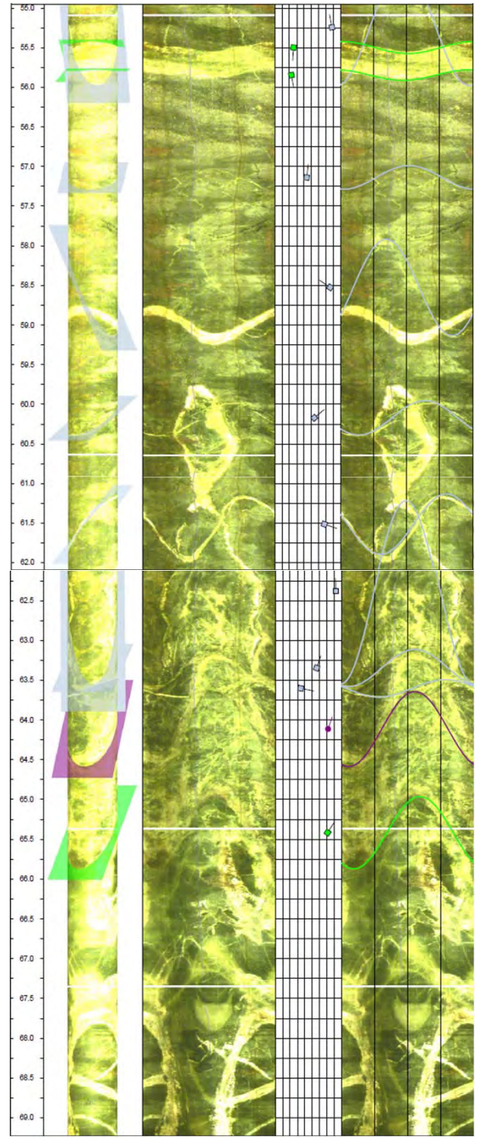

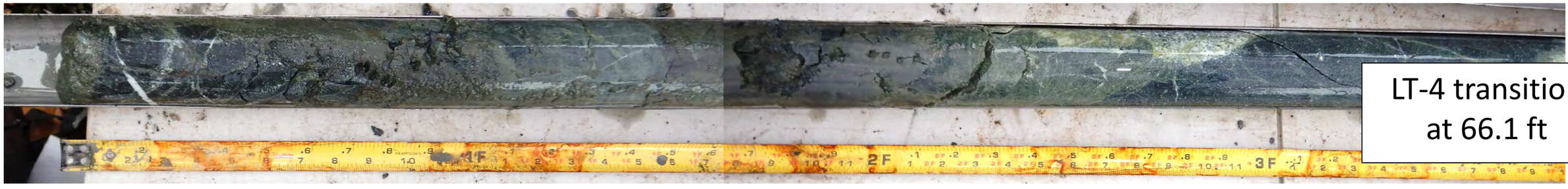

LT-4 transition at 66.1 ft

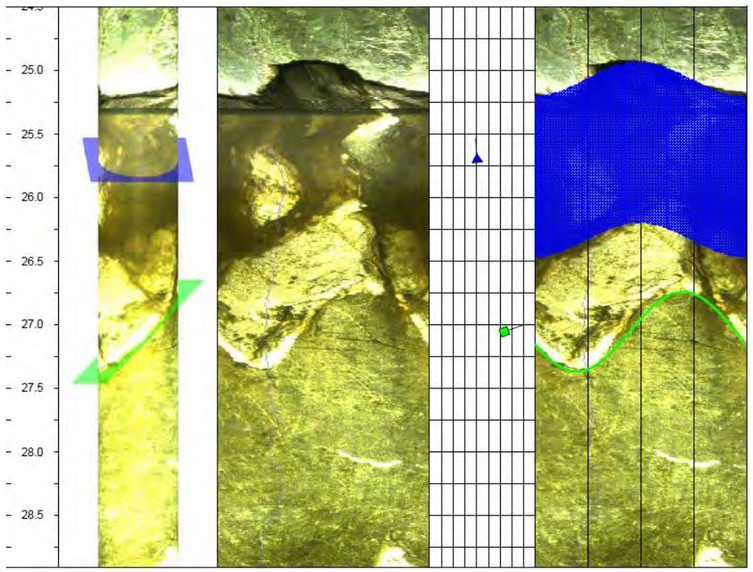

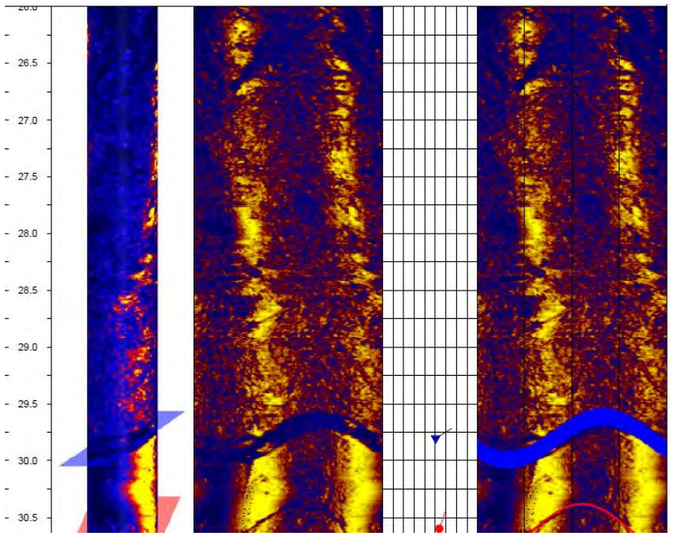

LT-5 transition
at 26.7 ft

LT-6 transition at 7.5 ft

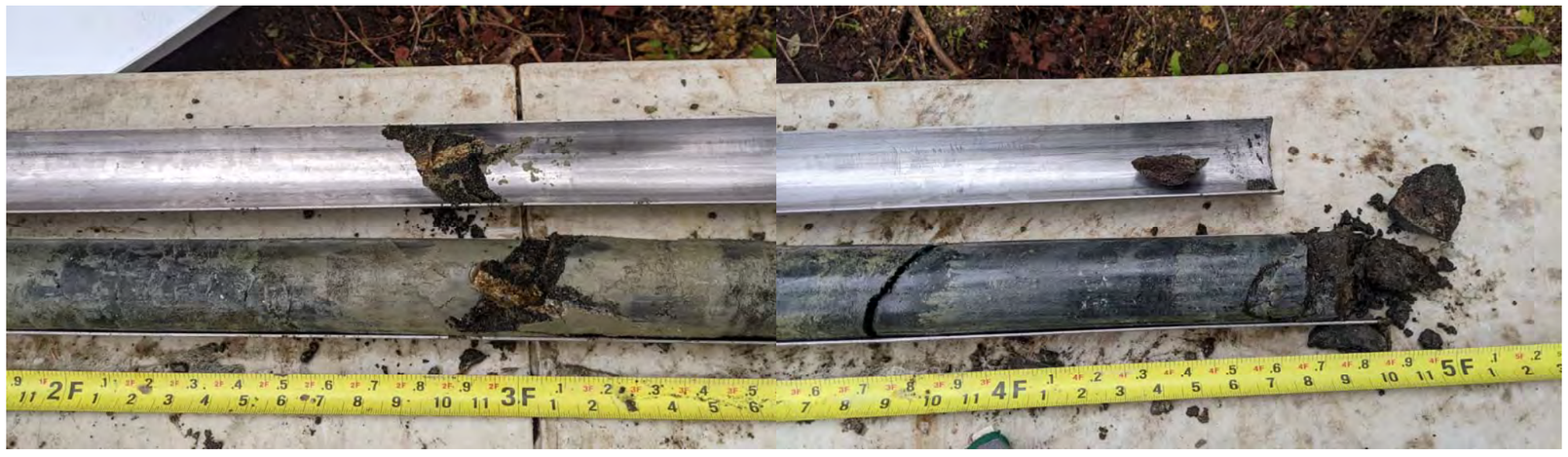

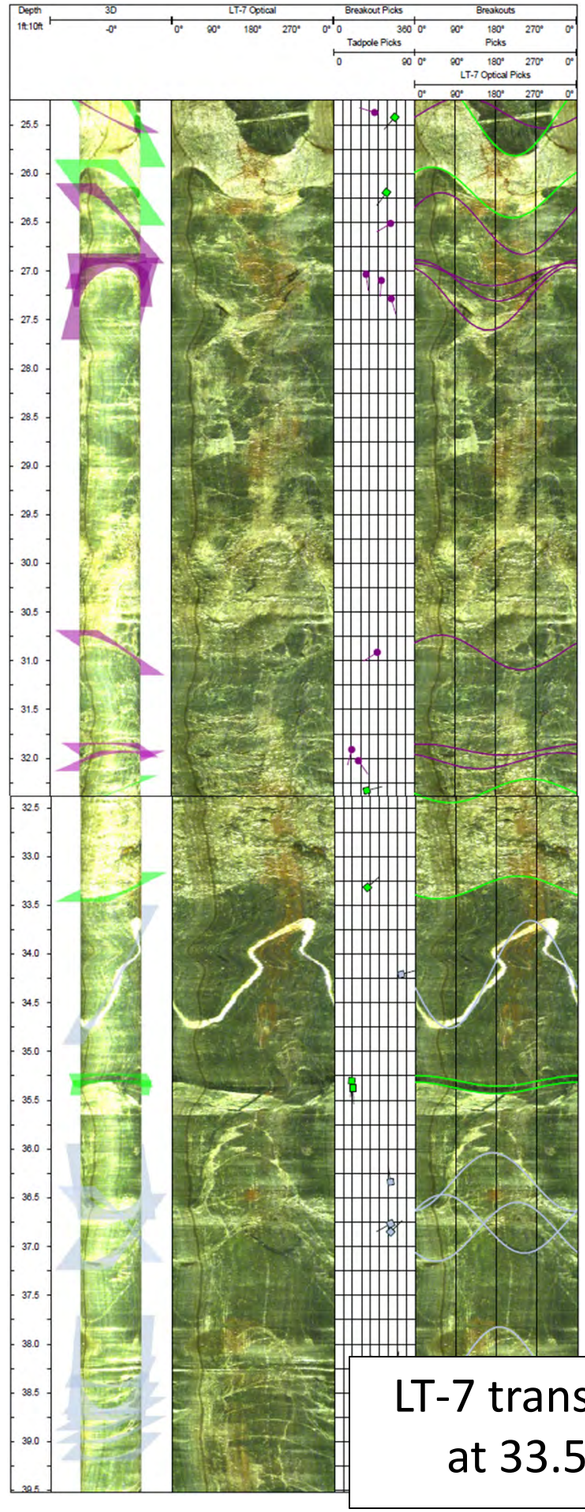

LT-7 transition at 33.5 ft

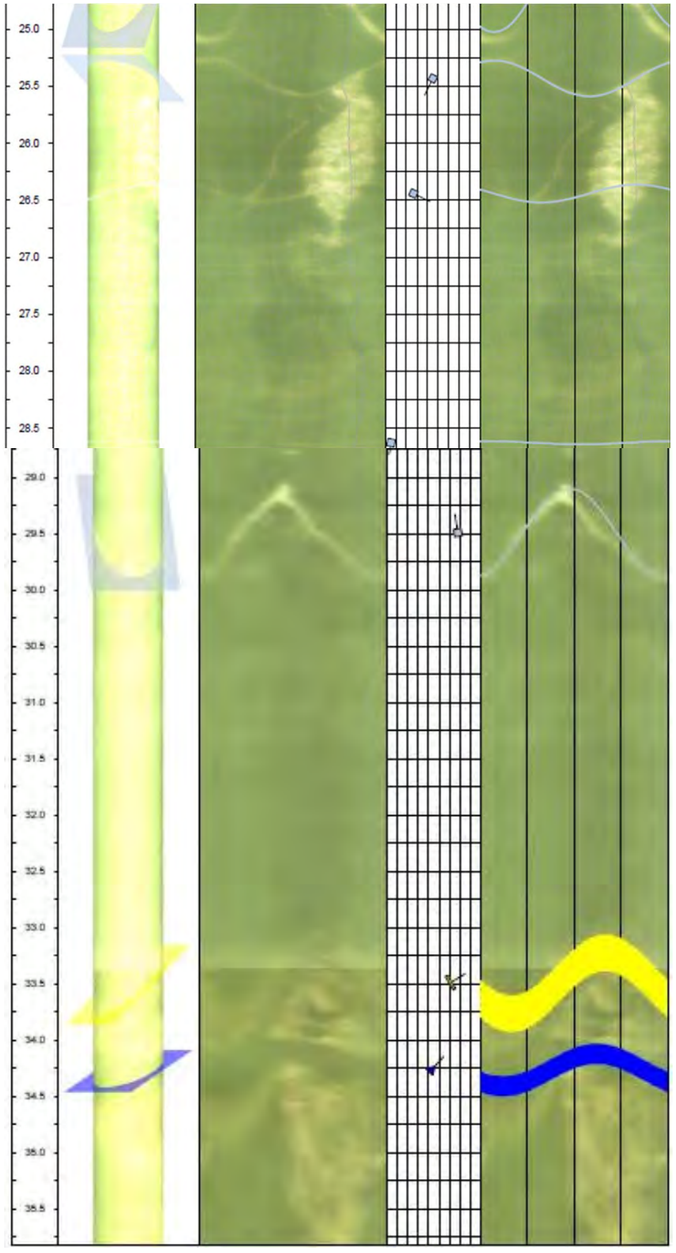

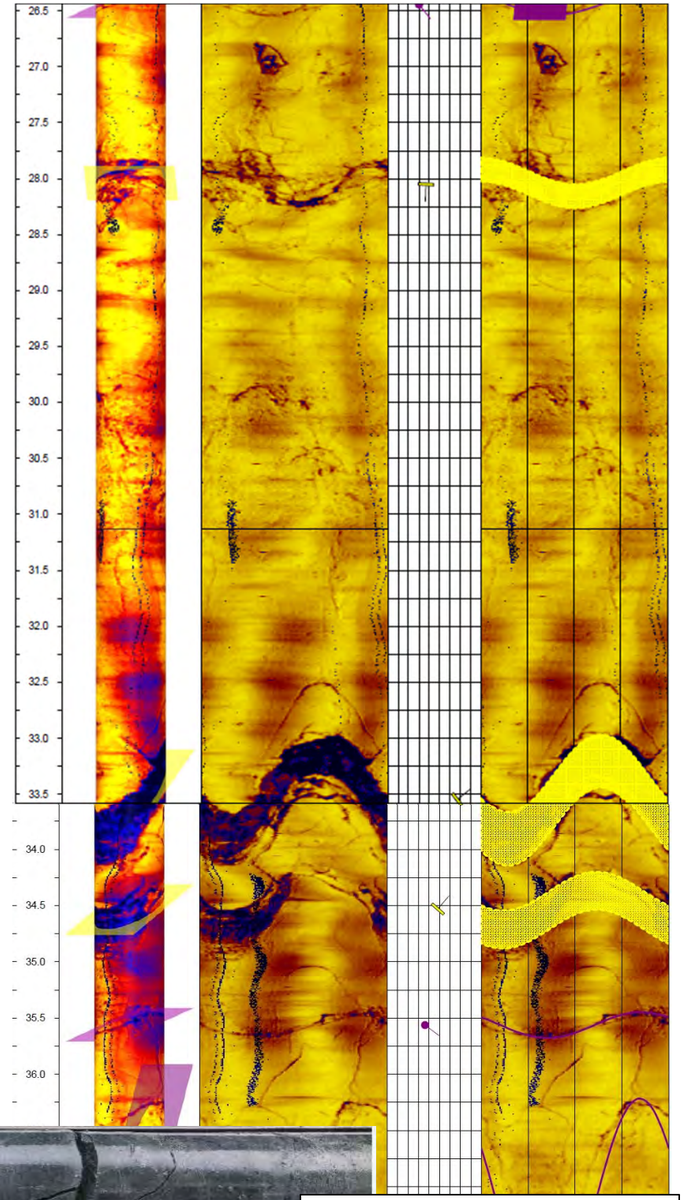

LT-8 transition at 35.2 ft

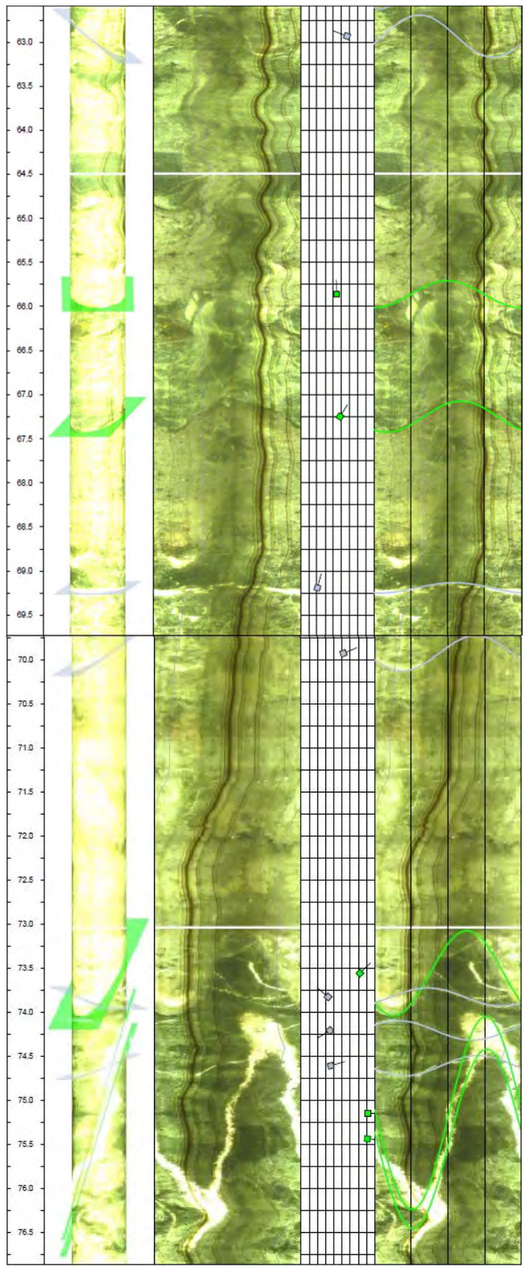

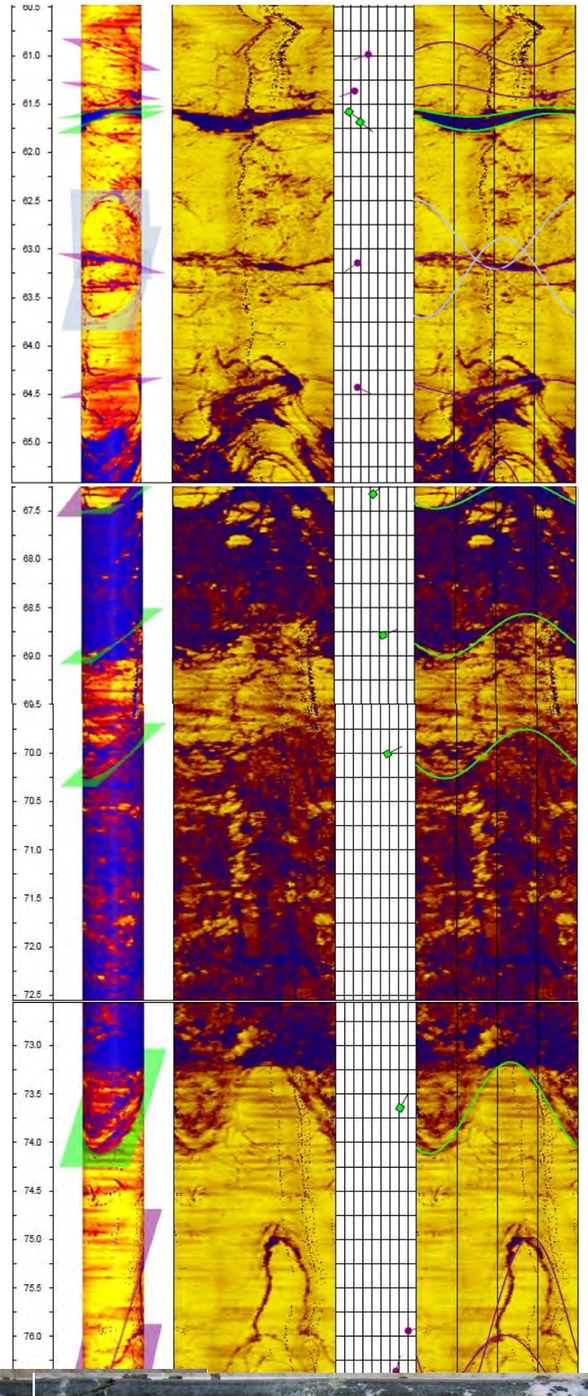

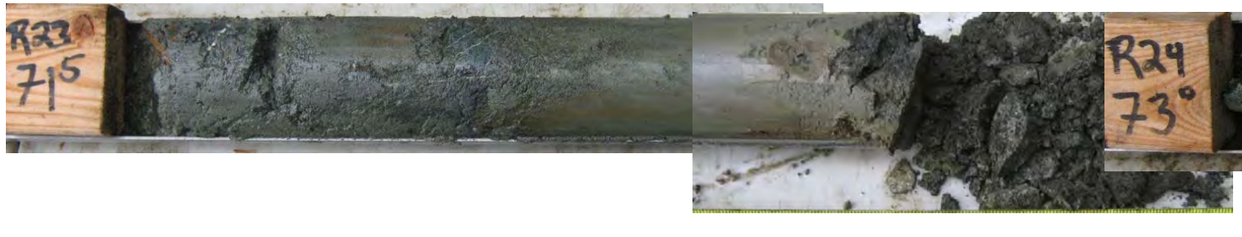

LT-9 transition
at 74.0 ft

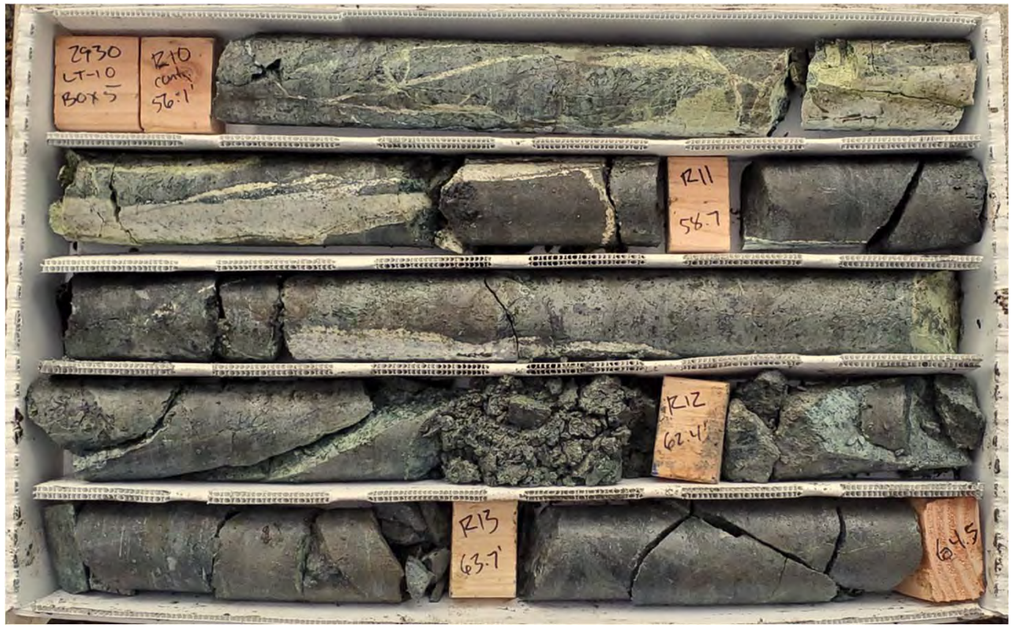

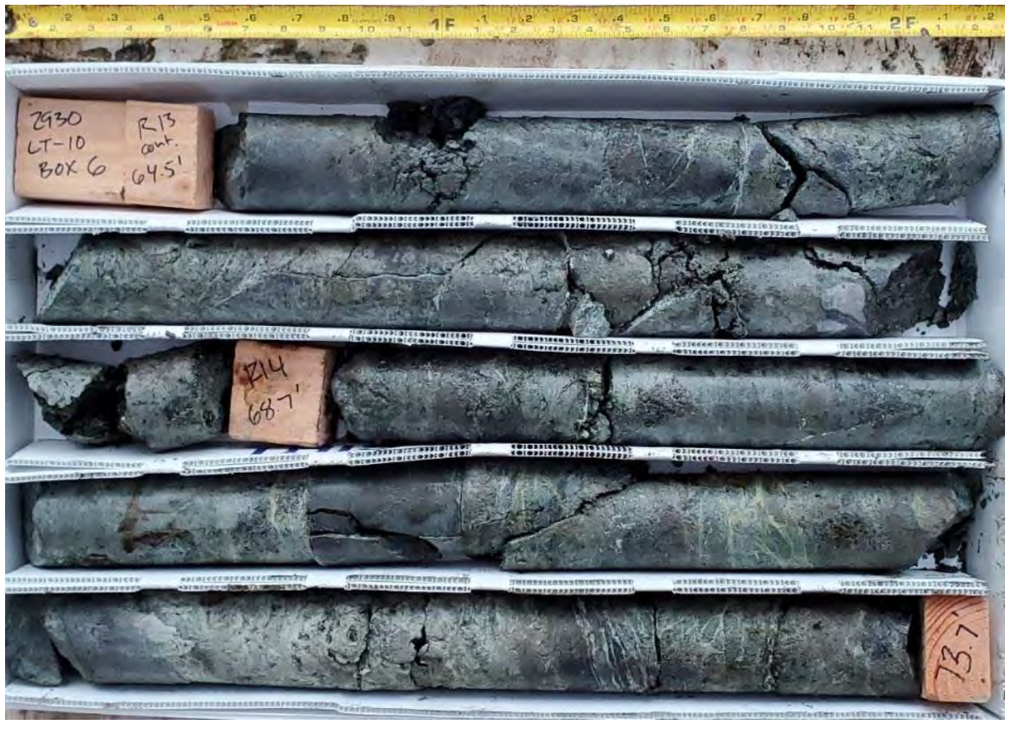

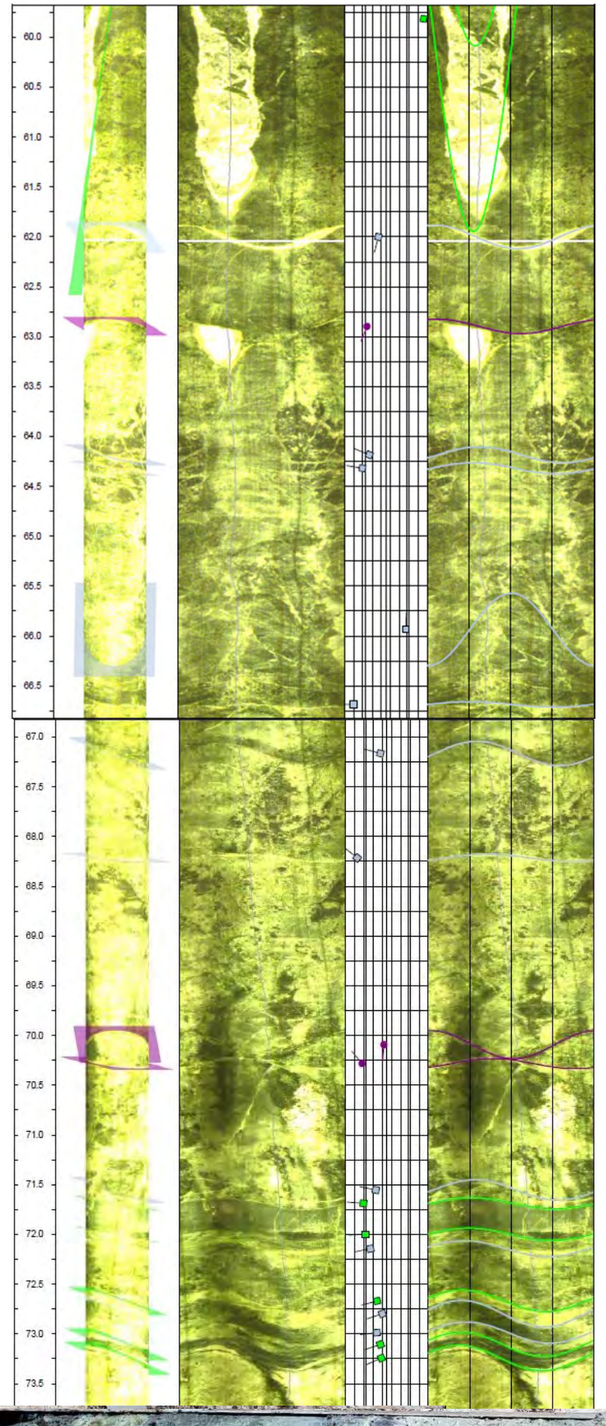

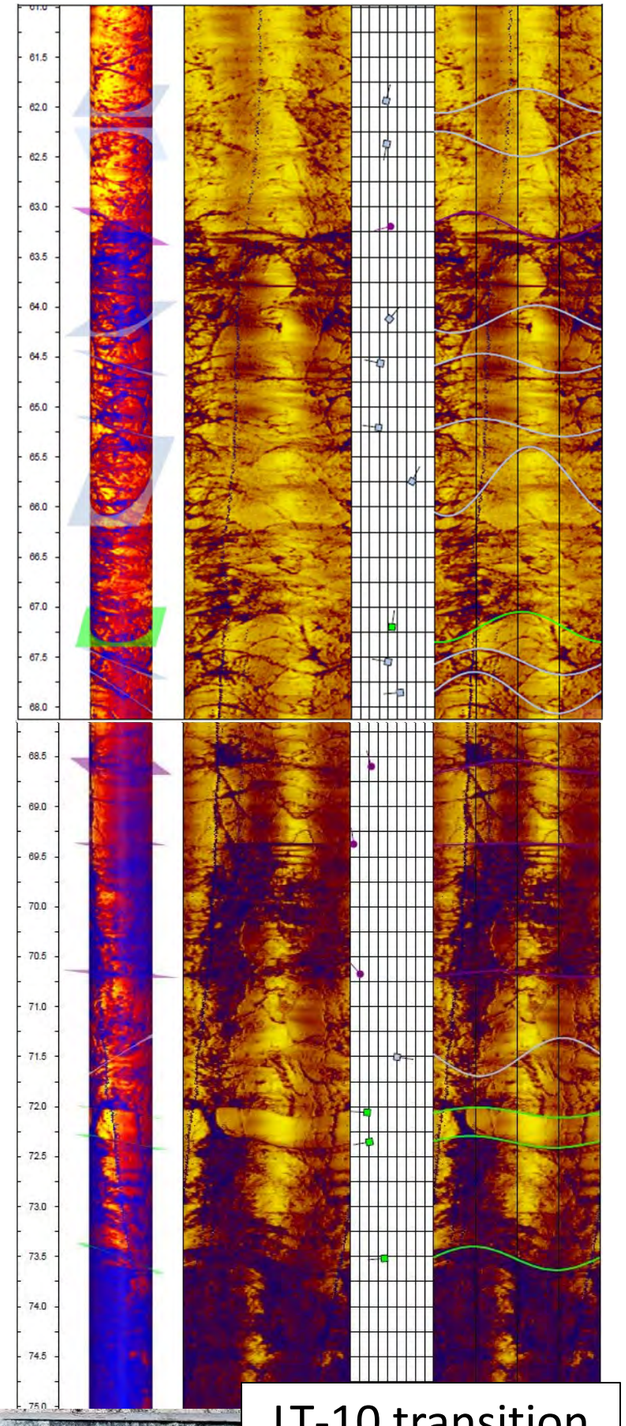

LT-10 transition at 71.8 ft

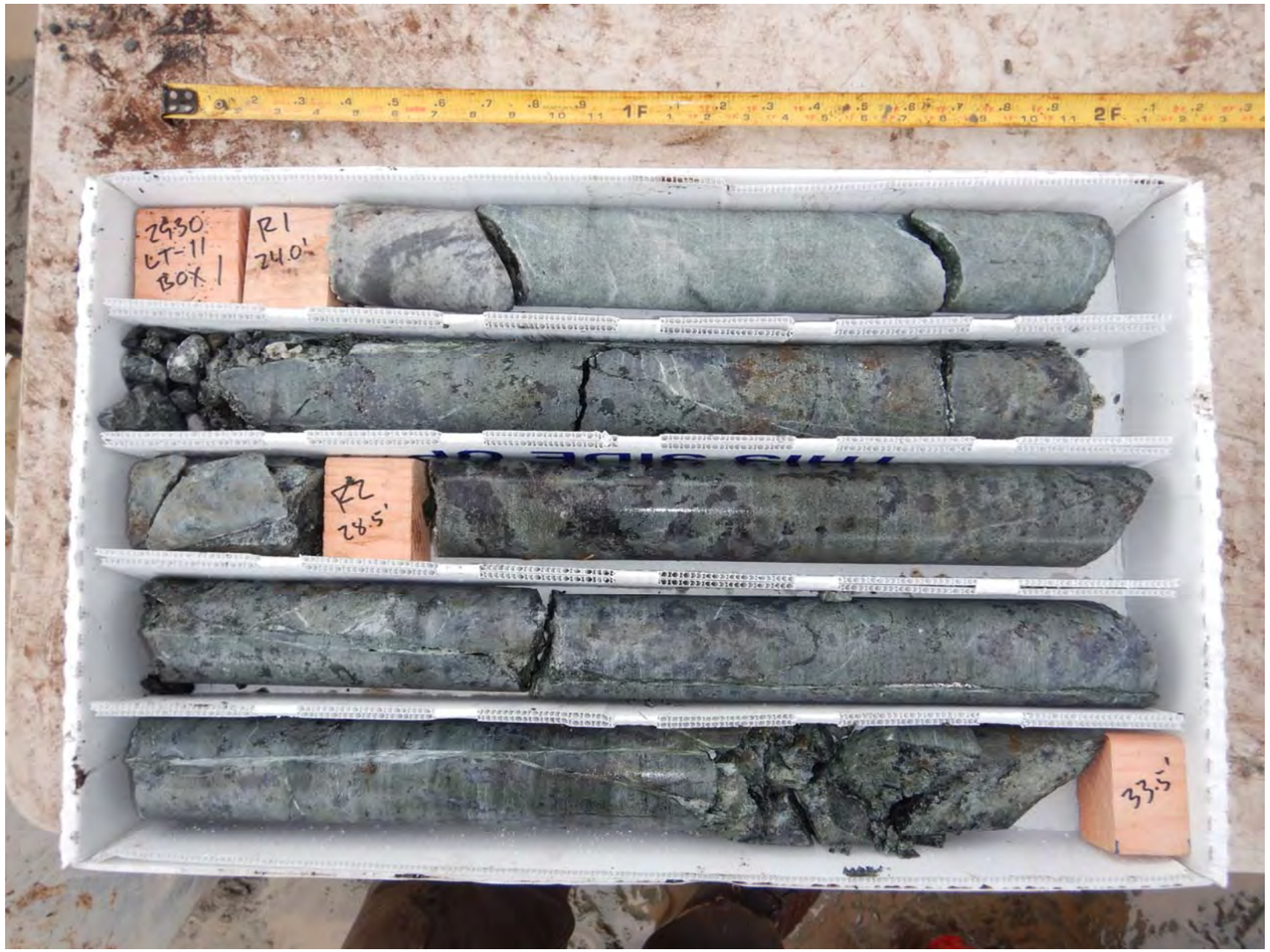

Note: no photos of LT-12 at Transition at 12.5 feet due to drilling methods

LT-11 transition at 25.8 ft

Appendix C: Source Specific Flow-R Runout Analyses

Beach Road

Mt. Riley Road

1

2

3

4

5

6

7

N

Flow-R Source Areas

Haines Borough Area of Concern

Geomorphic Interpretations

Likelihood of Flow Paths (%)

0

< 10

10 to 20

20 to 30

30 to 40

40 to 50

> 50

0 150 300 600 Feet

Note: Topography derived from 2020 LiDAR data provided by DGGS.

LANDSLIDE TECHNOLOGY
A DIVISION OF CORNFORTH CONSULTANTS
10250 S.W. Greenburg Road, Suite 111
Portland, Oregon 97223
Phone 503-452-1200 Fax 503-452-1528

Model A Applied to Source Area 1

Updated Findings Report - Beach Rd Landslide
Haines, Alaska

MAR 2022

PROJ. 2925

FIG. C-1

Beach Road

Mt. Riley Road

N

Flow-R Source Areas

Haines Borough Area of Concern

Geomorphic Interpretations

Likelihood of Flow Paths (%)

0

< 10

10 to 20

20 to 30

30 to 40

40 to 50

> 50

1

2

3

4

5

6

7

0 150 300 600 Feet

Note: Topography derived from 2020 LiDAR data provided by DGGS.

LANDSLIDE TECHNOLOGY
A DIVISION OF CORNFORTH CONSULTANTS
10250 S.W. Greenburg Road, Suite 111
Portland, Oregon 97223
Phone 503-452-1200 Fax 503-452-1528

Model B Applied to Source Area 1

Updated Findings Report - Beach Rd Landslide
Haines, Alaska

MAR 2022

PROJ. 2925

FIG. C-2

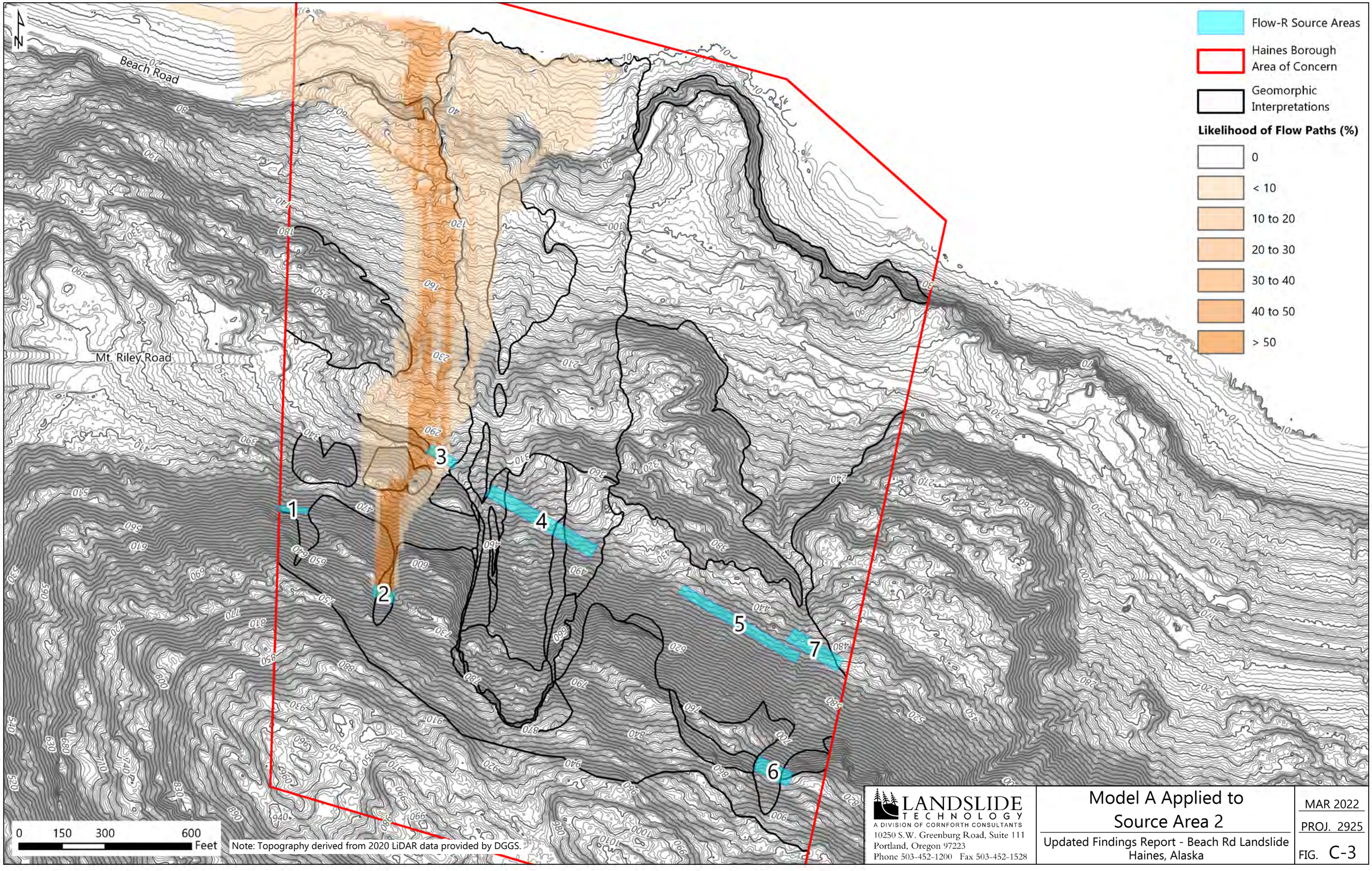

Note: Topography derived from 2020 LiDAR data provided by DGGS.

LANDSLIDE TECHNOLOGY
A DIVISION OF CORNFORTH CONSULTANTS
10250 S.W. Greenburg Road, Suite 111
Portland, Oregon 97223
Phone 503-452-1200 Fax 503-452-1528

Model A Applied to Source Area 2

Updated Findings Report - Beach Rd Landslide
Haines, Alaska

MAR 2022
PROJ. 2925
FIG. C-3

Flow-R Source Areas

Haines Borough Area of Concern

Geomorphic Interpretations

Likelihood of Flow Paths (%)

0

< 10

10 to 20

20 to 30

30 to 40

40 to 50

> 50

Beach Road

Mt. Riley Road

1

2

3

4

5

6

7

0 150 300 600 Feet

Note: Topography derived from 2020 LiDAR data provided by DGGS.

LANDSLIDE TECHNOLOGY
A DIVISION OF CORNFORTH CONSULTANTS
10250 S.W. Greenburg Road, Suite 111
Portland, Oregon 97223
Phone 503-452-1200 Fax 503-452-1528

Model B Applied to Source Area 2

Updated Findings Report - Beach Rd Landslide
Haines, Alaska

MAR 2022

PROJ. 2925

FIG. C-4

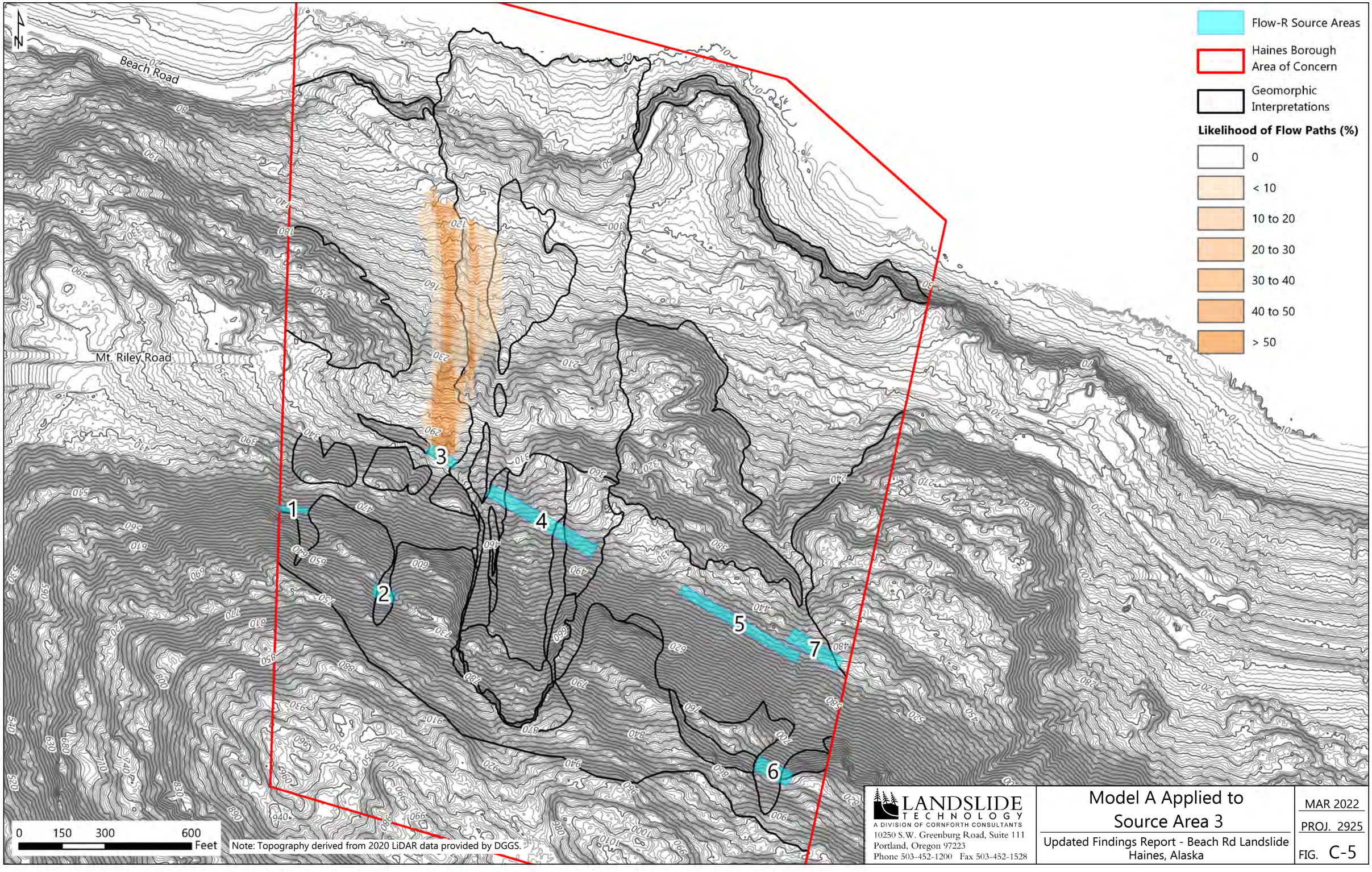

LANDSLIDE TECHNOLOGY
A DIVISION OF CORNFORTH CONSULTANTS
10250 S.W. Greenburg Road, Suite 111
Portland, Oregon 97223
Phone 503-452-1200 Fax 503-452-1528

Model A Applied to Source Area 3

Updated Findings Report - Beach Rd Landslide
Haines, Alaska

MAR 2022
PROJ. 2925
FIG. C-5

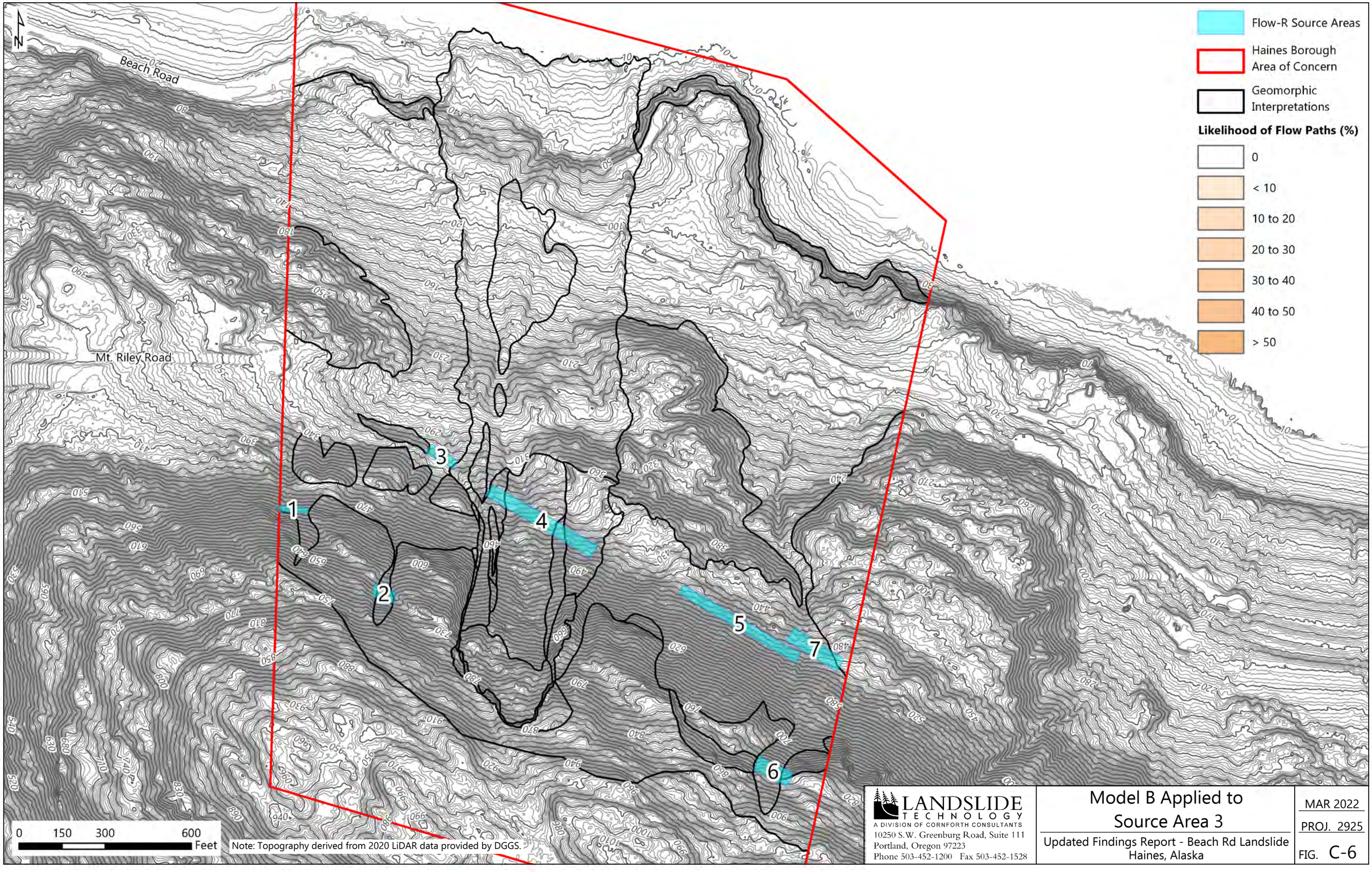

LANDSLIDE TECHNOLOGY
A DIVISION OF CORNFORTH CONSULTANTS
10250 S.W. Greenburg Road, Suite 111
Portland, Oregon 97223
Phone 503-452-1200 Fax 503-452-1528

Model B Applied to Source Area 3

Updated Findings Report - Beach Rd Landslide
Haines, Alaska

MAR 2022
PROJ. 2925
FIG. C-6

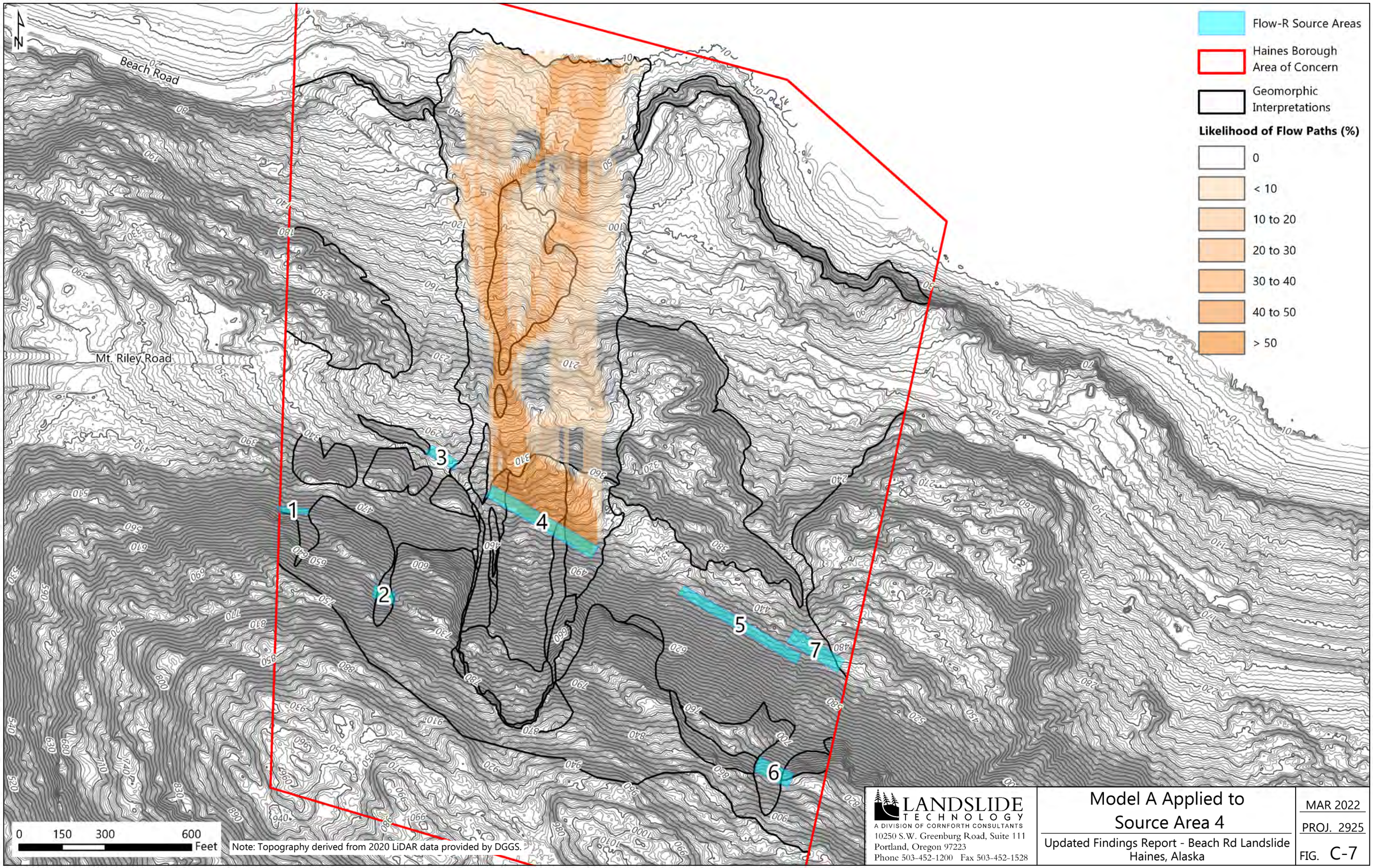

LANDSLIDE TECHNOLOGY
A DIVISION OF CORNFORTH CONSULTANTS
10250 S.W. Greenburg Road, Suite 111
Portland, Oregon 97223
Phone 503-452-1200 Fax 503-452-1528

Model A Applied to Source Area 4

Updated Findings Report - Beach Rd Landslide
Haines, Alaska

MAR 2022
PROJ. 2925
FIG. C-7

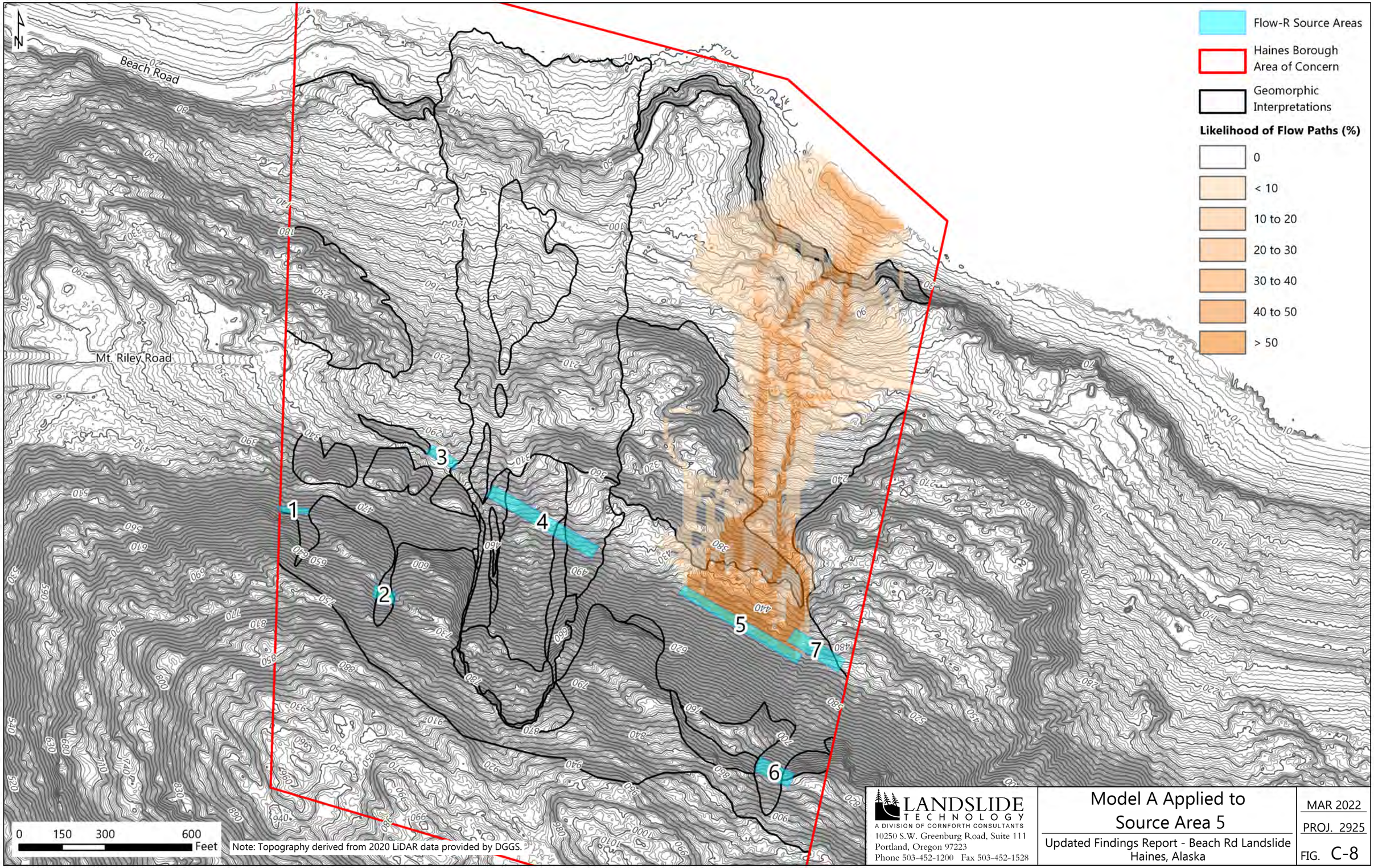

Note: Topography derived from 2020 LiDAR data provided by DGGS.

LANDSLIDE TECHNOLOGY
A DIVISION OF CORNFORTH CONSULTANTS
10250 S.W. Greenburg Road, Suite 111
Portland, Oregon 97223
Phone 503-452-1200 Fax 503-452-1528

Model A Applied to Source Area 5

Updated Findings Report - Beach Rd Landslide
Haines, Alaska

MAR 2022

PROJ. 2925

FIG. C-8

Beach Road

Mt. Riley Road

1

2

3

4

5

6

7

Flow-R Source Areas

Haines Borough Area of Concern

Geomorphic Interpretations

Likelihood of Flow Paths (%)

0

< 10

10 to 20

20 to 30

30 to 40

40 to 50

> 50

0 150 300 600 Feet

Note: Topography derived from 2020 LiDAR data provided by DGGS.

LANDSLIDE TECHNOLOGY
A DIVISION OF CORNFORTH CONSULTANTS
10250 S.W. Greenburg Road, Suite 111
Portland, Oregon 97223
Phone 503-452-1200 Fax 503-452-1528

Model B Applied to Source Area 5

Updated Findings Report - Beach Rd Landslide
Haines, Alaska

MAR 2022

PROJ. 2925

FIG. C-9

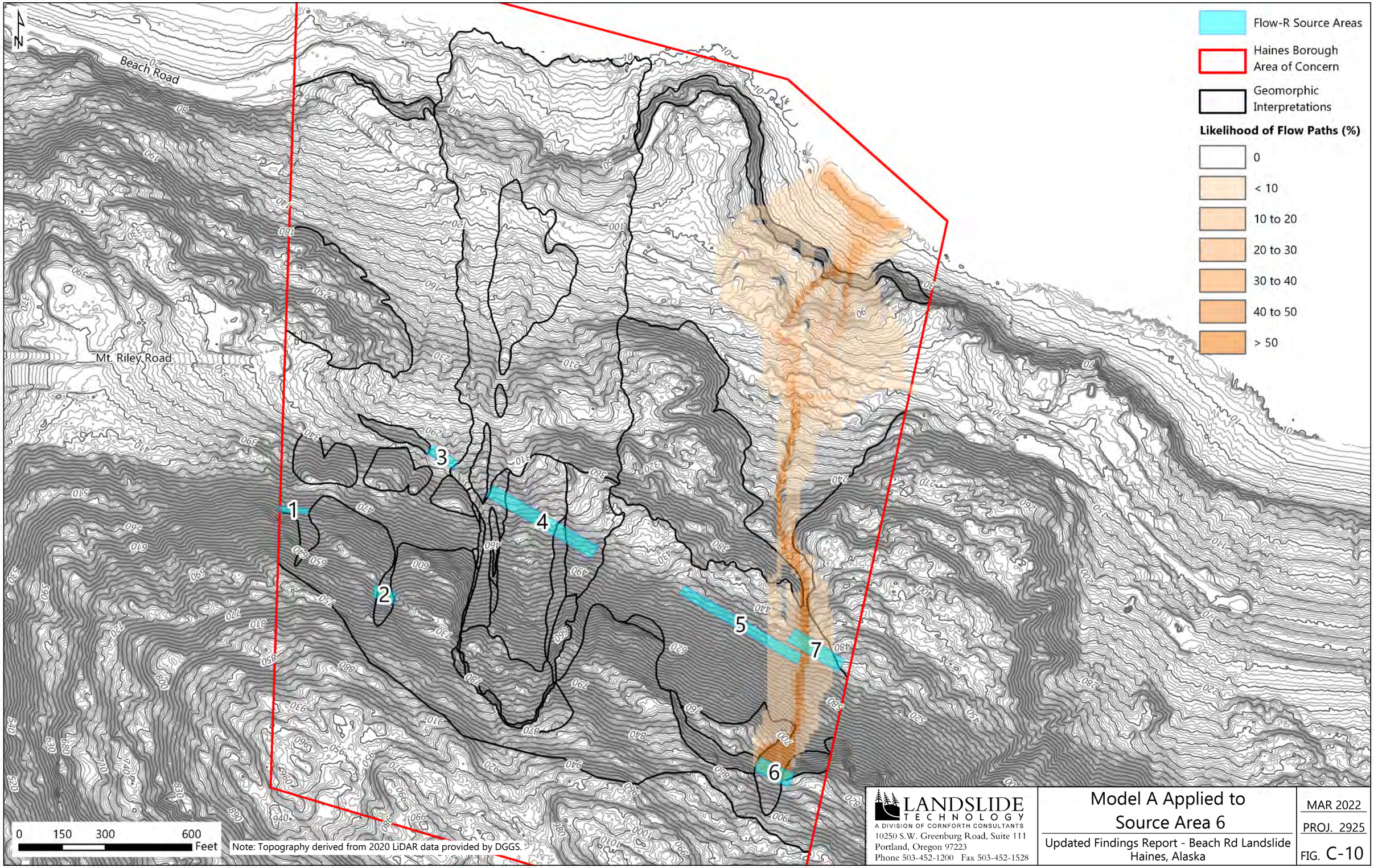

Note: Topography derived from 2020 LiDAR data provided by DGGS.

LANDSLIDE TECHNOLOGY
A DIVISION OF CORNFORTH CONSULTANTS
10250 S.W. Greenburg Road, Suite 111
Portland, Oregon 97223
Phone 503-452-1200 Fax 503-452-1528

Model A Applied to Source Area 6

Updated Findings Report - Beach Rd Landslide
Haines, Alaska

MAR 2022

PROJ. 2925

FIG. C-10

Flow-R Source Areas

Haines Borough Area of Concern

Geomorphic Interpretations

Likelihood of Flow Paths (%)

0

< 10

10 to 20

20 to 30

30 to 40

40 to 50

> 50

Beach Road

Mt. Riley Road

1

2

3

4

5

6

7

0 150 300 600 Feet

Note: Topography derived from 2020 LiDAR data provided by DGGS.

LANDSLIDE TECHNOLOGY
A DIVISION OF CORNFORTH CONSULTANTS
10250 S.W. Greenburg Road, Suite 111
Portland, Oregon 97223
Phone 503-452-1200 Fax 503-452-1528

Model B Applied to Source Area 6

Updated Findings Report - Beach Rd Landslide
Haines, Alaska

MAR 2022

PROJ. 2925

FIG. C-11

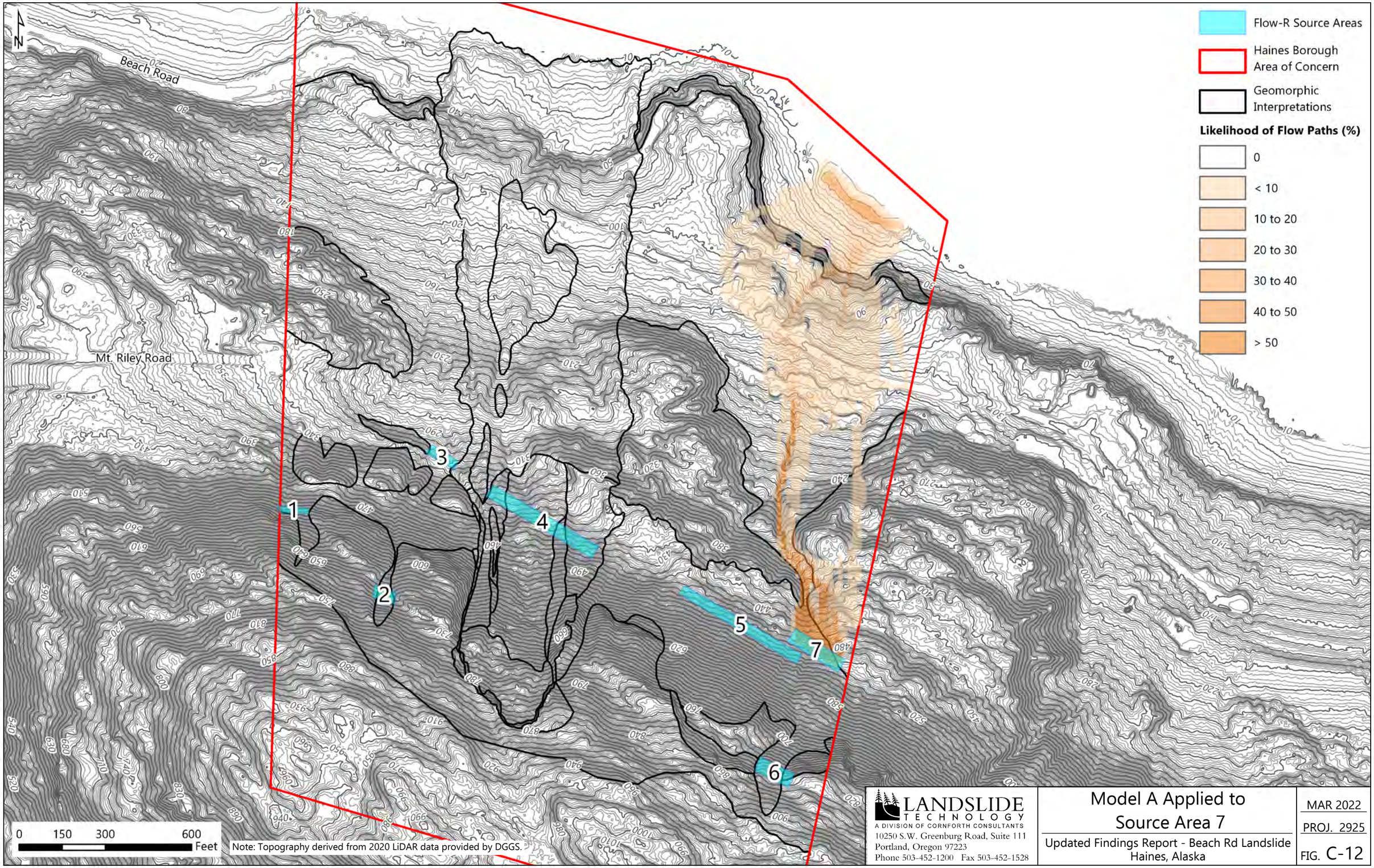

Note: Topography derived from 2020 LiDAR data provided by DGGS.

LANDSLIDE TECHNOLOGY
A DIVISION OF CORNFORTH CONSULTANTS
10250 S.W. Greenburg Road, Suite 111
Portland, Oregon 97223
Phone 503-452-1200 Fax 503-452-1528

Model A Applied to Source Area 7

Updated Findings Report - Beach Rd Landslide
Haines, Alaska

MAR 2022

PROJ. 2925

FIG. C-12

Flow-R Source Areas

Haines Borough Area of Concern

Geomorphic Interpretations

Likelihood of Flow Paths (%)

0

< 10

10 to 20

20 to 30

30 to 40

40 to 50

> 50

Beach Road

Mt. Riley Road

1

2

3

4

5

6

7

0 150 300 600 Feet

Note: Topography derived from 2020 LiDAR data provided by DGGS.

LANDSLIDE TECHNOLOGY
A DIVISION OF CORNFORTH CONSULTANTS
10250 S.W. Greenburg Road, Suite 111
Portland, Oregon 97223
Phone 503-452-1200 Fax 503-452-1528

Model B Applied to Source Area 7

Updated Findings Report - Beach Rd Landslide
Haines, Alaska

MAR 2022

PROJ. 2925

FIG. C-13